NASA CR-152186

An Analysis of Prop-Fan/Airframe Aerodynamic Integration

The Boeing Commercial Airplane Company
P.O. Box 3707
Seattle, Washington 98124

Prepared for
Ames Research Center
under contract NAS2-9104



NASA

National Aeronautics and
Space Administration

October 1978

1. Report No.	2. Government Accession No.	3. Recipient's Catalog No.
NASA CR-152186		

4. Title and Subtitle	5. Report Date
FINAL REPORT— An Analysis of Prop-Fan/Airframe Aerodynamic Integration	October 1978
	6. Performing Organization Code B-7200
7. Author(s) M.L. Boctor, C.W. Clay, C.F. Watson	8. Performing Organization Report No. D6-47113
	10. Work Unit No.
9. Performing Organization Name and Address Boeing Commercial Airplane Company P.O. Box 3707 Seattle, Washington 98124	11. Contract or Grant No. NAS2-9104
	13. Type of Report and Period Covered Final Report October 1978
12. Sponsoring Agency Name and Address National Aeronautics and Space Administration Ames Research Center Moffet Field, California 94035	14. Sponsoring Agency Code FVS

15. Supplementary Notes

Technical Monitor: Louis J. Williams
NASA Ames Research Center
Moffet Field, California 94035

16. Abstract

This study addresses an approach to aerodynamic integration of turbo-props and airframes, with emphasis placed upon wing-mounted installations. Potential flow analytical techniques were employed to study aerodynamic integration of the prop-fan propulsion concept with advanced, subsonic, commercial transport airframes. Three basic configurations were defined and analyzed:

- Wing-mounted prop-fan at a cruise Mach number of 0.8
- Wing-mounted prop-fan in a low-speed configuration
- Aft-mounted prop-fan at a cruise Mach number of 0.8

17. Key Words (Suggested by Author(s))	18. Distribution Statement
potential-flow analysis prop-fan slipstream prop-fan swirl	[redacted]

19. Security Classif. (of this report)	20. Security Classif. (of this page)	21. No. of Pages	22. Price*
Unclassified	Unclassified	—	

* For sale by the National Technical Information Service, Springfield, Virginia 22161

CONTENTS

		Page
1.0	SUMMARY	1
	1.1 General	1
	1.2 Conclusions	1
	1.3 Recommendations	4
2.0	INTRODUCTION	6
	2.1 Background	6
	2.2 Study Objective and Scope	7
3.0	ABBREVIATIONS AND SYMBOLS	8
4.0	ANALYSIS AND DESIGN METHODS	10
	4.1 Computer Program A 230 Description	10
	4.2 Analysis Using Slipstream and Pre- and Post-Processors	10
	4.3 Computer Program A 236 Description	12
	4.4 Design Method	13
5.0	WING-MOUNTED PROP-FAN–CRUISE	17
	5.1 Configuration and Flight Conditions	17
	5.2 Slipstream Characteristics	20
	5.3 Pressure Coefficient Data	21
	5.4 Wing Isobars	26
	5.5 Force Data	28
	5.6 Propeller Thrust Recovery Assessment	30
	5.7 Assessment	33
6.0	WING-MOUNTED PROP-FAN–LOW SPEED	34
	6.1 Geometrical Definition	34
	6.2 Design Procedure	37
	6.3 Slipstream Characteristics	39
	6.4 Pressure Coefficient Data	40
	6.5 Force Data	40
	6.6 Drag and Thrust Recovery	44
	6.7 Effect of One-Engine Failure	44
	6.8 Assessment	46
7.0	AFT-MOUNTED PROP-FAN	47
	7.1 Configuration and Flight Conditions	47
	7.2 Slipstream Characteristics	49
	7.3 Pressure Distribution and Span Loading	49
	7.4 Drag and Thrust Recovery	54
	7.5 Assessment	55
8.0	REFERENCES	56
APPENDIX A	BASELINE AND MODIFIED WING GEOMETRY	A1

FIGURES

No.		Page
	SECTION 1.0	
1	Summary of Study Approach and Results	2
2	Typical Modification Concept for Prop-Fan Cruise Wing	5
	SECTION 4.0	
3	Technique for Modeling Prop Slipstream	11
4	Test Case–Flow Over Stub Wing: Strip 2	12
5	Prop-Fan Wing Design Technique	14
6	Cruise Wing Geometry	15
7	Cruise Wing Twist Distribution	16
8	Cruise Wing Thickness Distribution	16
	SECTION 5.0	
9	Baseline Wing Body Model	17
10	Baseline Wing Body/Nacelle Model	18
11	Paneling of Modified Cruise Wing	19
12	Modified Cruise Wing	19
13	Radial Distribution of Swirl and Total Pressure in Prop Slipstream	20
14	Effect of Slipstream on Chordwise Pressure Distribution: Strip 3	22
15	Effect of Slipstream on Chordwise Pressure Distribution: Strip 4	22
16	Effect of Slipstream on Chordwise Pressure Distribution: Strip 5	23
17	Effect of Slipstream on Chordwise Pressure Distribution: Strip 6	23
18	Wing Pressure Profiles: Strip 3	24
19	Wing Pressure Profiles: Strip 4	24
20	Wing Pressure Profiles: Strip 5	25
21	Wing Pressure Profiles: Strip 6	25
22	Upper Surface Wing Isobars–Clean Wing	26
23	Upper Surface Wing Isobars–Baseline Wing + Nacelle	27
24	Upper Surface Wing Isobars–Baseline Wing + Nacelle + Slipstream	27
25	Upper Surface Wing Isobars–Modified Wing + Nacelle + Slipstream	28
26	Cruise Wing Lift Curves	29
27	Effect of Slipstream on Span Loading	29
28	Wing Spanwise Load Distribution	30
29	Spanwise Distribution of $C_{p_{MIN}}$	31
30	Wing Drags Incremented from Clean Wing	32

No. Page

SECTION 6.0

31 Leading- and Trailing-Edge Flaps for Low-Speed Configuration 34
32 Krueger Flap Definition 35
33 Paneling Scheme–Low-Speed Configuration 36
34 Krueger Wing–Low-Speed Configuration 36
35 Krueger Flap Deflection Schedule 37
36 Low-Speed Wing Pressure Profiles: Strip 3 38
37 Low-Speed Wing Pressure Profiles: Strip 6 38
38 Radial Distribution of Swirl and Total Pressure in Prop Slipstream 39
39 Radial Distribution of Axial Velocity Increment in Prop Slipstream 40
40 Low-Speed Wing Pressure Profiles with Slipstream: Strip 3 41
41 Low-Speed Wing Pressure Profiles with Slipstream: Strip 4 41
42 Low-Speed Wing Pressure Profiles with Slipstream: Strip 5 42
43 Low-Speed Wing Pressure Profiles with Slipstream: Strip 6 42
44 Krueger Wing–Low-Speed Configuration Lift Curve 43
45 Krueger Wing–Low-Speed Configuration Spanwise Load Distribution 43
46 Krueger Wing–Low-Speed Configuration Induced Drag Due to Slipstream 44
47 Krueger Wing–Low-Speed Configuration Rolling Moment Coefficient 45
48 Rolling Moment Due to Engine-Out Comparison with Preliminary Estimates 45

SECTION 7.0

49 Paneling of Aft-Mounted Prop-Fan 47
50 Aft-Mounted Prop-Fan Isometric Projection 48
51 Aft-Mounted Prop-Fan Cross Sectional Area Distribution 48
52 Aft-Mounted Prop-Fan Side-of-Body Pressure Profile 49
53 Aft-Mounted Prop-Fan Strut Pressure Profiles: Strip 1 50
54 Aft-Mounted Prop-Fan Strut Pressure Profiles: Strip 2 51
55 Aft-Mounted Prop-Fan Strut Pressure Profiles: Strip 3 51
56 Aft-Mounted Prop-Fan Vertical Tail Pressure Profiles: Strip 1 52
57 Aft-Mounted Prop-Fan Vertical Tail Pressure Profiles: Strip 2 52
58 Aft-Mounted Prop-Fan Vertical Tail Pressure Profiles: Strip 3 53
59 Aft-Mounted Prop-Fan Vertical Tail Pressure Profiles: Strip 4 53
60 Aft-Mounted Prop-Fan Effect of Slipstream on Strut Loading 54
61 Aft-Mounted Prop-Fan Effect of Slipstream on Induced Drag 55

APPENDIX A

A-1 Wing Planform Dimensions A1

1.0 SUMMARY

1.1 GENERAL

Previous NASA/industry advanced-turboprop-propeller and prop-fan studies and wind tunnel tests indicate that point design, installed propulsive efficiencies on the order of 80% at Mach 0.8 are achievable; and that a net reduction of 18% in TSFC could be expected over a comparable, bypass-ratio-six, turbofan-powered airplane. In the absence of any associated penalties, this reduction in TSFC (18%) would result in a net fuel saving of approximately 25% for a twin-engine, 180-passenger, Mach 0.8, commercial transport designed for 3300-km (1800-nmi) range. However, the weight and drag of the prop-fan-powered airplanes were judged to be larger than those of the turbo-fan-powered airplanes. When these penalties were assessed in one study (ref 1), the fuel savings of 25% for the 3300-km (1800-nmi) design range were reduced to 9.7% for the wing-mounted prop-fan and 5.8% for the aft-mounted prop-fan airplanes. This earlier study recommended additional analysis and design to add realism to these preliminary assessments.

This study, implemented in response to one of these recommendations, addresses an approach to the aerodynamic integration of turbo-props and airframes. Both the wing-mounted and aft-mounted prop-fan installations were considered, but emphasis was placed upon the wing-mounted installation as it represented the most difficult task.

Potential flow techniques were employed to study the aerodynamic integration of the prop-fan propulsion concept with the airframe of advanced subsonic commercial transports. Three basic configurations were defined and analyzed:

- A wing-mounted prop-fan at a cruise Mach number of 0.8
- A wing-mounted prop-fan in a low-speed configuration
- An aft-mounted prop-fan at cruise Mach number of 0.8

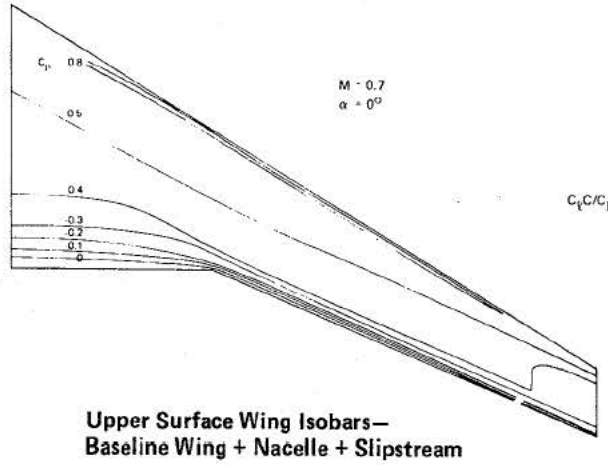
In each case, the propeller slipstream was modeled and its interaction with the configuration calculated.

To minimize aerodynamic interference penalties, the cruise wing of the wing-mounted configuration was redesigned to reproduce or approximate the clean-wing pressure distribution after inclusion of nacelle and slipstream effects.

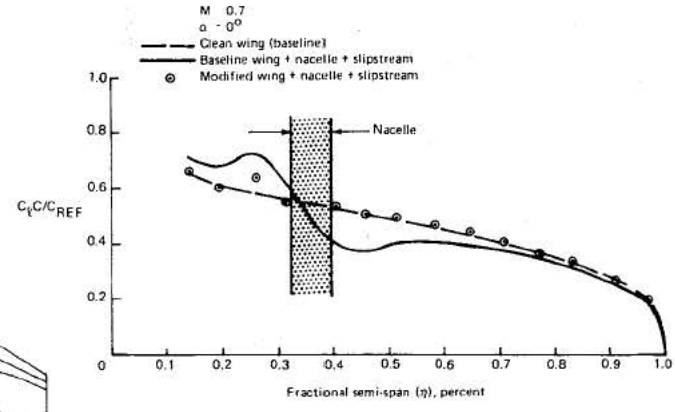
1.2 CONCLUSIONS

This study has demonstrated the feasibility of using potential flow analysis techniques to calculate prop-fan airplane aerodynamics. The study objective of minimizing propeller slipstream effects upon a wing was accomplished (fig. 1). However, the resulting wing was structurally unsatisfactory because of an arbitrary ground rule to hold the leading edge constant, with the remaining wing geometry contoured to reduce or eliminate prop slipstream effects. The resulting wing with sheared front and rear spars would be impractical due to excessive weight penalties, particularly when other solutions would be available with addi-

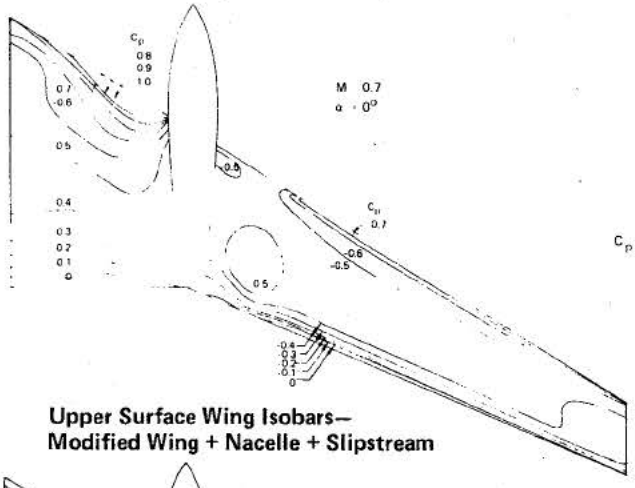
Upper Surface Wing Isobars—
Clean Wing



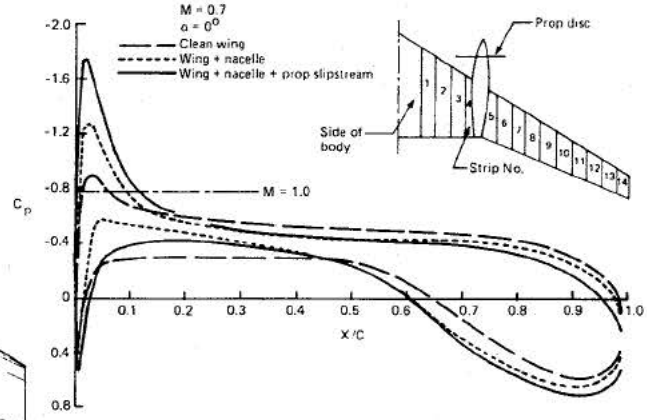
Wing Spanwise Load Distribution



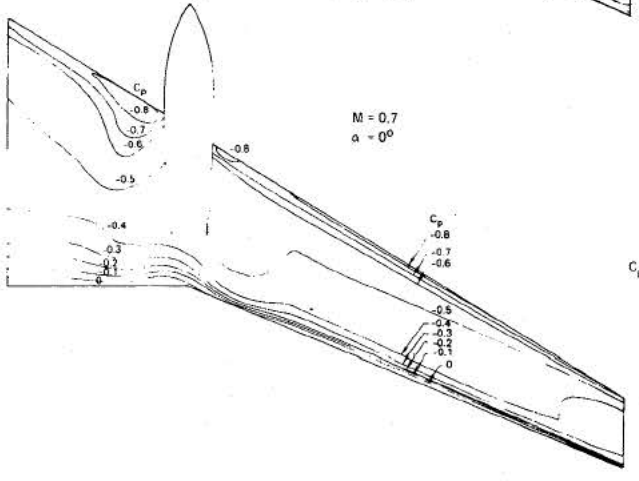
Upper Surface Wing Isobars—
Baseline Wing + Nacelle + Slipstream



Wing Pressure Profiles: Strip 4



Upper Surface Wing Isobars—
Modified Wing + Nacelle + Slipstream



Wing Pressure Profiles: Strip 5

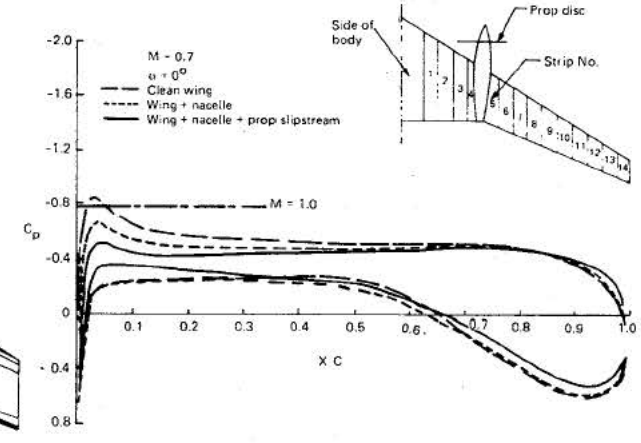


Figure 1. Summary of Study Approach and Results

tional analysis and/or wind tunnel testing. Therefore, wind tunnel testing of the configuration developed by this study is not recommended. Additional studies of alternate means to achieve the same or better aerodynamic results for a practical wing design are needed, and wind tunnel testing should then be done to validate the resulting wing design.

Additional conclusions resulting from this study are discussed in the following paragraphs.

1.2.1 WING-MOUNTED PROP-FAN–HIGHSPEED

- Predicated on the assumption of isentropic flow over the inboard wing, the baseline wing has the potential for recovering up to 50% of the thrust lost due to swirl by de-rotating the slipstream. However, the upwash from the propeller results in high pressure peaks on the upper surface of the inboard wing, a condition that renders the wing susceptible to shock waves, flow separation, high drag, and buffet. This condition could more than offset the potential thrust recovery.

- The wing, modified for minimum cruise drag, generally accomplishes the objective of neutralizing the adverse effects of the slipstream, but in so doing fails to de-rotate the slipstream. The profile drag penalties are mostly eliminated; however, the potential thrust recovery gains are also eliminated.

- The approach taken results in a modified wing that has large variations in twist and thickness and is considered structurally undesirable due to potential manufacturing cost and weight penalties. Alternate approaches for modifying the wing and/or nacelle are recommended for further study.

1.2.2 WING-MOUNTED PROP-FAN–LOW SPEED

- The chordwise velocity increase in the slipstream is the predominant effect at low speed, and is more important than the effect of swirl.

- Large increments in chordwise velocity result in overloading the wing both inboard and outboard of the nacelle.

- A high-lift system designed for achieving high power-off $C_{L_{MAX}}$ does de-rotate the slipstream to some extent and results in partial thrust recovery.

- When considering all-engine slipstream effects, the high-lift condition drag polar is improved because of the large increase in C_L combined with thrust recovery.

- Rolling moment caused by one engine being inoperative is much less than the estimates for the Reference 1 study and does not appear to be a major concern.

1.2.3 AFT-MOUNTED PROP-FAN

- The aft-mounted prop-fan configuration is aerodynamically similar to a comparable turbofan configuration.

- The prop slipstream effects extend beyond the strut to the body and vertical tail and influence the longitudinal cross section area distribution.

- Partial ($\cong$ 10%) thrust recovery resulting from the straightening effect of the strut on the slipstream appears as an increment in strut C_L, rather than a decrement in drag. The opposing tendencies of the wing downwash and the propeller swirl influence the flow about the leading edge of the strut and in turn, the thrust recovery vector.

- Overall, the prop slipstream has little effect on the aerodynamics of the airplane for aftmounted engines as compared to wing-mounted engines.

1.3 RECOMMENDATIONS

This study was directed at applying analytical techniques to minimize propeller slipstream/airplane aerodynamic interference effects and to maximize overall aircraft aerodynamic efficiency during cruise. Potential flow analysis techniques to calculate prop-fan airplane aerodynamics were applied. Additional studies of alternate methods for achieving the same or better results with a more practical wing design are required. Therefore, the following efforts are recommended to ensure a balanced, logical development of prop-fan technology; and ultimately, a convincing evaluation of the economic and energy saving potential for prop-fan propulsion systems.

1.3.1 PROP-FAN/AIRFRAME AERODYNAMIC INTEGRATION

- Develop a cruise wing design that incorporates changes to the planform and leading/trailing edges, but that essentially maintains the structural wing box. This may include changes in local wing sweep, leading- and trailing-edge camber, wing aspect ratio, thickness ratio, and nacelle contouring.

- Determine the influence of the wing on wing propeller environment and aft-mounted propfan installations.

1.3.2 NOISE RADIATION AND ATTENUATION

- These recommendations result from the Reference 1 study.

- Develop a data base and theoretical methods for predicting noise radiation from prop-fans.

- Develop a light-weight structure to attenuate noise at the prop-fan blade passing frequencies.

1.3.3 PROP-FAN MISSIONS AND APPLICATION

- Determine the optimum range and Mach number for a prop-fan airplane.

- Conduct a fully integrated study that includes all technical elements of airplane design.

As indicated, the cruise wing design should incorporate changes to the planform. For example, leading-edge extensions on both sides of the nacelle could effectively reduce the local thickness ratio without reducing the physical wing thickness. This leading-edge extension permits incorporation of local leading-edge camber without distorting the wing structural box. The large suction peaks caused by the swirling slipstream inboard of the nacelle could be mitigated by merely drooping the extended leading-edge. Conversely, the wing leading-edge could be upcambered on the outboard side to compensate for the loss of load on that side. This concept is shown in Figure 2.

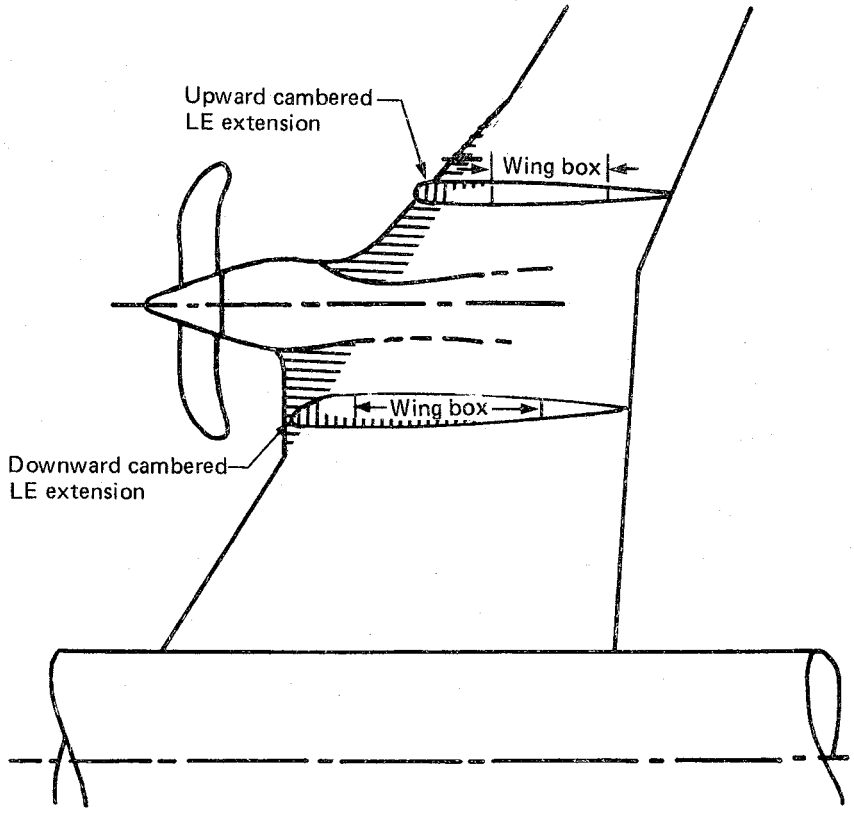


Figure 2. Typical Modification Concept for Prop-Fan Cruise Wing

2.0 INTRODUCTION

2.1 BACKGROUND

Elementary considerations of momentum and energy lead to the conclusion that, in the absence of compensating losses, propulsive efficiency is improved by accelerating more fluid by a smaller velocity increment. Introduction of the high-bypass-ratio turbofan engine stimulated a new generation of transport aircraft by using this principle to reduce fuel consumption without substantially sacrificing the simplicity, reliability, and low maintenance costs that have come to be expected by the airlines since reciprocating engines were replaced by turbojets.

The increase in the relative cost of fuel following the 1973 Arab oil embargo, along with national concern over the need of fuel conservation, have prompted Government and industry to examine possibilities for further reducing aircraft fuel consumption.

A 1976 NASA-sponsored study (ref 1) concluded that modest gains in efficiency could be achieved by pushing turbofan technology further through the application of geared fans, higher overall pressure ratios, and higher turbine inlet temperatures. The same study also noted that the propeller offered more dramatic gains than advanced turbofans if it could be adapted to the Mach 0.75+ cruise speed favored by airframe technology and expected by the traveling public.

The high propulsive efficiency of propellers is difficult to maintain at cruise speeds above Mach 0.7 because:

- The helical-tip Mach number becomes supersonic, and the outer section of the blade incurs increased drag, leading to increased noise and the associated penalties,

  or,

- The rotational speed must be reduced to the point where excessive slipstream swirl necessitates the added weight and complexity of dual rotation.

In 1975, the Hamilton Standard Division of United Technologies Corporation proposed the prop-fan concept. This concept is one in which a slightly supersonic outer blade speed is accepted, and alleviation of increased drag and noise is accomplished by the use of thin and swept-back blade sections. Also, to keep the diameter reasonable while absorbing the very high power required for high-speed transport designs, eight to ten broad blades are used.

Wind tunnel tests conducted by Hamilton Standard and the NASA Lewis Research Center indicate a point-design installed propulsive efficiency of 80% at Mach 0.8 cruise is achievable, and a net reduction of 18% in TSFC over a comparable technology bypass-ratio-six turbofan may be expected.

Study results reported in Reference 1 indicate that this 18% advantage in cruise TSFC for a twin-engine, Mach 0.8 commercial transport designed for 3300-km (1800-nmi) range with

180 passengers could result in a net fuel savings of approximately 25% if there were not compensating penalties. However, both the installation weight and drag penalties of the prop-fan-powered airplanes were judged to be larger than those of the turbo-fan.

When these penalties are assessed, the estimated fuel savings are reduced to 9.7% for the wing-mounted prop-fan airplane and 5.8% for the aft-mounted prop-fan.

Early analysis and design work are necessary to add realism to these assessments and to help guide decisions regarding the development of prop-fan technology.

2.2 STUDY OBJECTIVE AND SCOPE

The objective of the current study is to apply analytical techniques to the problem of the wing and aft-body installation, thus minimizing propeller slipstream/airplane interference, to maximize overall aircraft aerodynamic efficiency in cruise, and to define appropriate high-lift devices for takeoff and landings.

2.2.1 TASK I–WING-MOUNTED PROP-FAN–HIGH SPEED

A "clean" wing of appropriate geometry is defined and analyzed (using a 3-D potential-flow computer program, Boeing A 230) to provide a baseline pressure distribution. The nacelle and slipstream then are added, and the resulting distorted isobar pattern examined to identify problem areas associated with pressure peaks, adverse pressure gradients, and local loss of effective sweepback. Design changes are defined to alleviate these problems, and a revised wing-nacelle geometry analyzed to provide new pressure distribution data for validation of the proposed changes. A wing model for high-speed wing tunnel testing is defined and thrust recovery due to slipstream de-rotation estimated.

2.2.2 TASK II–WING-MOUNTED PROP-FAN–LOW SPEED

Leading- and trailing-edge flap geometry and the fan flow field is examined at takeoff and landing approach flight conditions. Pressures and streamline patterns at the leading edge (with and without slipstream) are computed, and leading-edge devices required to mitigate pressure peaks and to provide reasonable protection from flow separation are defined and analyzed. Probable power-off behavior and requirements for automatic retraction or angle adjustment in case of engine failure are estimated and thrust recovery due to slipstream de-rotation is calculated.

2.2.3 TASK III–AFT–MOUNTED PROP-FAN

Aerodynamic integration of aft-mounted engines poses a completely different set of problems. Most of the requirements constraining the wing do not apply to a strut having only the function of supporting the propulsion pod (and possibly to develop some thrust by removing slipstream swirl). On the other hand, the drag of the aft-body may be sensitive to disturbances caused by the nacelle and propeller because of the thick boundary layer and adverse pressure gradient to be expected there. Potential flow methods are used to compute pressure distributions and streamline paths.

3.0 ABBREVIATIONS AND SYMBOLS

A	Cross sectional area
b_{REF}	Reference span
C	Chord
C_D	Drag coefficient
C_{D_i}	Induced drag coefficient
C_{D_p}	Profile drag coefficient
C_k	Krueger flap chord
C_ℓ	Lift coefficient per unit span
C_L	Lift coefficient
$C_{L_{MAX}}$	Maximum lift coefficient
C_{MX}	Rolling moment coefficient
C_p	Pressure coefficient
$C_{p_{MIN}}$	Minimum pressure coefficient
C_{REF}	Reference chord
D	Propeller diameter
G	Geometry
G_F	Error-free initial geometry
G_0	Clean-wing initial geometry
LE	Leading edge
M	Local Mach number
MAC	Mean aerodynamic chord
M_∞	Freestream Mach number
n	Unit normal
nmi	Nautical mile
p(r)	Static pressure at radius r
p_∞	Static pressure at infinity
P(r)	Total pressure at radius r
P_0	Total pressure at infinity
q	Dynamic head
r	Radial distance
R	Propeller radius
S	Arc length
S/C	Arc length from leading edge/chord
SHP	Shaft horsepower

T	Thrust
TE	Trailing edge
t/c	Thickness ratio
TSFC	Thrust specific fuel consumption
U_∞	Freestream velocity
V	Local velocity
V_n	Normal velocity component
V_{PROP}	Slipstream perturbation velocity
V_t	Tangential velocity component
V_x	Axial velocity
w/U	Uniform cross-flow
W	Vertical component of velocity vector
WBL	Wing buttock line
WL	Water line
X,Y,Z	Cartesian coordinates
α	Angle-of-attack
δ	Swirl angle
δ_F	Trailing-edge flap deflection
δ_K	Krueger flap deflection
Δ	Incremental quantity
η	Fractional semispan
θ	Wing twist
γ	Ratio of specific heats for air

4.0 ANALYSIS AND DESIGN METHODS

Three-dimensional potential flow techniques have been in use for many years for analysis and design of complex aerodynamic configurations. These techniques have been found to be adequate even though local patches of supersonic flow and shock waves at high subsonic Mach numbers are not simulated. Consistent with current design practices, this analysis was conducted at Mach 0.7.

4.1 COMPUTER PROGRAM A 230 DESCRIPTION

The Boeing-developed computer program A 230 (ref 2) is a general boundary-value problem solver that uses source and doublet panels distributed on the configuration boundary surfaces and internally. The flow field over the configuration is determined by a computational routine, which calculates the strengths of the sources and doublets that produce a flow field satisfying the boundary conditions. Each boundary condition statement consists of the following specifications:

- Spacial coordinates of the boundary point
- Direction cosines of a unit vector
- The desired velocity component along the unit vector

For a general impermeable surface, the boundary point is positioned at the panel centroid, with the unit vector directed normal to the panel. The condition of zero velocity along the normal vector produces a flow that is parallel to the surface. This type of boundary condition is provided automatically by the program and requires no input from the user. However, if a nonzero velocity component is specified along the unit normal vector, problems such as controlling the inflow distribution into a simulated fan face may be formulated. This option has been exercised in the present study to represent the interaction of the slipstream with the configuration without actually generating the swirling flow behind the propeller.

4.2 ANALYSIS USING SLIPSTREAM AND PRE- AND POST-PROCESSORS

The methodology for inclusion of the prop slipstream in the three-dimensional, potential-flow analysis model is presented in this section. The swirling flow behind the propeller disc, impinging on the surface of the configuration is simulated mathematically through a restatement of the boundary conditions at those boundary points that are washed by the wake. The obtained solution is corrected to ensure satisfaction of the tangency condition at all points in the presence of the slipstream.

The boundary conditions underlying the potential flow problem are described schematically in Figure 3. The slipstream perturbation velocity (V_{PROP}) is resolved into a normal (V_n) and tangential (V_t) component to the local panel. The boundary condition at the panel center is expressed as:

$$V.\, n = -V_n$$

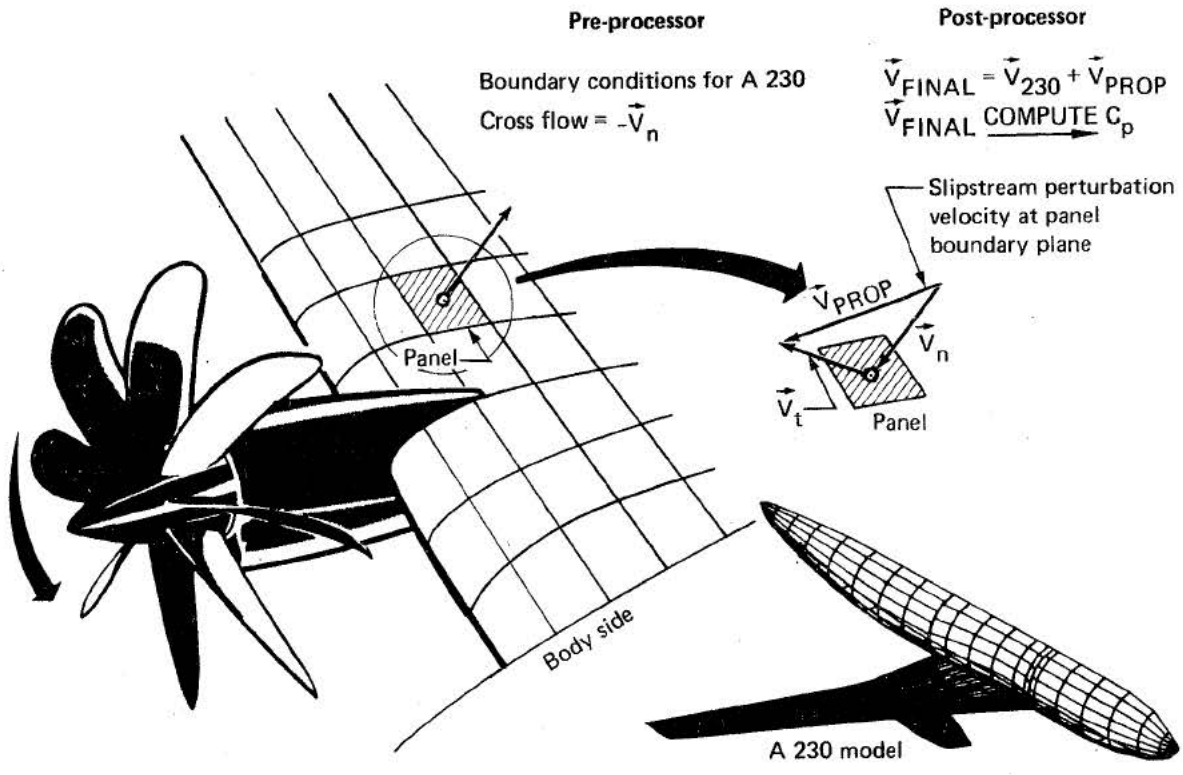


Figure 3. Technique for Modeling Prop Slipstream

The requirement that there be a normal flow through the surface of magnitude $-V_n$ is equivalent to requiring the local singularity strength to oppose V_{PROP}, had the latter been generated by an appropriate distribution of singularities in the flow field. Post-solution addition of V_{PROP} to the local velocity vector ensures satisfaction of the tangency condition and yields the effect of the slipstream on the configuration.

A pre- and post-processor computer program has been developed to handle the boundary value problem described above. In the pre-processor section, the slipstream velocity vector V_{PROP} is generated from swirl angle and total pressure data aft of the propeller (see derivation in Section 5.0). This vector (V_{PROP}) is then resolved normal to the configuration panels within reach of the wake. The normal velocity ($-V_n$) is generated and entered (as the boundary condition) into potential flow program A 230. A solution is obtained and the post-processor then is called upon to:

1. Regenerate the slipstream velocity vector V_{PROP} at all affected boundary points
2. Vectorially add V_{PROP} to the velocity vector arising from the potential flow solution
3. Recompute pressure coefficient, C_p
4. Integrate the pressures for forces and moments on a column-by-column basis

This technique described above can be used to superimpose any velocity field on a boundary value problem. An example is given in Figure 4 for the flow over a stub wing at an angle of attack, $\alpha = 5^{o}$. The solution obtained superimposes a uniform cross-flow of magnitude $w/U = \tan \alpha$ to the configuration at $\alpha = 0^{o}$. The excellent agreement with the exact solution at $\alpha = 5^{o}$ supports applicability of the method.

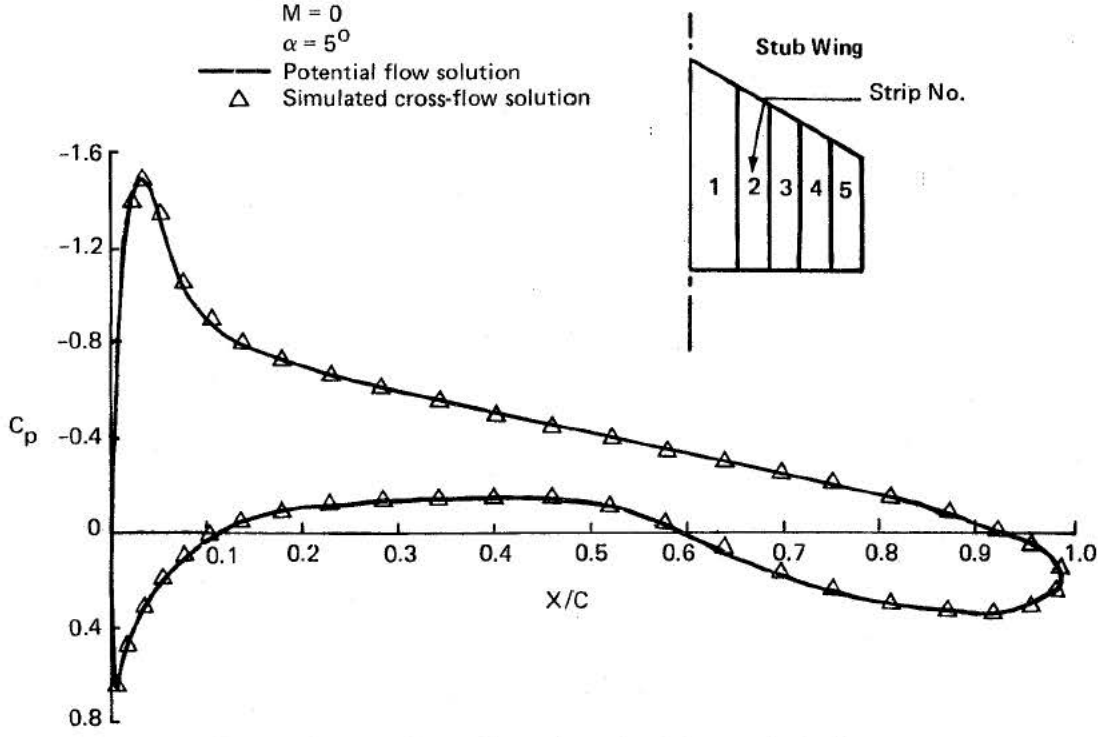


Figure 4. Test Case—Flow Over Stub Wing: Strip 2

4.3 DESCRIPTION OF COMPUTER PROGRAM A 236

The Boeing A 236 computer program (ref 3) is a design-analysis-optimization program, which has been used in the present study to redesign the baseline wing of the wing-mounted prop-fan. In the design mode, A 236 calculates the wing geometry required to support a specified pressure distribution. To achieve design capabilities, a number of limitations were

imposed upon A 236, as compared with the more general program, A 230. The variations between these two programs are:

	A 230	A 236
1.	Analysis only	Analysis, design, and optimization
2.	Accepts general configurations of any shape	Accepts wing/body only
3.	Exact boundary conditions (applied on surface)	Linearized wing boundary conditions (applied on wing design plane, exact boundary conditions on body
4.	Lifting surfaces treated as a whole	Wing split into camber and thickness
5.	Paneling external to program	Automatic paneling provided

Features of A 236 include:

- It handles wing/body configurations only. The wing may be designed in the presence of the body, but nacelle and slipstream are excluded.
- Linearized boundary conditions are applied on the wing design plane, eliminating the need to estimate the initial geometry when designing the wing.
- Wing camber and thickness are treated separately and their effects are superimposed. This is a necessary limitation of the linear theory.
- Since only wing/body configurations are admissible into A 236, automatic paneling is provided. The wing is considered flat and is paneled over its planform.

4.4 DESIGN METHOD

The problem of redesigning the baseline wing of the wing-mounted prop-fan for favorable interaction with the slipstream was as follows:

"Find the wing geometry which, in the presence of the nacelle and slipstream will support the pressure distribution of the clean wing". Because the nacelle and slipstream could not be modeled on the design program A 236, a scheme employing both programs A 230 and A 236 was devised (fig. 5). The clean wing-body configuration was analyzed on A 236, resulting in the pressure distribution, C_{p_I} (only one wing section is used for illustration in the figure). The increment C_p of the nacelle-slipstream over the clean wing, calculated by A 230, was then subtracted from C_{P_I} to produce $C_{P_{II}}$, thus:

$$C_{pII} = C_{pI} - \Delta C_p$$

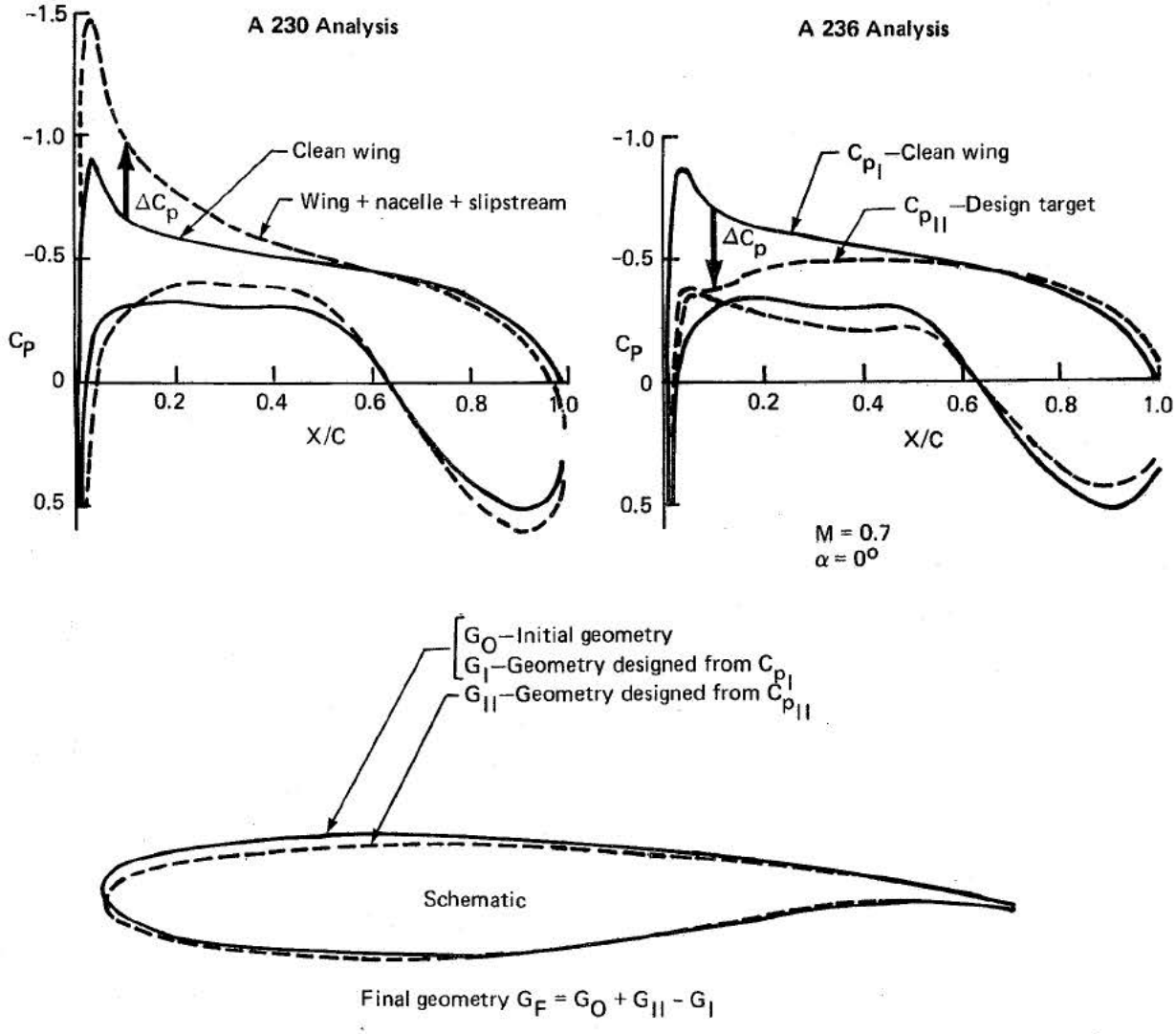


Figure 5. Prop-Fan Wing Design Technique

In an attempt to eliminate errors inherent in the solution of the design problem, two design runs were executed on A 236; one for C_{pI} and another for C_{pII}. The resulting wing geometries are symbolically denoted G_I and G_{II}, respectively in the figure. The final wing geometry was then calculated from:

$$G_F = G_O + G_{II} - G_I$$

where G_O is the initial geometry of the clean wing. $G_I - G_O$ represents the error attributable to the lack of reversibility in the analysis-design-analysis cycle on A 236. By subtracting it from G_{II}, an error-free final geometry (G_F) is obtained.

Figure 6 shows a comparison of baseline and redesigned wing sections on the two sides of the nacelle. Large changes in twist, thickness, and airfoil shape are evident as a result of the design exercise. Figure 7 defines the twist distribution of the baseline and modified wings. A twist increment of approximately $+6^{o}$ outboard and -5^{o} inboard of the nacelle appears to be almost equal and opposite to the swirl angles at cruise stated in Section 5.0. The wing thickness distribution of the baseline and modified wings is shown in Figure 8. As a result of this design exercise, the maximum wing thickness ratio has been reduced by 18% inboard and by 10% outboard of the nacelle.

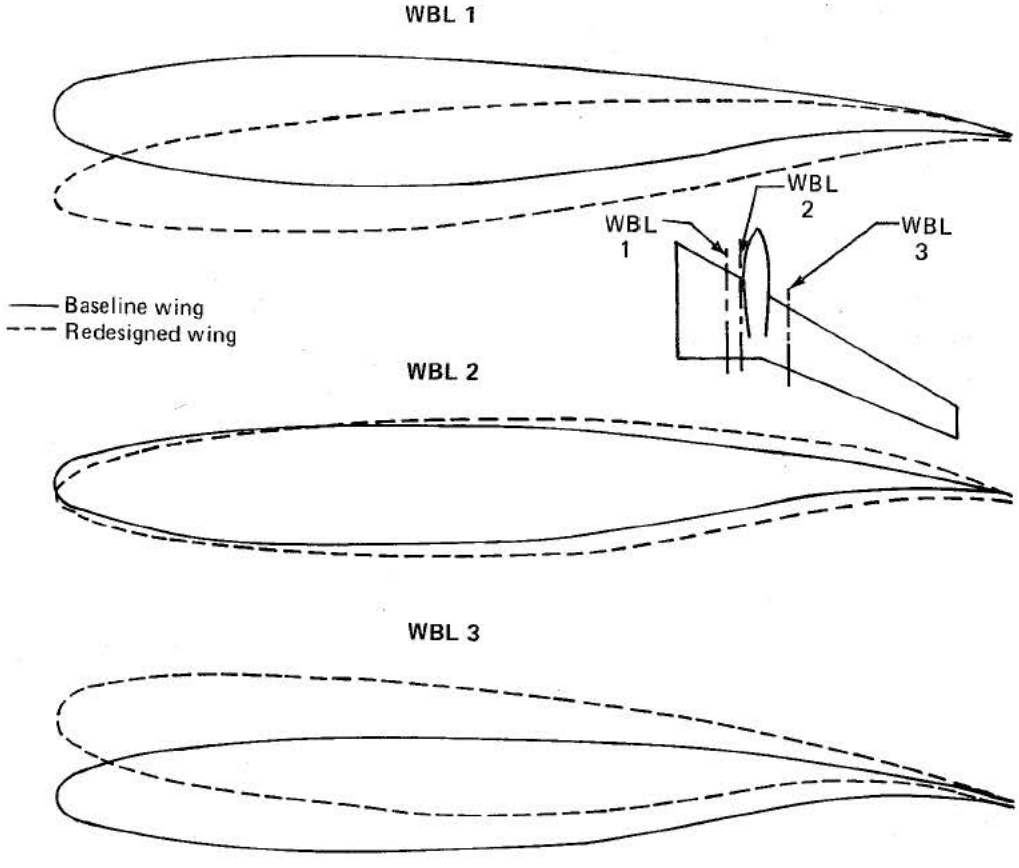


Figure 6. Cruise Wing Geometry

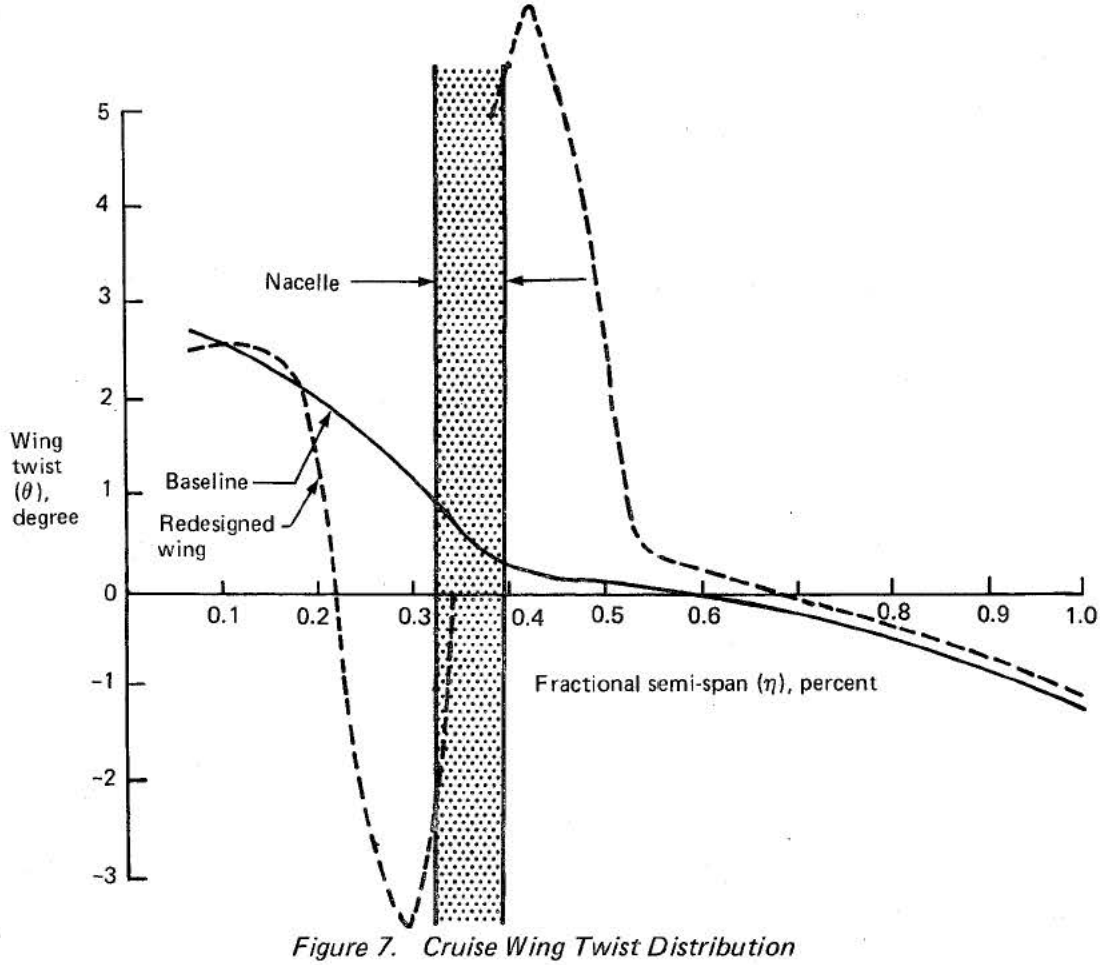


Figure 7. Cruise Wing Twist Distribution

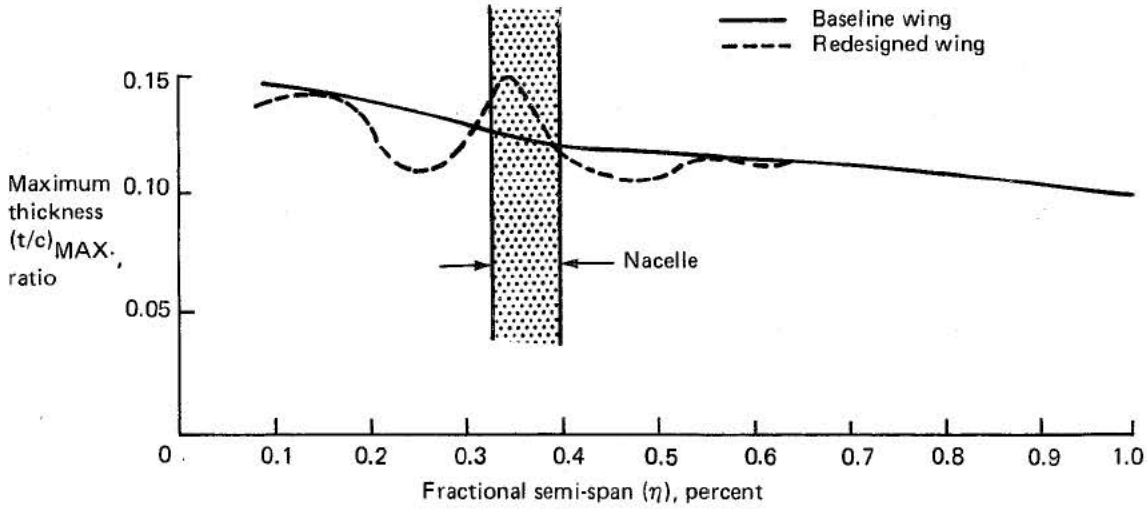


Figure 8. Cruise Wing Thickness Distribution

5.0 WING-MOUNTED PROP-FAN–CRUISE

5.1 CONFIGURATION AND FLIGHT CONDITIONS

Potential-flow analysis of the wing-mounted prop-fan in a cruise configuration is presented in this section. The analysis was carried out on the Boeing A 230 general potential flow computer system (Section 4.0) at values of α from -3° to $+3^{\circ}$, and at 0.7 freestream Mach number. Several configurations comprising wing, body, nacelle and slipstream were modeled and analyzed in a systematic buildup toward achieving a broad understanding of the phenomena involved. The baseline wing employed in the study was essentially that of a twin-turbofan airplane meeting similar requirements and available from previous Boeing studies. This wing was subsequently redesigned, using the method described in Section 4.0, with the objective of achieving the clean wing pressure distribution in the presence of the nacelle and slipstream. Figures 9 and 10 show the paneling arrangement for the clean wing and the

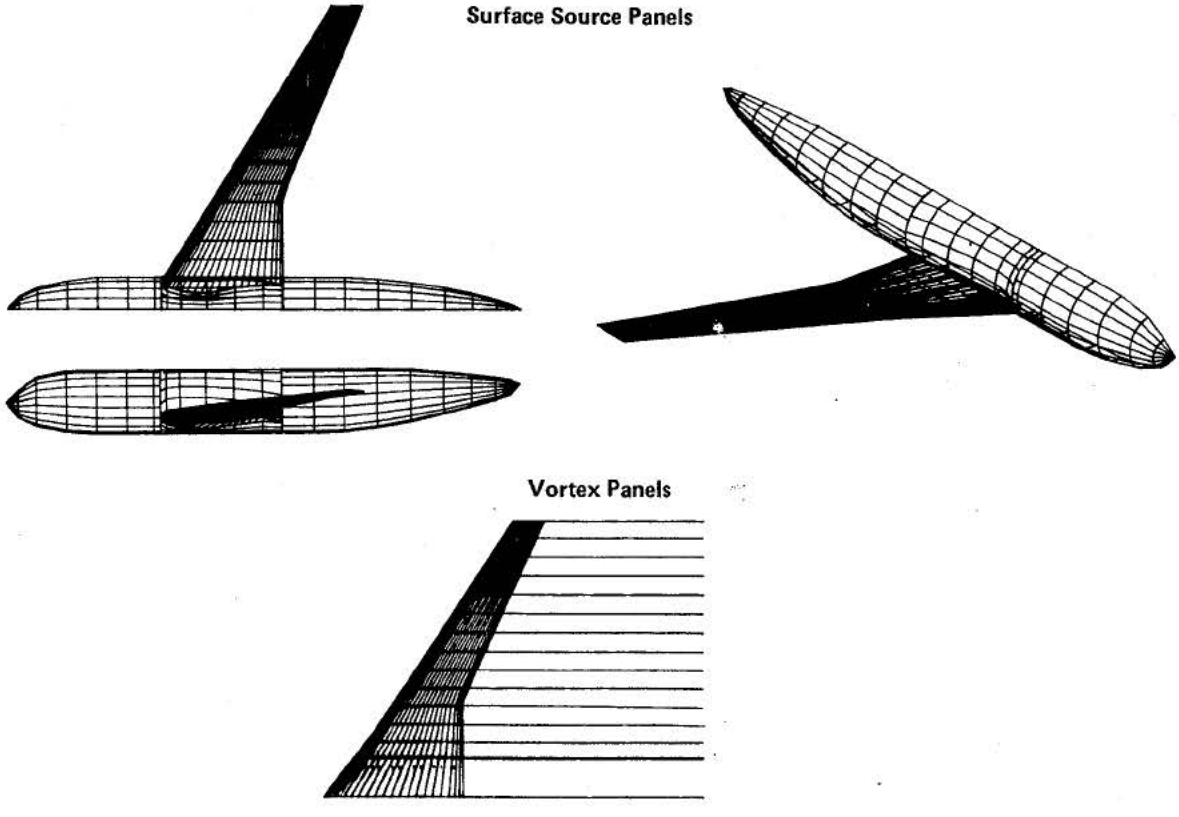


Figure 9. Baseline Wing Body Model

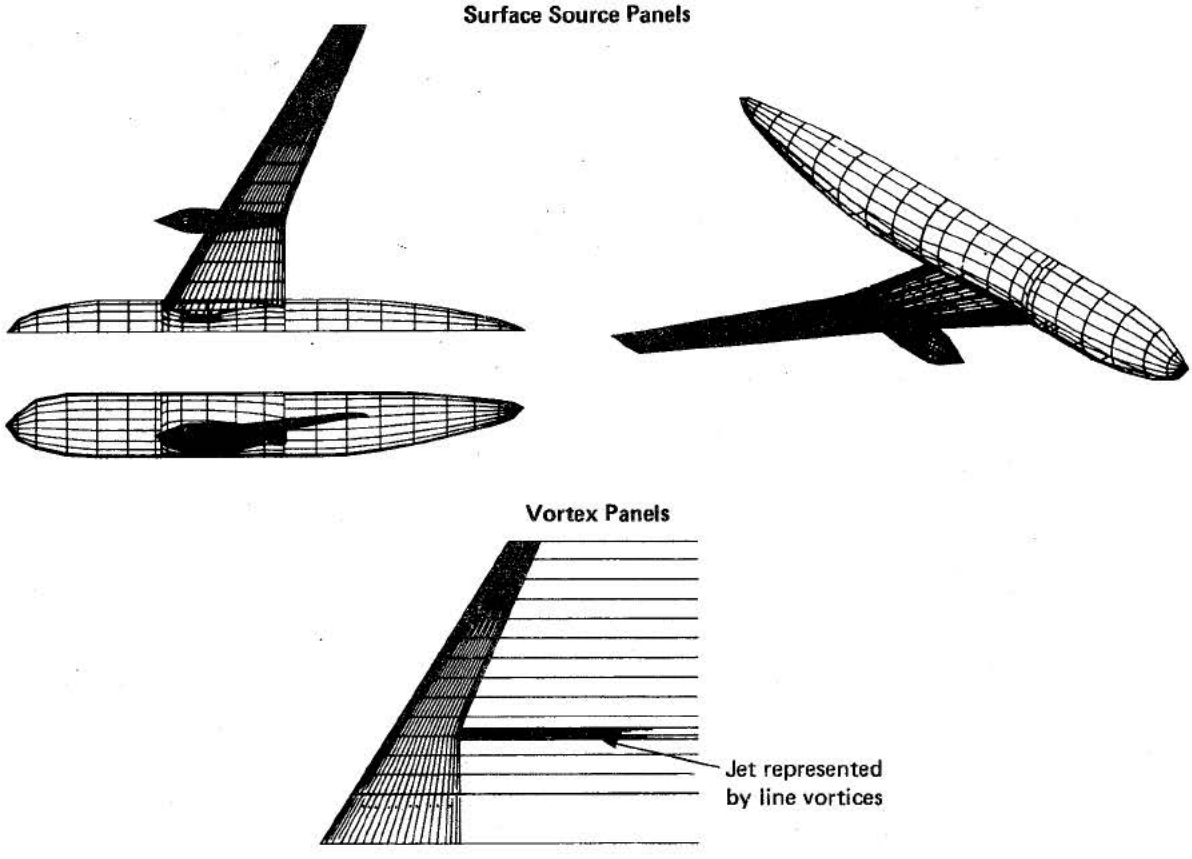


Figure 10. Baseline Wing Body/Nacelle Model

wing plus nacelle, respectively, as defined for potential flow analysis. In each case, the wing has been subdivided into 14 strips having 48 source panels each. The modified wing-nacelle-body configuration is shown in Figures 11 and 12. Definition of the baseline and modified wings is given in Appendix A. Sharp discontinuities in twist and thickness across the nacelle make this wing structurally undesirable. For this reason, although wind tunnel testing to validate the theory and to assess the extent to which the design objectives were achieved could be conducted, they are not recommended for this wing geometry, Instead, further research to define a more realistic wing geometry is recommended.

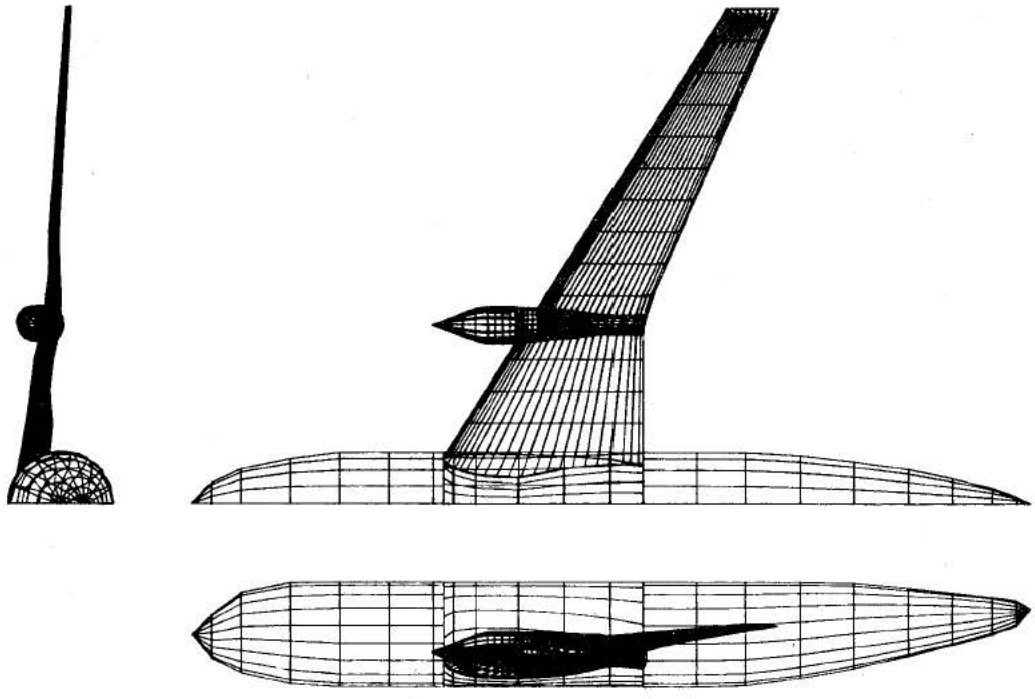


Figure 11. Paneling of Modified Cruise Wing

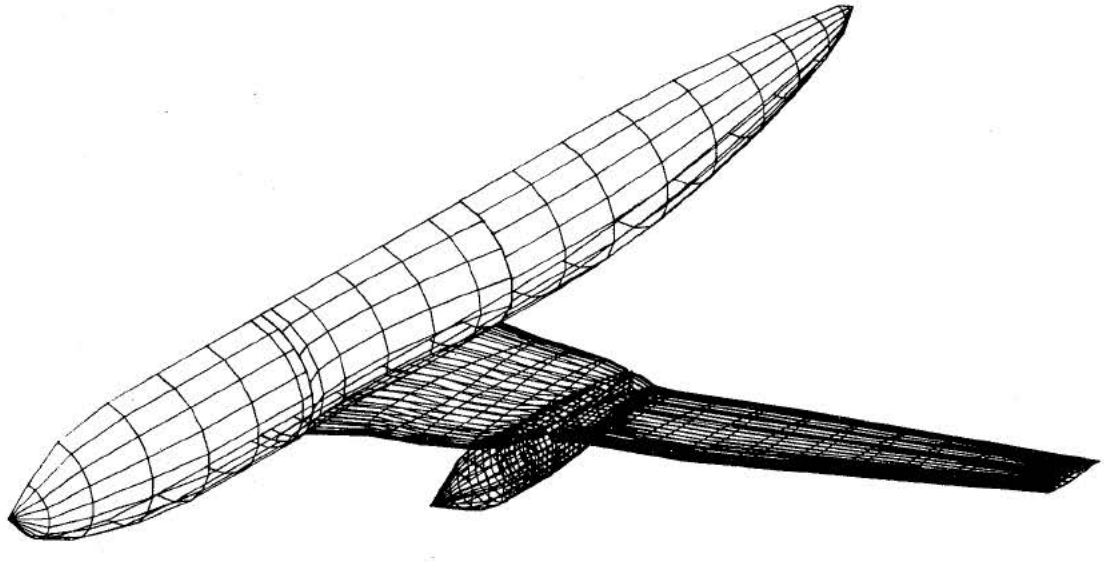


Figure 12. Modified Cruise Wing

5.2 SLIPSTREAM CHARACTERISTICS

Figure 13 presents a comparison of the measured and calculated total pressure ratios and swirl angles along the blade radius as stated by Hamilton Standard in reference 4. The measured data, taken one blade chord behind the propeller, indicated that the root sections were overloaded and the top portions were underloaded compared to the design objectives. Because further refinements were contemplated by Hamilton Standard to achieve the design objectives, the theoretical distribution was selected for inclusion in the potential flow model.

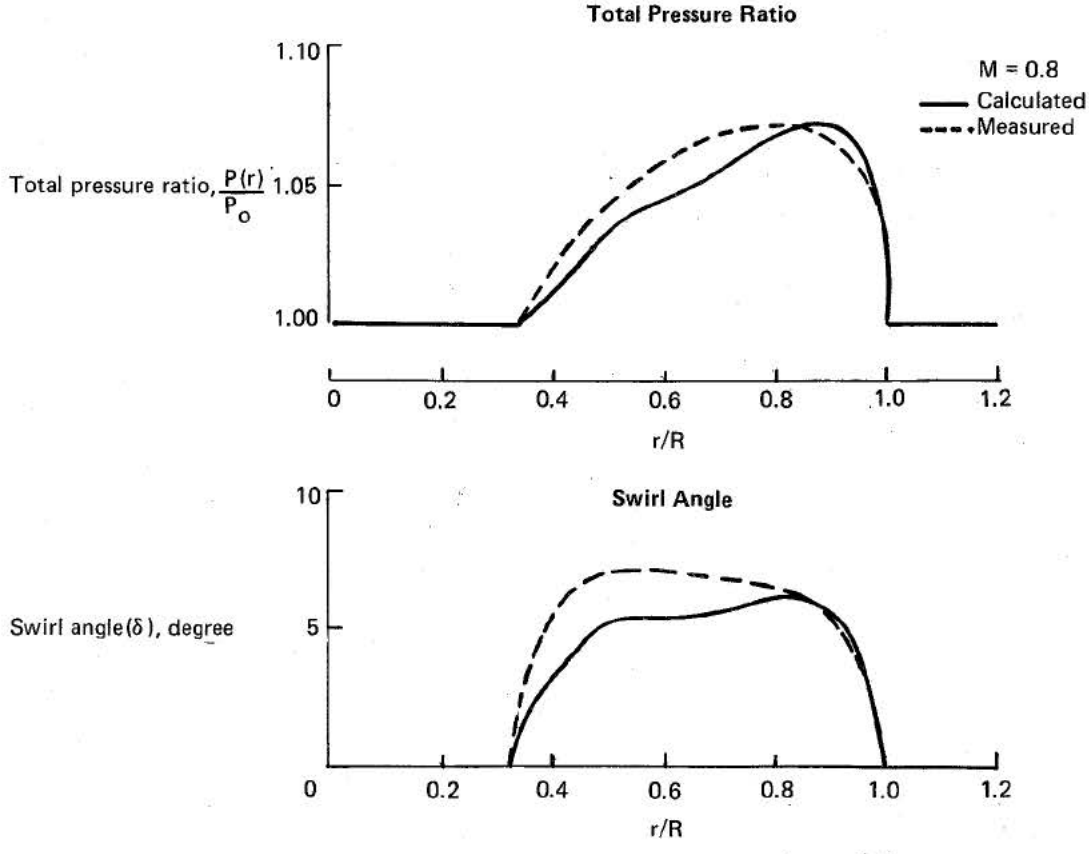


Figure 13. Radial Distribution of Swirl and Total Pressure in Prop Slipstream

The magnitude of the velocity vector V(r) in the propeller slipstream is isentropically related to the total pressure ratio $P(r)/P_O$ as follows:

$$\frac{V(r)}{U_\infty} = \frac{1}{M_\infty}\left[\left(\frac{P(r)}{P_O}\right)^{\frac{\gamma-1}{\gamma}}\left(\frac{2}{\gamma-1} + M_\infty^2\right) - \frac{2}{\gamma-1}\right]^{1/2}$$

with the assumption that the local static pressure is constant: $p(r) = p$

The axial velocity component, V_X/U_∞ is determined from V(r) and the swirl angle $\delta(r)$ thus,

$$\frac{V_X}{U_\infty} = \frac{V(r)}{U_\infty} \cos \delta(r)$$

The pressure coefficient is calculated from:

$$C_p = \frac{\left[1 + \frac{\gamma - 1}{2} M_\infty^2 \left(1 - \frac{V(r)^2}{U_\infty^2}\right)\right]^{\frac{\gamma}{\gamma - 1}} - 1}{\frac{\gamma}{2} M_\infty^2} + \frac{\Delta P(r)}{q}$$

where q is the dynamic head and $\Delta P(r)/a$ is a correction term to account for the change in total head across the propeller disc. It is given by:

$$\frac{\Delta P(r)}{q} = \left(\frac{P(r)}{P_o} - 1\right) \frac{\left[1 + \frac{\gamma - 1}{2} M_\infty^2\right]^{\frac{\gamma}{\gamma - 1}}}{\frac{\gamma}{2} M_\infty^2}$$

The above formulation has been used for all potential flow calculations in the present document.

5.3 PRESSURE COEFFICIENT DATA

Pressure profiles for the baseline wing on the two sides of the nacelle are shown in Figures 14 through 17. On the inboard side (strips 3 and 4), the effect of the nacelle is to increase the supervelocities on both upper and lower surfaces. This is equivalent to an increased-thickness effect. The propeller slipstream induces a local upwash which further aggravates the upper surface pressure peaks. Local Mach numbers of up to 1.5, corresponding to a freestream Mach number of 0.7, have been calculated. It is thus postulated that severe penalties in drag may be incurred as a result of shock formation on the inboard wing. On the outboard side of the nacelle (strips 4 and 5), both the nacelle and the slipstream contribute to unloading the local wing sections. The nacelle produces a diminished-thickness effect, whereas the swirl reduces the effective local incidence.

Pressure profiles for the modified wing are compared with the baseline profiles in Figures 18 through 21. These figures indicate that, to a large extent, the design objective of achieving the clean wing pressure distribution has been attained. The design procedure (outlined in Section 4.0) necessitated changes in the wing twist, thickness, and airfoil shape and was limited to a single design cycle.

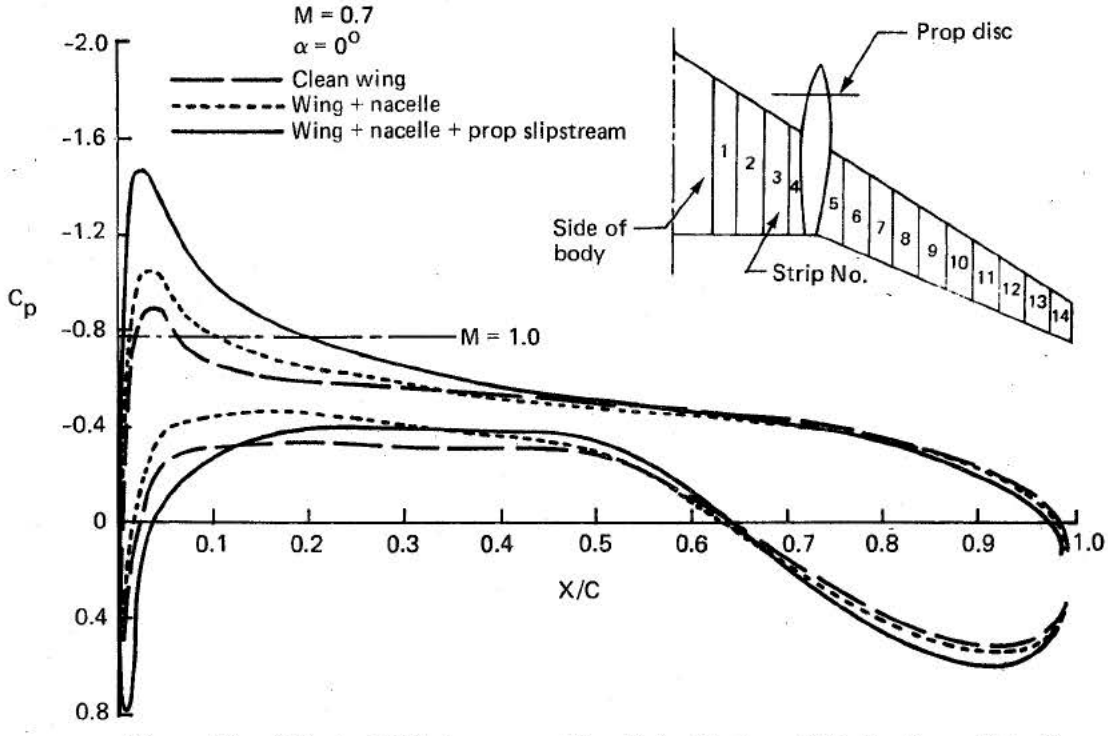


Figure 14. Effect of Slipstream on Chordwise Pressure Distribution: Strip 3

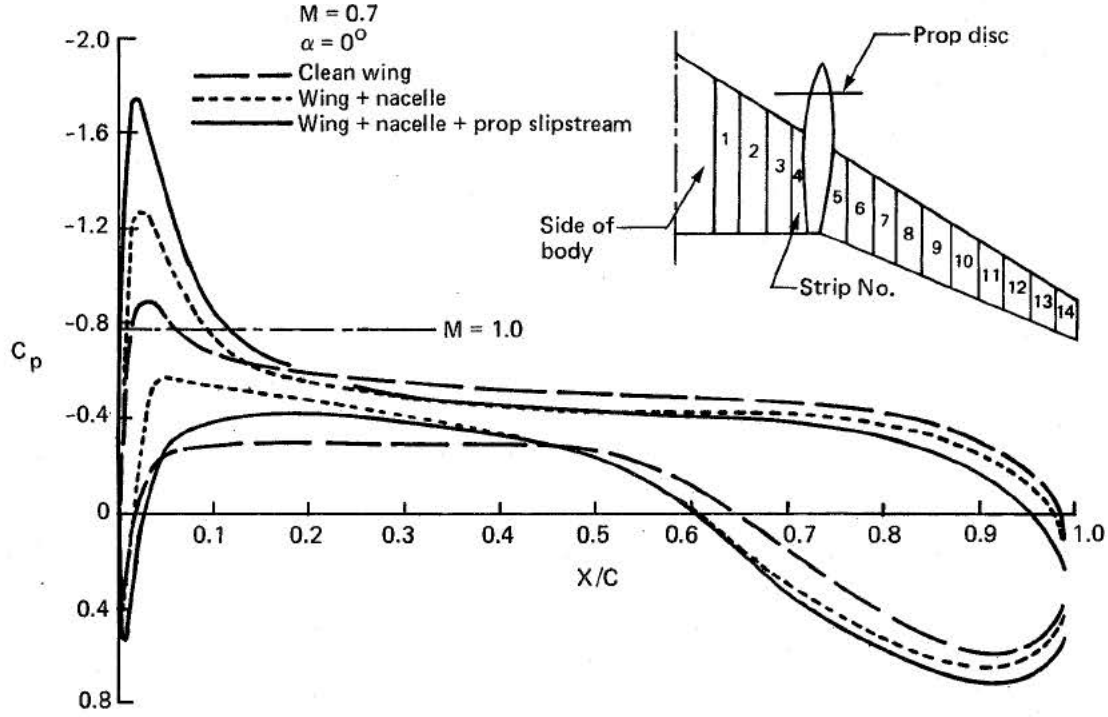


Figure 15. Effect of Slipstream on Chordwise Pressure Distribution: Strip 4

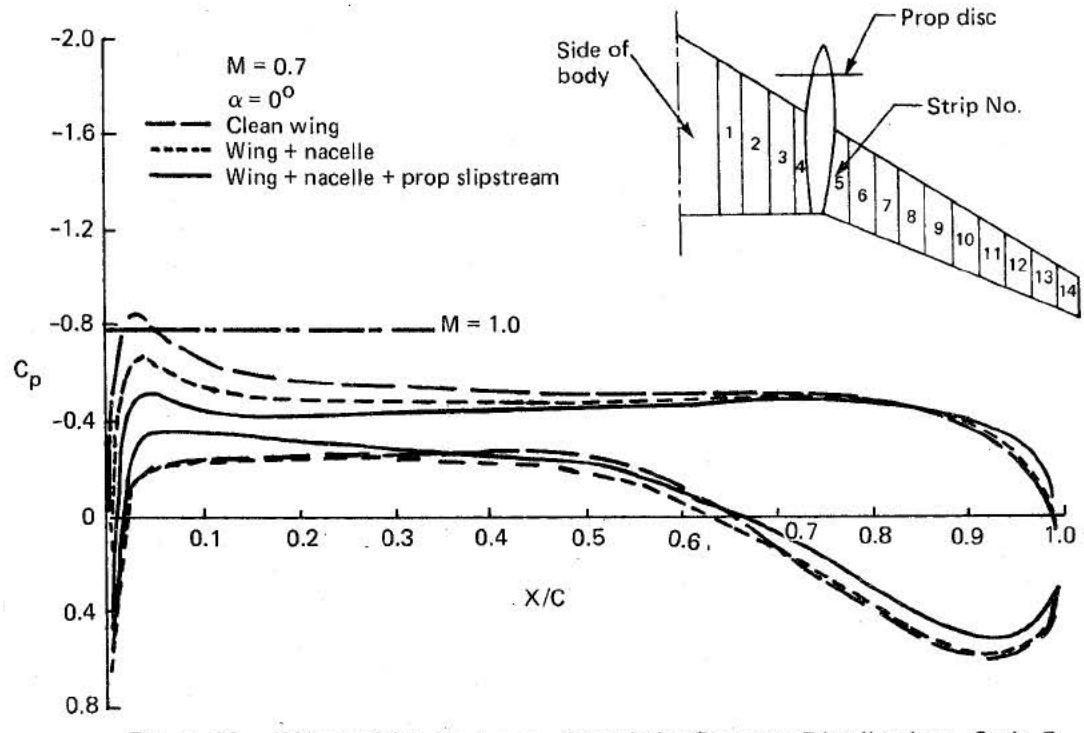


Figure 16. Effect of Slipstream on Chordwise Pressure Distribution: Strip 5

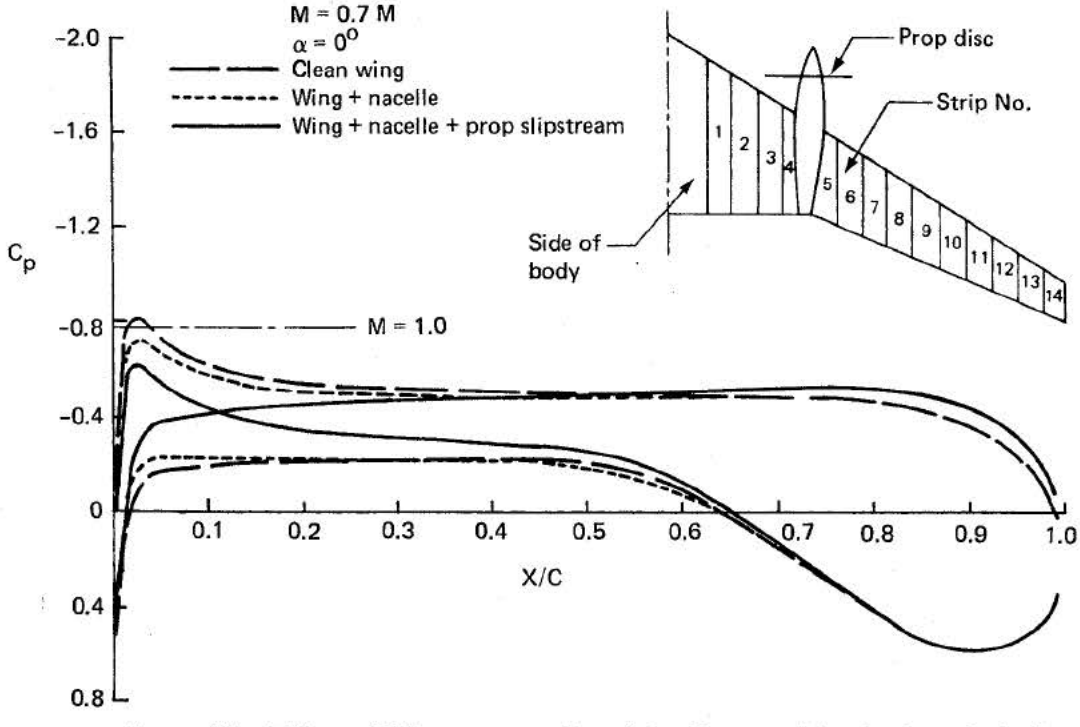


Figure 17. Effect of Slipstream on Chordwise Pressure Distribution: Strip 6

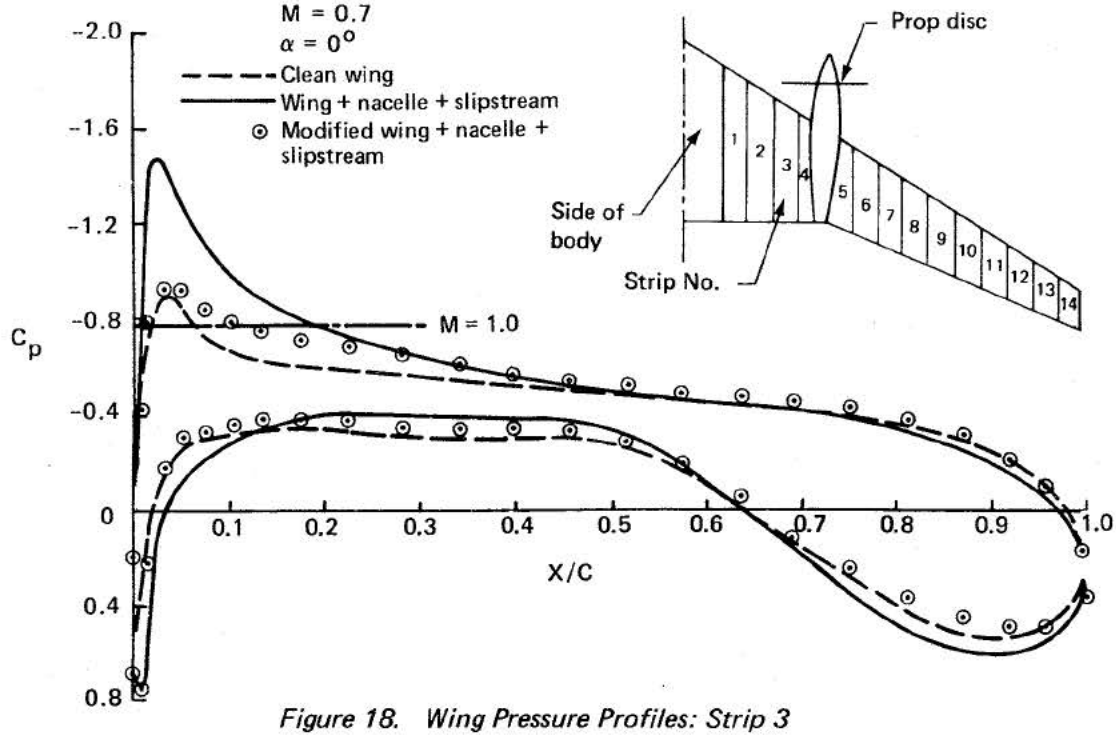


Figure 18. Wing Pressure Profiles: Strip 3

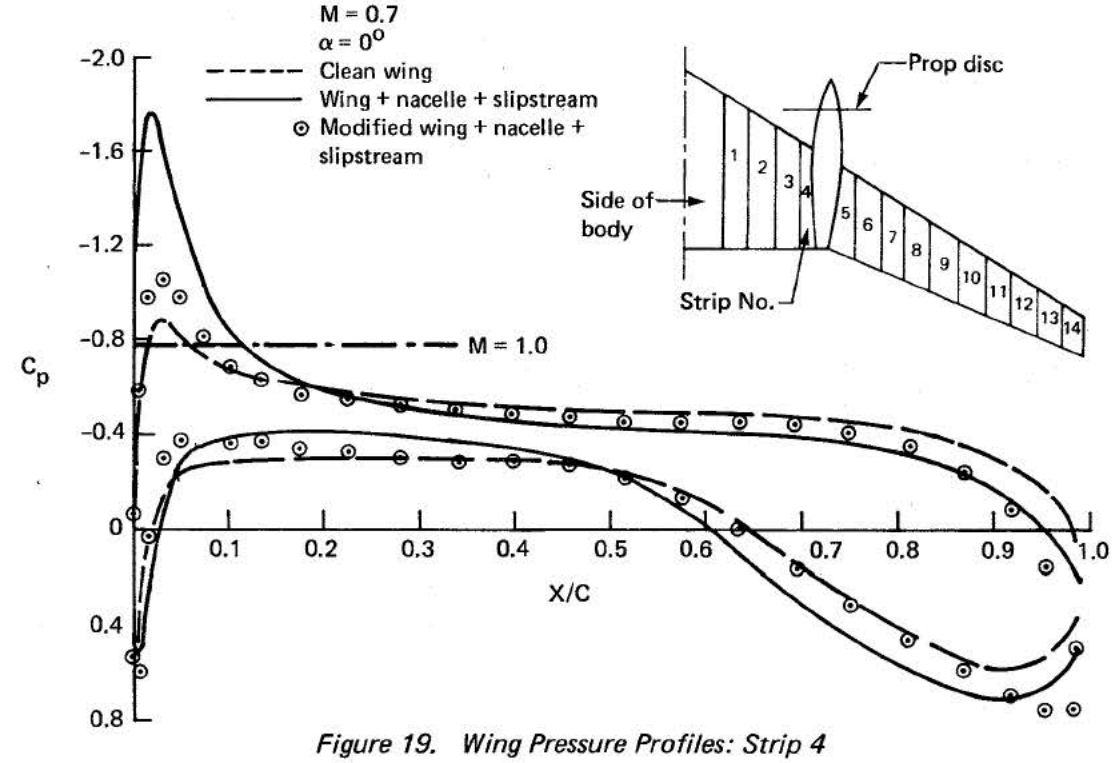


Figure 19. Wing Pressure Profiles: Strip 4

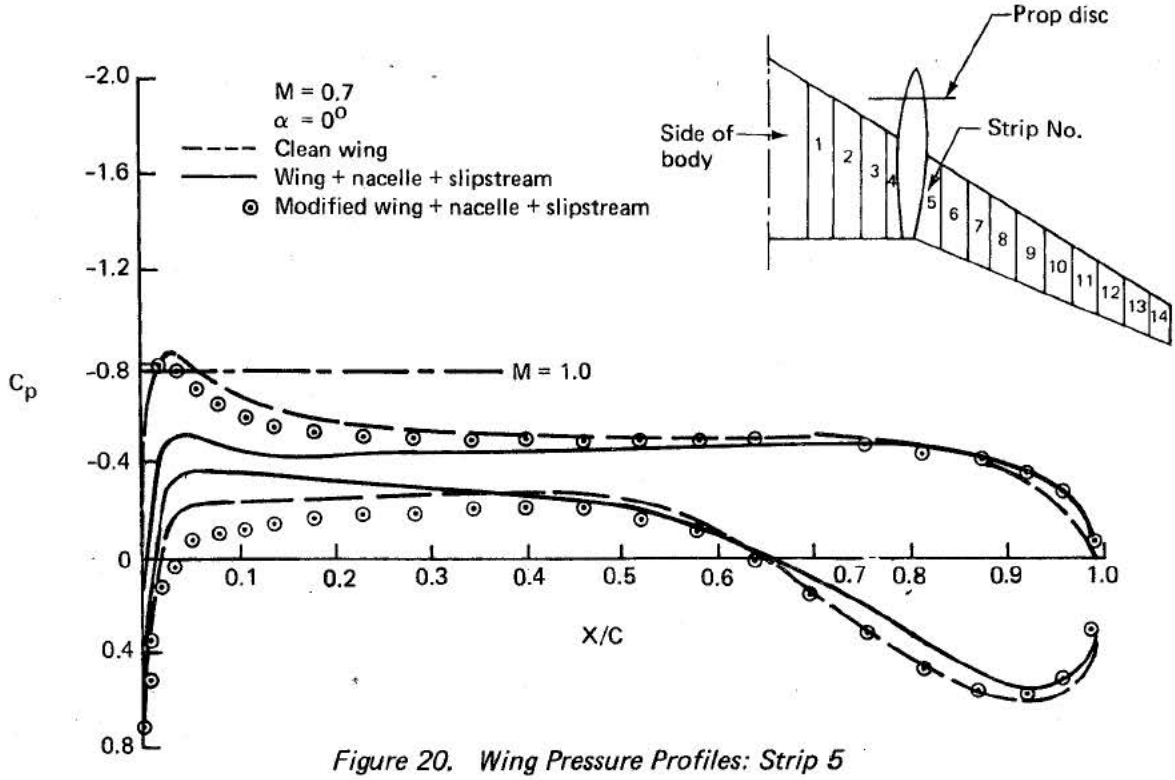


Figure 20. Wing Pressure Profiles: Strip 5

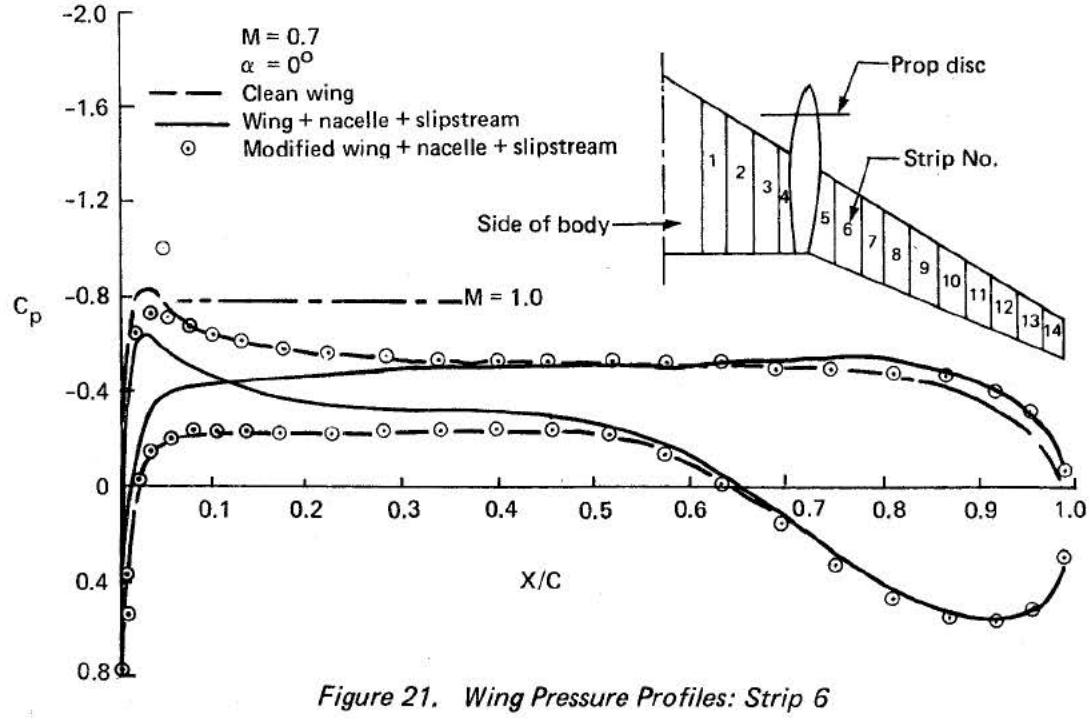


Figure 21. Wing Pressure Profiles: Strip 6

5.4 WING ISOBARS

Wing upper surface isobars for the baseline and modified wings are presented in Figures 22 through 25. The effect of the nacelle alone (fig. 23) is to disrupt the isobar pattern near the wing leading edge. Increased suction peaks inboard of the nacelle, which die out near the side of the body, appear as elongated puddles. The effect of the swirl (fig. 24) is to further increase the suction peaks inboard of the nacelle and to cause puddling of the isobars on the outboard side.

The modified wing (fig. 25) exhibits an outboard isobar pattern similar to that of the clean wing. Inboard, the isobar pattern reveals the presence of suction peaks higher than those of the clean wing that have not been fully mitigated through the design exercise.

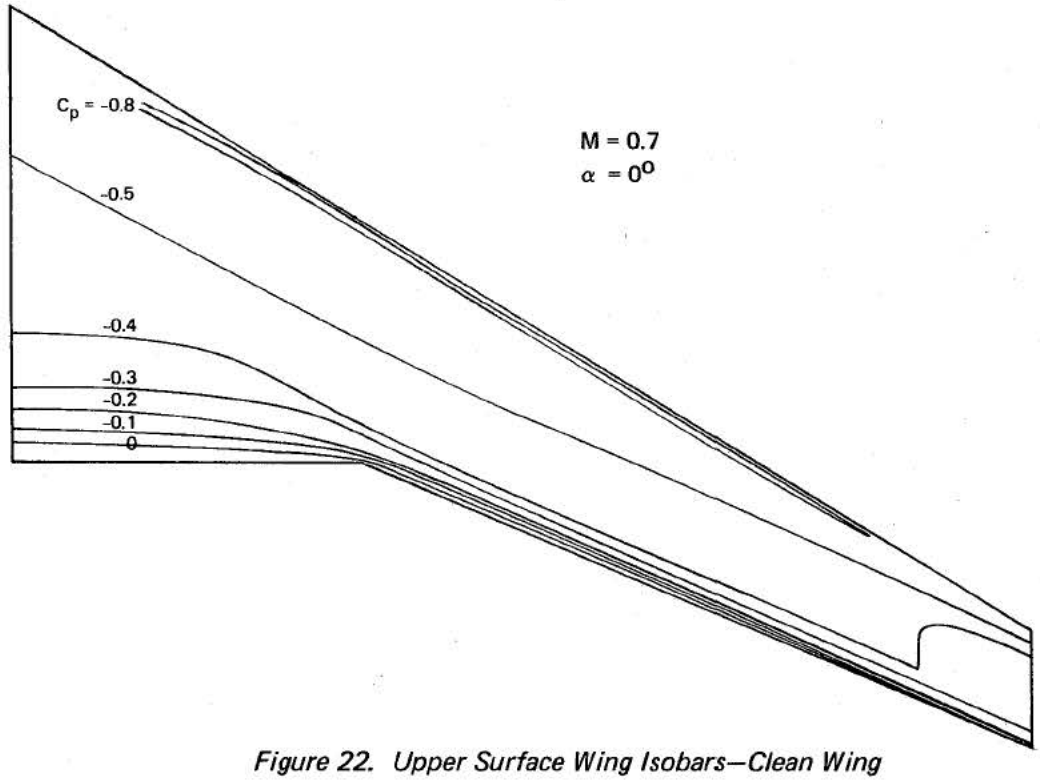


Figure 22. Upper Surface Wing Isobars—Clean Wing

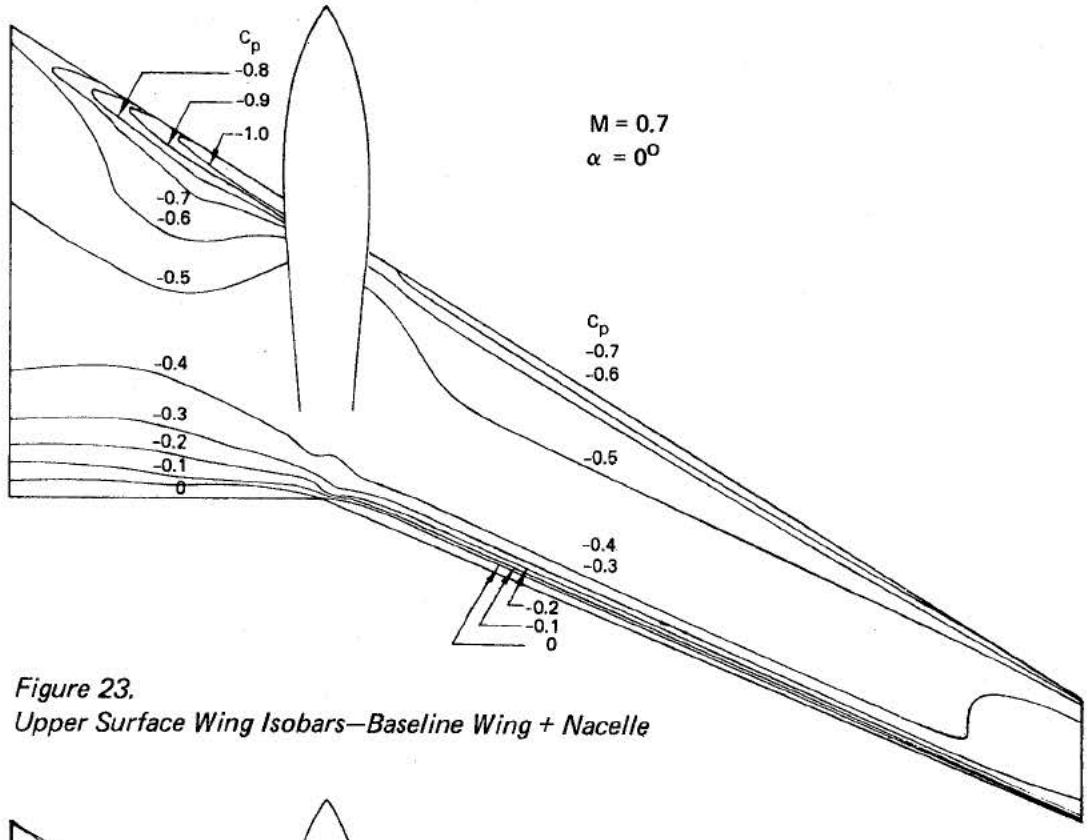


Figure 23.
Upper Surface Wing Isobars—Baseline Wing + Nacelle

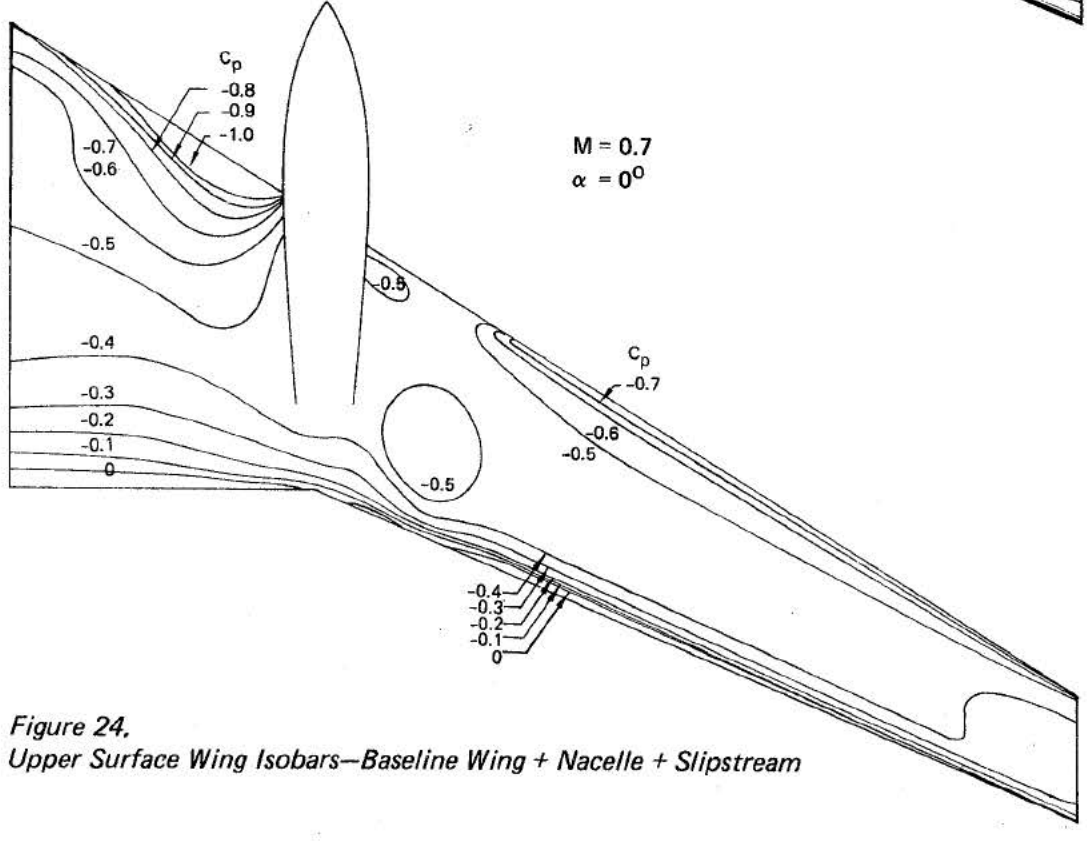


Figure 24.
Upper Surface Wing Isobars—Baseline Wing + Nacelle + Slipstream

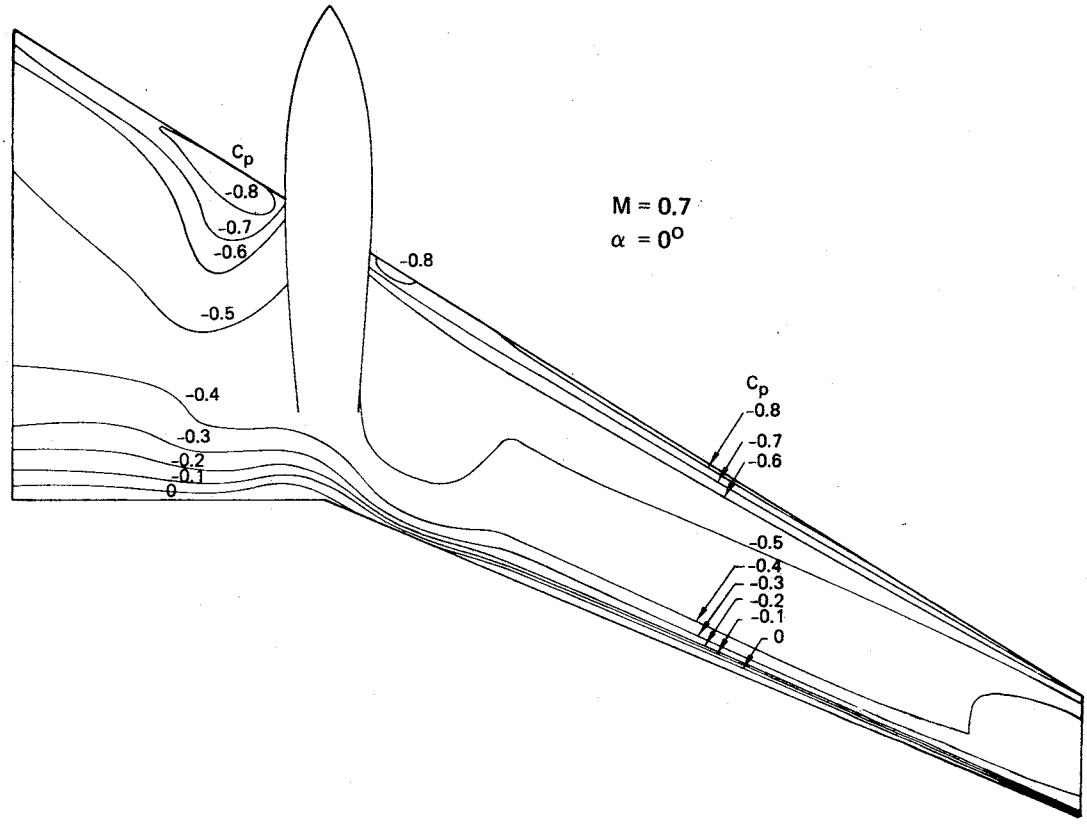


Figure 25. Upper Surface Wing Isobars—Modified Wing + Nacelle + Slipstream

5.5 FORCE DATA

C_L vs a curves for the cruise wing-body-nacelle configuration are shown in Figure 26. At $a = 0^o$, the effect of the slipstream is to increase the total lift by approximately 5%. The slope of the lift curve is slightly lower for the modified wing relative to the baseline in the absence of slipstream effects. In all cases, a design C_L value of 0.5 is achieved at a close to 0^o.

Wing spanwise load distributions are presented in Figures 27 and 28. Figure 27 shows the incremental effects of the nacelle and slipstream on the loading of the baseline wing. The asymmetry created by the prop slipstream is compatible with the pressure profiles of Figures 13 through 16. The wing, in this case, acts as a pair of stators tending to straighten the swirling flow behind the propeller and thus contribute to thrust recovery. Figure 28 gives the span load distribution for the modified wing which is in agreement with that of the clean wing, as set forth in the design objective.

Spanwise distribution of $C_{p_{MIN}}$ for the baseline and modified wing is presented in Figure 29 at $a = 0^o$. Inboard of the nacelle, the baseline wing is highly critical because of upwash from the swirling slipstream. At 0.8 cruise Mach number, strong shock waves and, possibly,

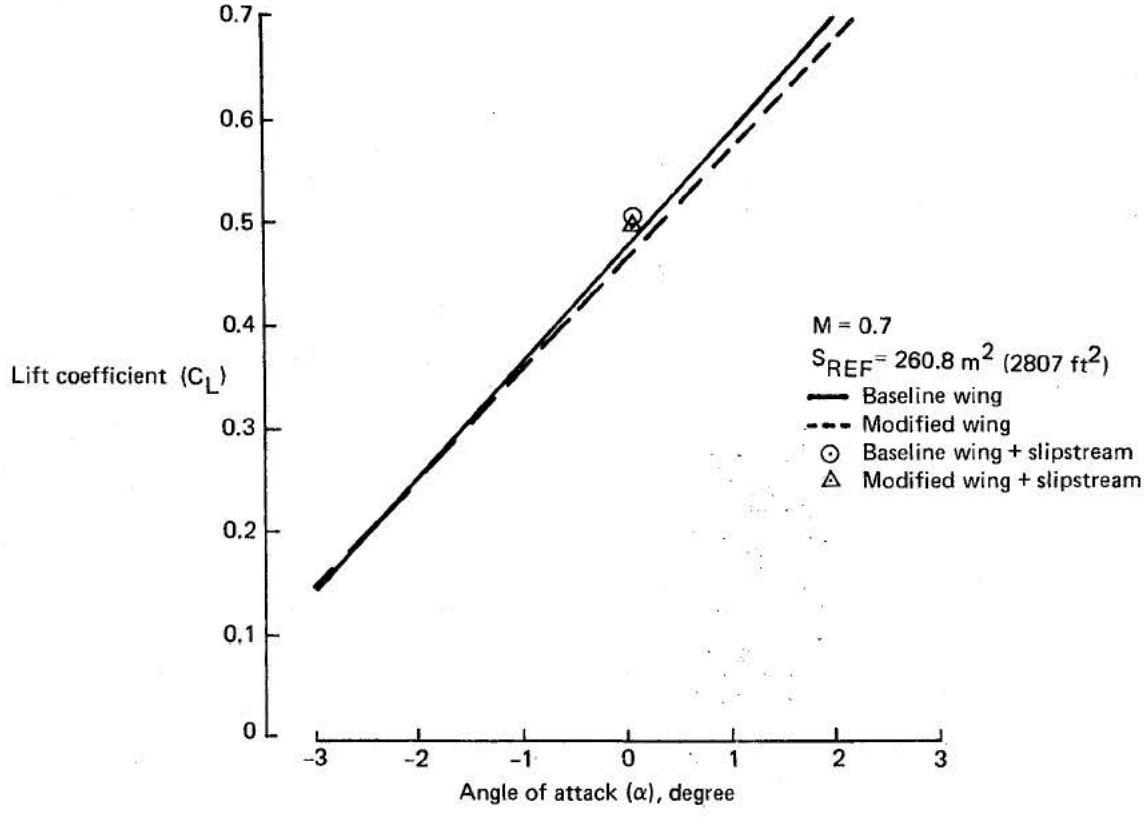


Figure 26. Cruise Wing Lift Curves

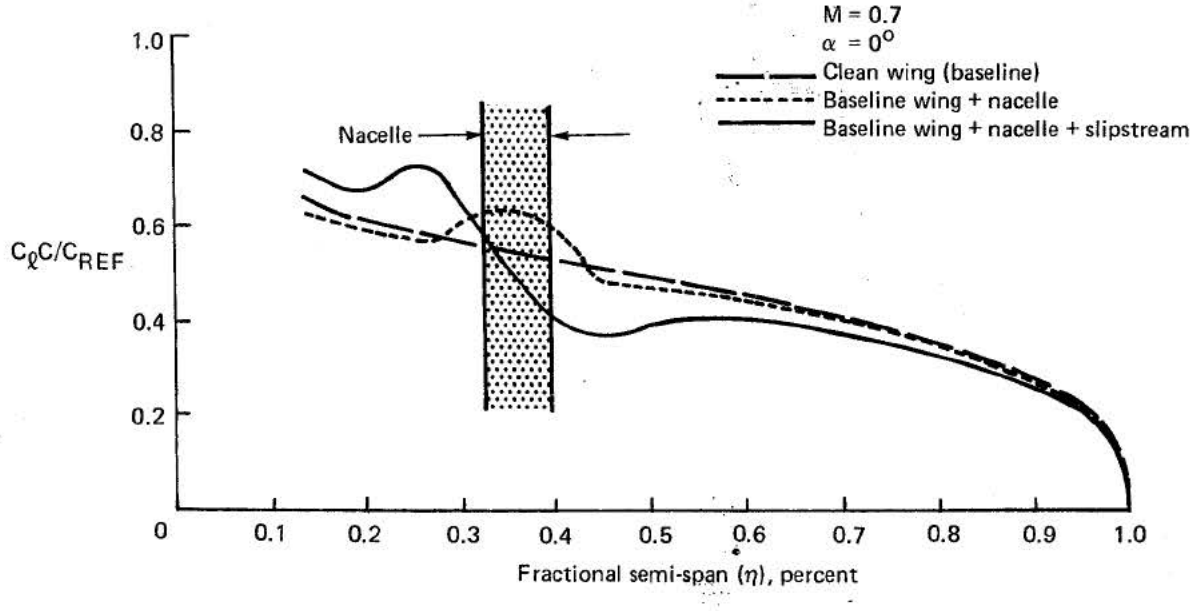


Figure 27. Effect of Slipstream on Span Loading

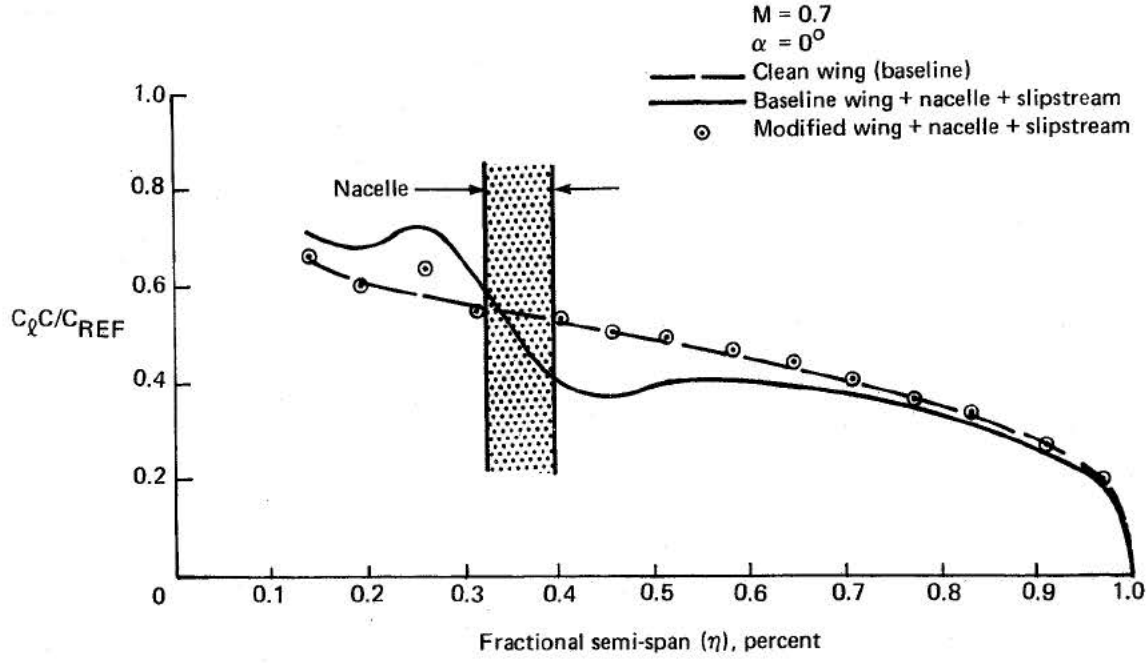


Figure 28. Wing Spanwise Load Distribution

shock-induced separation are likely to occur on the inboard baseline wing. Corresponding penalties in profile drag are difficult to assess without a full-scale wind tunnel test. However, these penalties are expected to outweigh gains accrued from propeller thrust recovery. The modifed wing (fig. 29) exhibits substantially reduced pressure peaks, although still higher than those of the clean wing.

5.6 PROPELLER THRUST RECOVERY

Swirl velocities in the prop slipstream represent lost thrust and hence lower efficiency. In Reference 1, these losses were estimated at 8% during cruise and 13% at takeoff. The wing, acting as a large chord stator, may be expected to recover some of the lost thrust by de-rotating the slipstream. Physically, the slipstream induces a local angle-of-attack, which causes the lift vector to tilt forward, producing thrust.

In the present context, the thrust increment due to the slipstream has been obtained by integration of the surface pressure. Figure 30 gives a drag buildup for the baseline and the modified wing, each incremented from the clean wing. The increments in profile drag (C_{DP}) were postulated on the basis of the spanwise distribution of C_{PMIN} of Figure 29. Early shock formation could lead to an early break in the polar as suggested in Figure 30. Uncertainty factors for the increments in C_{D_p} may be as high as 100%.

Vector ΔC_{Di} in Figure 30 represents the increment in induced drag between the wing plus nacelle and the clean wing. It was calculated by the induced drag program A 323 (ref. 5) and is strictly a function of the span load distribution. This vector is negligible for the baseline wing, but significant (4.5 drag counts) for the modified wing.

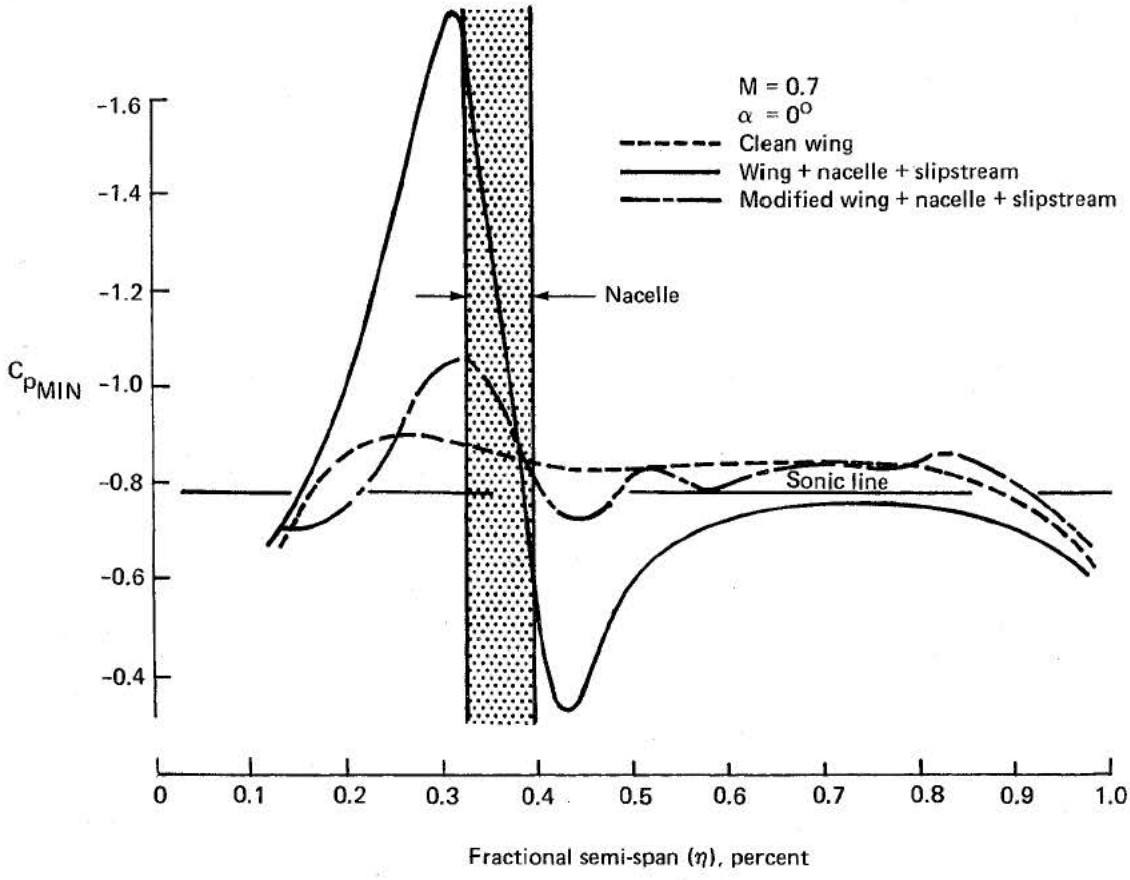


Figure 29. Spanwise Distribution of $C_{P_{MIN}}$

The thrust recovery vector was calculated by potential flow program A 230 as the difference in integrated surface pressures between the configuration with and without swirl. For the modified wing this vector is composed of a ΔC_L of 0.026 and a ΔC_D of one drag count. It is considered inconsequential.

The baseline wing shows a thrust recovery vector equivalent to 11 counts of thrust. At Mach 0.8 and 10 700m (35 000 ft), this translates into 2.97 kN (668 lb) of thrust. The total thrust of the airplane may be estimated from the propeller power loading given by Reference 4:

$$\frac{SHP}{D^2} = 37.5 \text{ per engine}$$

Where SHP is shaft horsepower and D = 5.97m (19.6 ft) is propeller diameter. At Mach 0.8 and 10 700m (35 000 ft), the total thrust, assuming a propeller efficiency of 0.8, is:

T = 72.427 kN (16 283 lb)

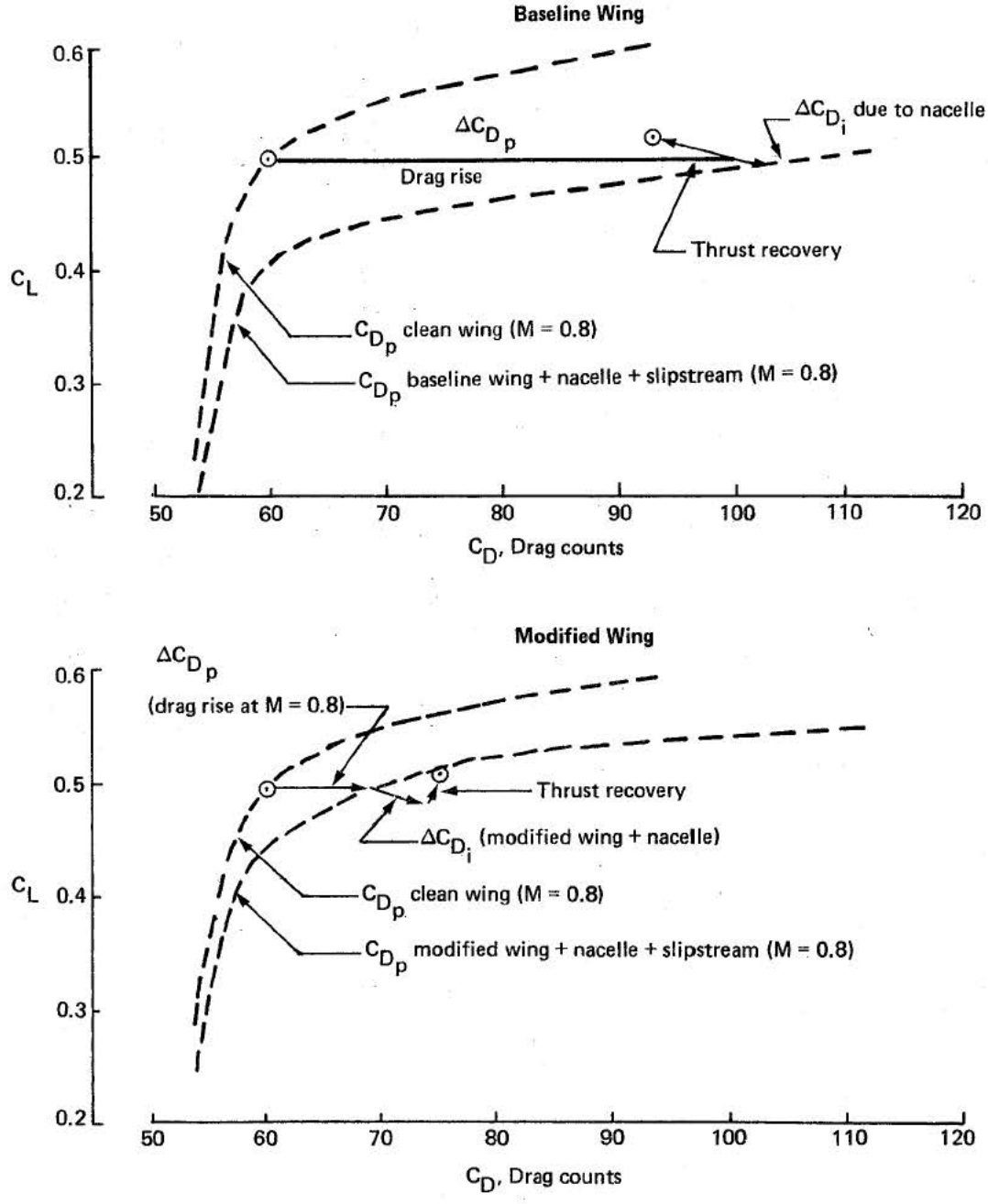


Figure 30. Wing Drags Incremented from Clean Wing

From the above, the recovered thrust for the baseline wing is 4.1% of the total, or approximately 50% of the estimated thrust lost due to swirl.

This estimate of thrust recovery is predicated on the ability of the baseline wing to sustain the calculated pressure profiles in shock and separation-free flow.

5.7 ASSESSMENT

The influence of the nacelle (without slipstream) on the baseline wing is significant as is indicated in Figures 14, 15, 24, and 27. The present study did not consider recontouring the nacelle. However, future study efforts should include this consideration, perhaps in combination with some thrust line toe-out to align it with the local flow.

The swirl produced by the wing-mounted prop-fan imparts a strong local upwash to the wing inboard of the nacelle and a downwash on the outboard side. Large leading edge suction pressures appearing on the inboard wing were found to produce a thrust force, equivalent to the momentum removed from the swirling slipstream through the straightening effect of the wing. The analysis further indicated that at high cruise Mach number (M = 0.8), isentropic flow could not be maintained on the inboard wing and that shock waves were likely to occur. If this occurs, the readjustment of pressure on the inboard wing would largely eliminate the calculated thrust increment and would further lead to sizeable penalties in profile drag. To alleviate the adverse effects of the nacelle and swirl on the wing, the latter was redesigned to neutralize these effects. The resulting wing is characterized by large variations in twist and thickness and shows little potential for thrust recovery. The trade between profile drag and thrust recovery must ultimately be determined through wind tunnel testing.

6.0 WING-MOUNTED PROP-FAN–LOW SPEED

Low-speed analysis of the takeoff configuration and flight condition was selected because the slipstream effects are much greater than in the landing approach condition.

6.1 GEOMETRICAL DEFINITION

Leading- and trailing-edge flap geometries have been defined for the modified cruise wing (described in sec. 5.0) to simulate the takeoff flight condition. Figure 31 depicts a streamwise section of the flapped wing as defined for potential flow analysis. A trailing-edge flap of 22% chord, extending over the entire wing span was assumed. A flap deflection δ_F of 10^o was selected for the takeoff condition and was achieved by rotating the trailing-edge about the 78% chord line.

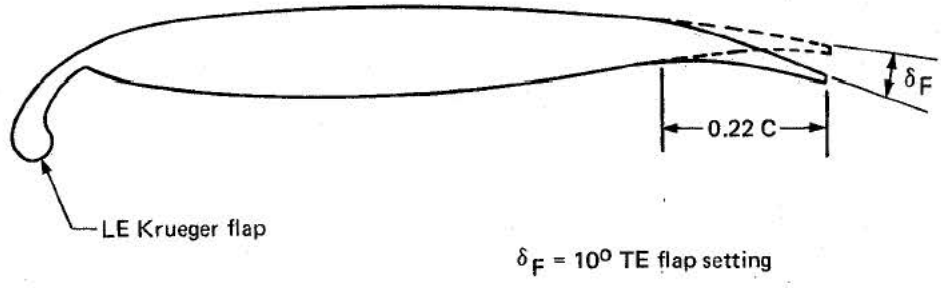


Figure 31. Leading- and Trailing-Edge Flaps for Low-Speed Configuration

The leading-edge Krueger flap geometry was defined as shown in Figure 32 and described below:

- Point A–A point of tangency on the wing upper surface at 2% chord from the leading-edge.
- Point B–Located at the intersection of the tangent from A and the wing chord line.
- The Krueger leading edge (point C) was determined by constructing from point B a line at an angle δ_K to the wing chord line and equal in length to the Krueger flap chord. The latter was fixed at 15% of the basic wing chord. The Krueger angle δ_K was initially selected equal to 63^o. In a subsequent design cycle, it was varied between 50^o and 55^o spanwise, in an attempt to improve the flow pattern over the leading edge.

- The Krueger upper surface profile was extracted from an existing Boeing design and geometrically stretched to fit between points B and C while remaining tangent to line AB.

- The Krueger lower surface profile was faired in arbitrarily to complete the section definition. It does not significantly impact the performance of the wing.

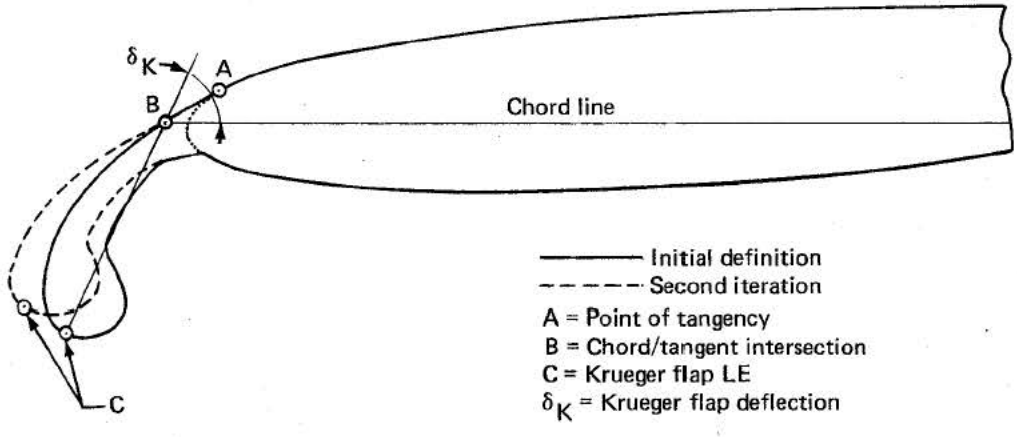


Figure 32. Krueger Flap Definition

The above procedure was fully automated for rapid generation of the entire wing, given a set of Krueger flap angles and chord ratios (C_K/C).

Paneling of the low-speed configuration for potential flow analysis is shown in Figures 33 and 34. Particular attention was required in modeling the wing-body intersection because of the Krueger flap dipping below the body. Bound vortices within the wing lifting system, located in the Kreuger flap region, could not be extended to the body centerplane as is normally done. Instead, they were routed to a point aft of the Krueger, deflected to the plane of symmetry, then shed aft to infinity.

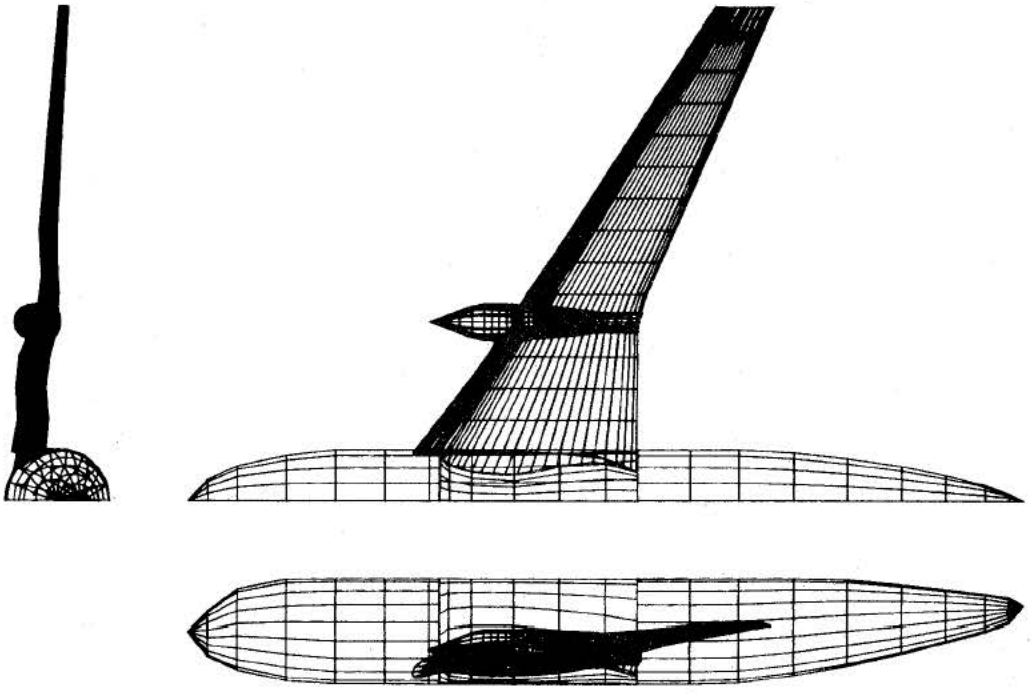


Figure 33. Paneling Scheme—Low-Speed Configuration

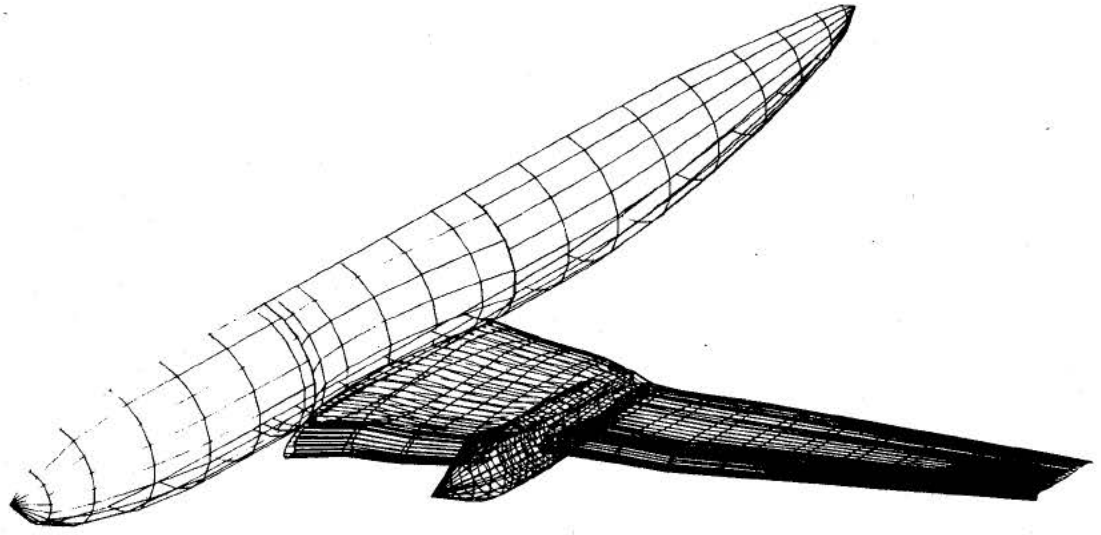


Figure 34. Krueger Wing—Low-Speed Configuration

6.2 DESIGN PROCEDURE

Initial definition of the low-speed configuration included a Krueger flap of constant deflection angle, $\delta_K = 63^o$ and chord ratio $C_K/C = 0.15$ (see fig. 32). This configuration was analyzed, less slipstream effects on potential flow program A 230. The results indicated a nonuniform stagnation pattern along the Krueger leading edge, partly because of the large variations in the wing twist distribution. In a second design cycle, the Krueger flap was redefined in accordance with the deflection schedule of Figure 35. A comparison of pressure profiles along strips 3 and 6 for the two design cases is given in Figures 36 and 37. The data are plotted versus arc length (S/C) from the Krueger flap leading edge. At $\alpha = 4^o$, the stagnation point is located on the upper side of the leading edge in both design cases. At higher angles-of-attack and/or increasing trailing-edge flap deflections (δ_F), the stagnation point is expected to move down past the leading edge toward a more favorable location corresponding to $C_{L_{MAX}}$. Because of a more uniform distribution of the stagnation line along the wing leading edge, the second iteration design was selected for further analysis.

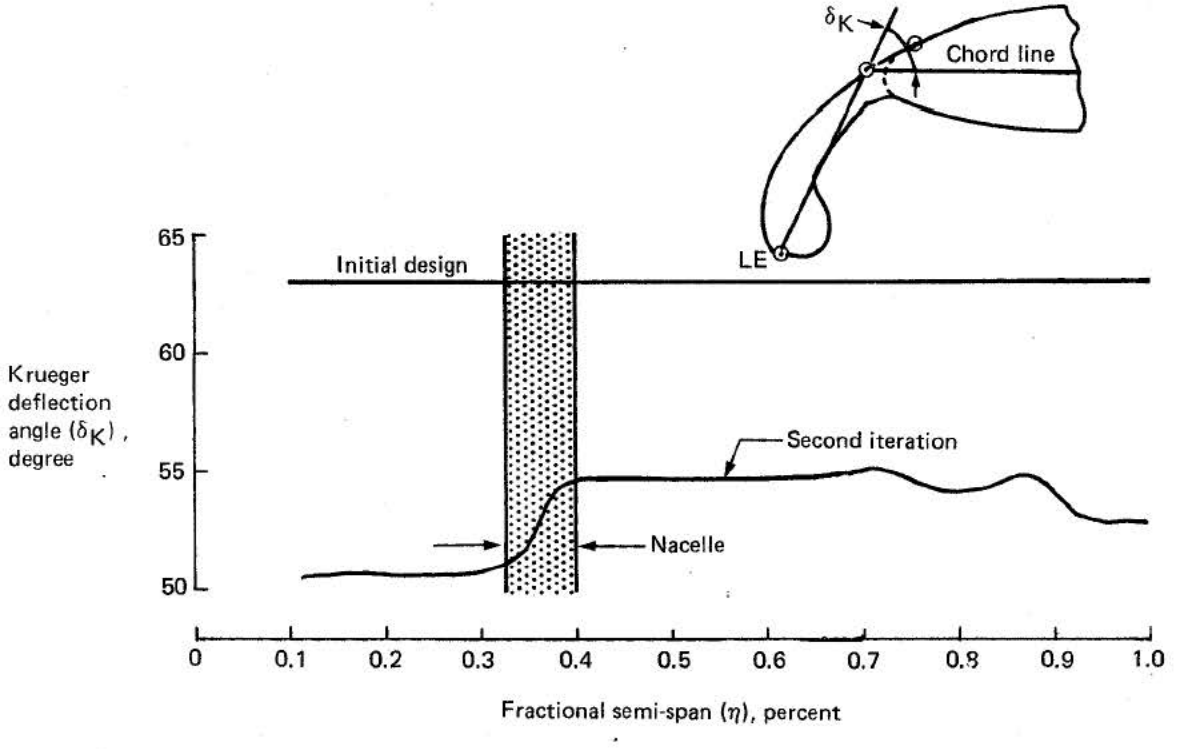


Figure 35. Krueger Flap Deflection Schedule

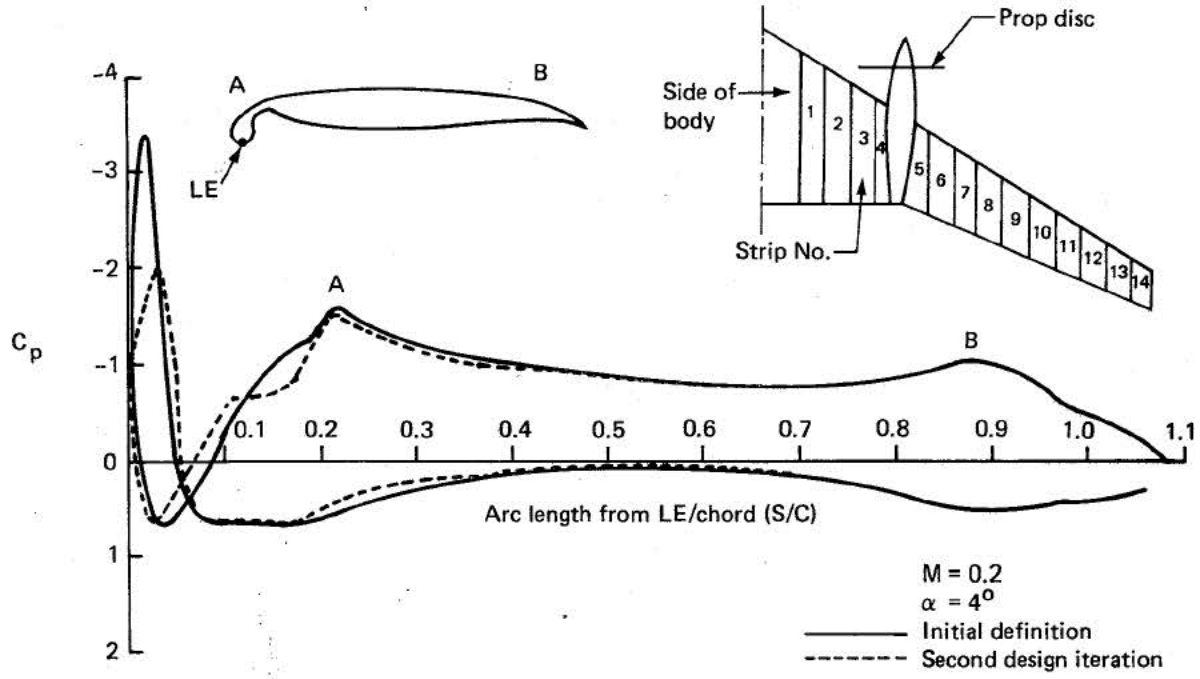


Figure 36. Low-Speed Wing Pressure Profiles: Strip 3

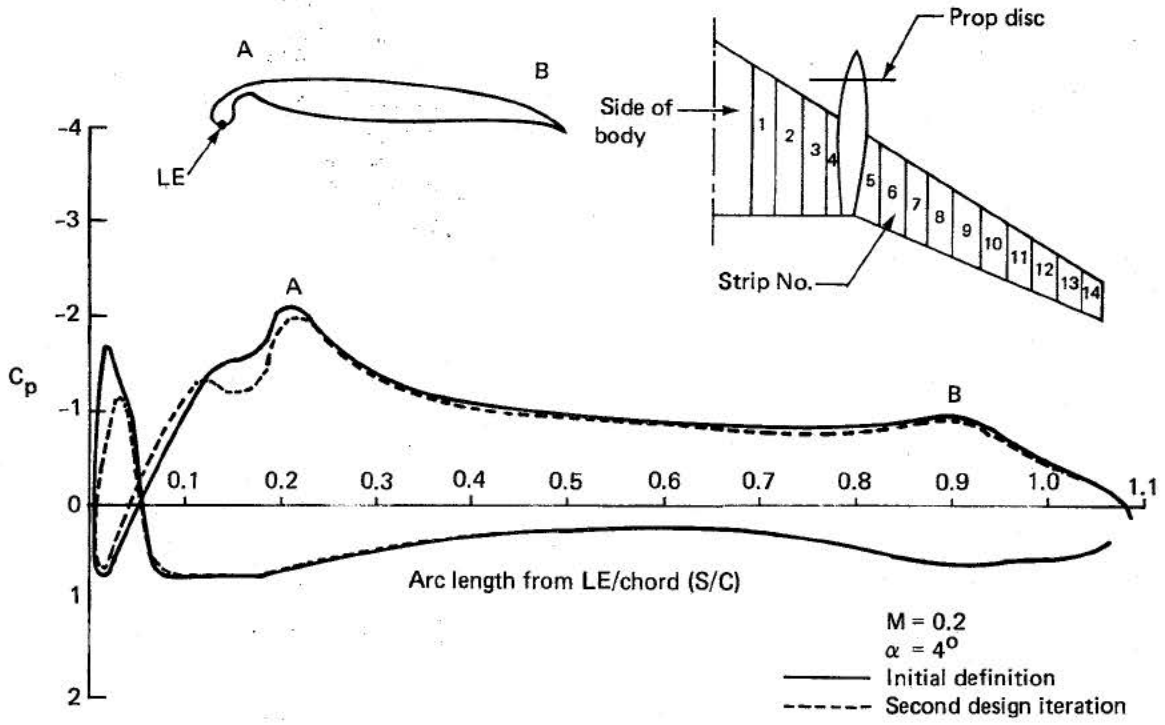


Figure 37. Low-Speed Wing Pressure Profiles: Strip 6

6.3 SLIPSTREAM CHARACTERISTICS

Radial distribution of total pressure ratio and swirl angle aft of the propeller for the cruise and takeoff conditions are given in Figure 38. The takeoff data at Mach 0.2 were obtained by Hamilton Standard through wind tunnel testing. Swirl angles of about 9 degrees are predicted, compared to 6 degrees at cruise. The incremental axial velocity ($\Delta V_X/U_\infty$) corresponding to the above data (calculated by the method described in sec. 5.0) is presented in Figure 39. These increments are very large during takeoff and have a significant impact on the wing aerodynamic characteristics.

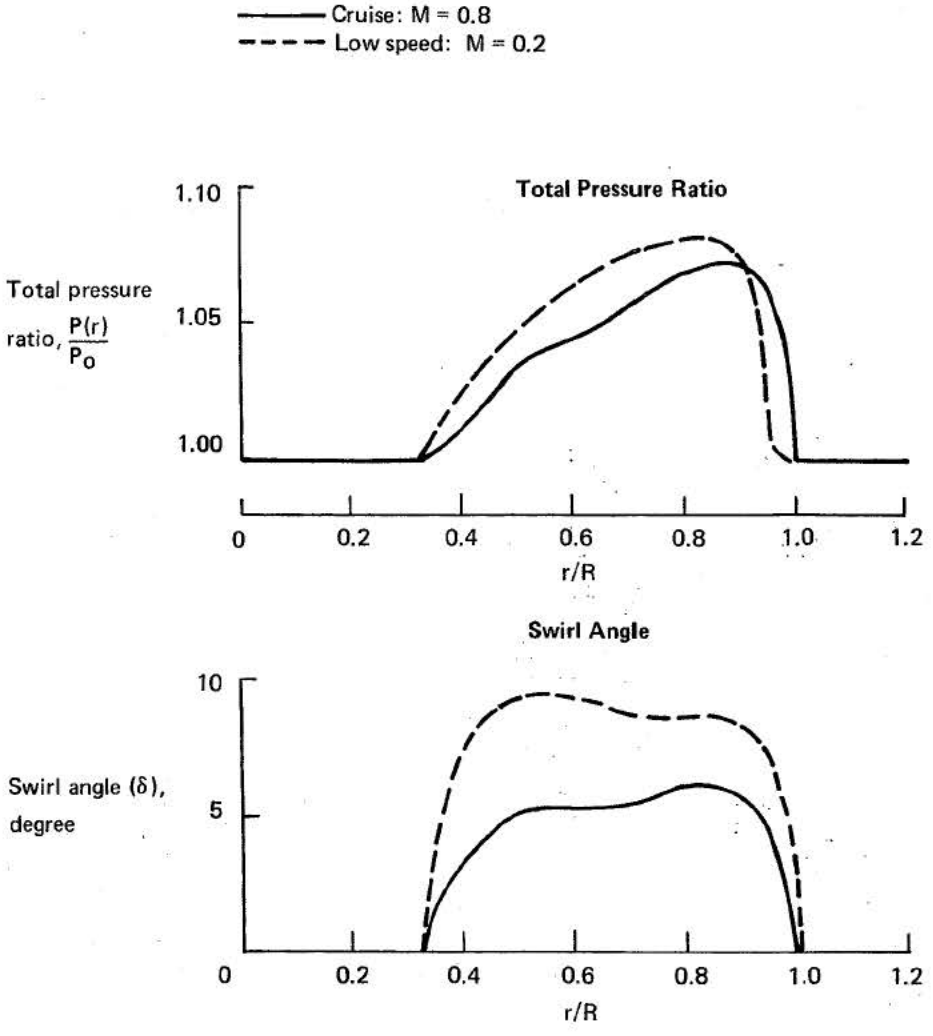


Figure 38. Radial Distribution of Swirl and Total Pressure in Prop Slipstream

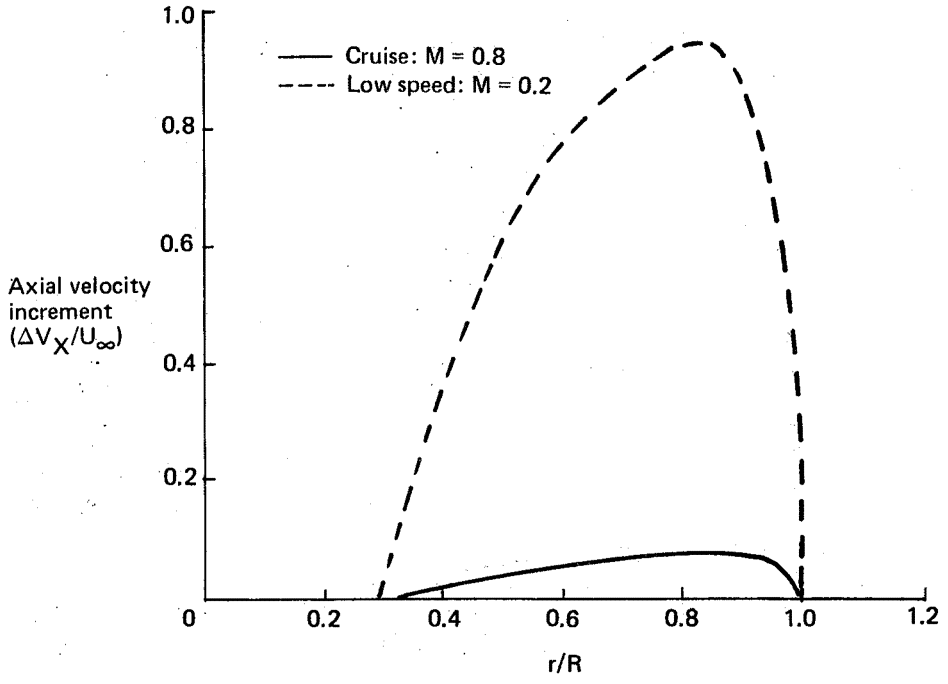


Figure 39. Radial Distribution of Axial Velocity Increment in Prop Slipstream

6.4 PRESSURE COEFFICIENT DATA

Pressure profiles for strips 3 through 6 at $\alpha = 4^{\circ}$, showing the effect of the propeller slipstream, are given in Figures 40 through 43. On the inboard side of the nacelle, the swirl angles and the increments in axial velocity have additive effects, resulting in high loading of the local wing sections. On the outboard side, these effects are subtractive with the axial velocity slightly more predominant. The net effect is an increase in load on the outboard, as well as the inboard wing. The effect of the slipstream on the wing as a whole is discussed further below.

6.5 FORCE DATA

The lift curve for the low-speed configuration is shown in Figure 44. At $\alpha = 4^{\circ}$, the effect of the slipstream is to increase C_L from 1.328 to 1.610, a 21% increase. Preliminary design estimates in Reference 1 give a climbout C_L value of 1.63 with a trailing-edge flap setting of 10°.

Figure 45 shows the effect of the slipstream on the wing-span load distribution. Local increases in the wing loading on both sides of the nacelle correspond to the pressure profiles of Figures 40 through 43.

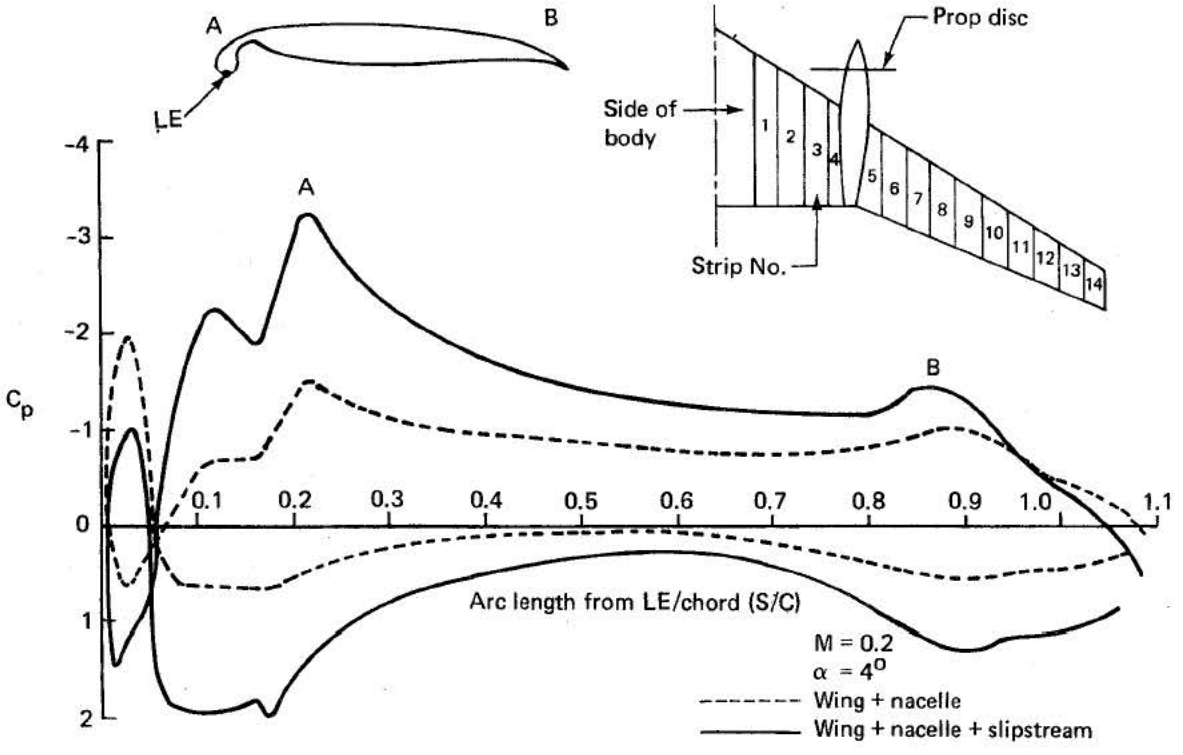


Figure 40. Low-Speed Wing Pressure Profiles with Slipstream: Strip 3

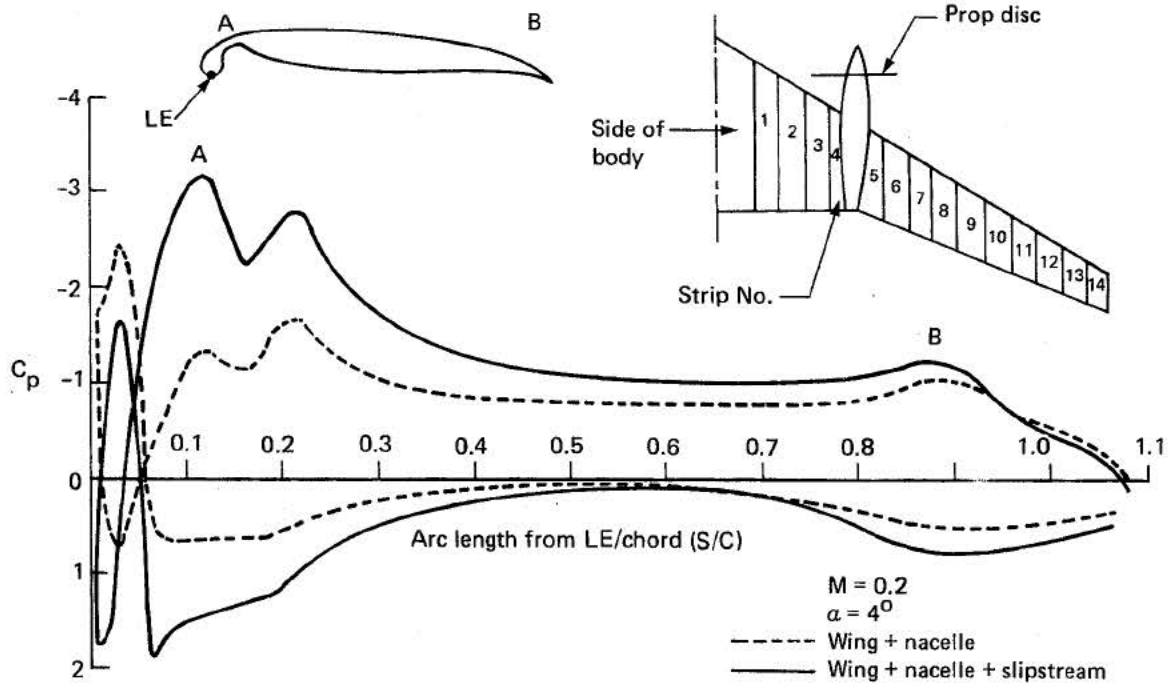


Figure 41. Low-Speed Wing Pressure Profiles with Slipstream: Strip 4

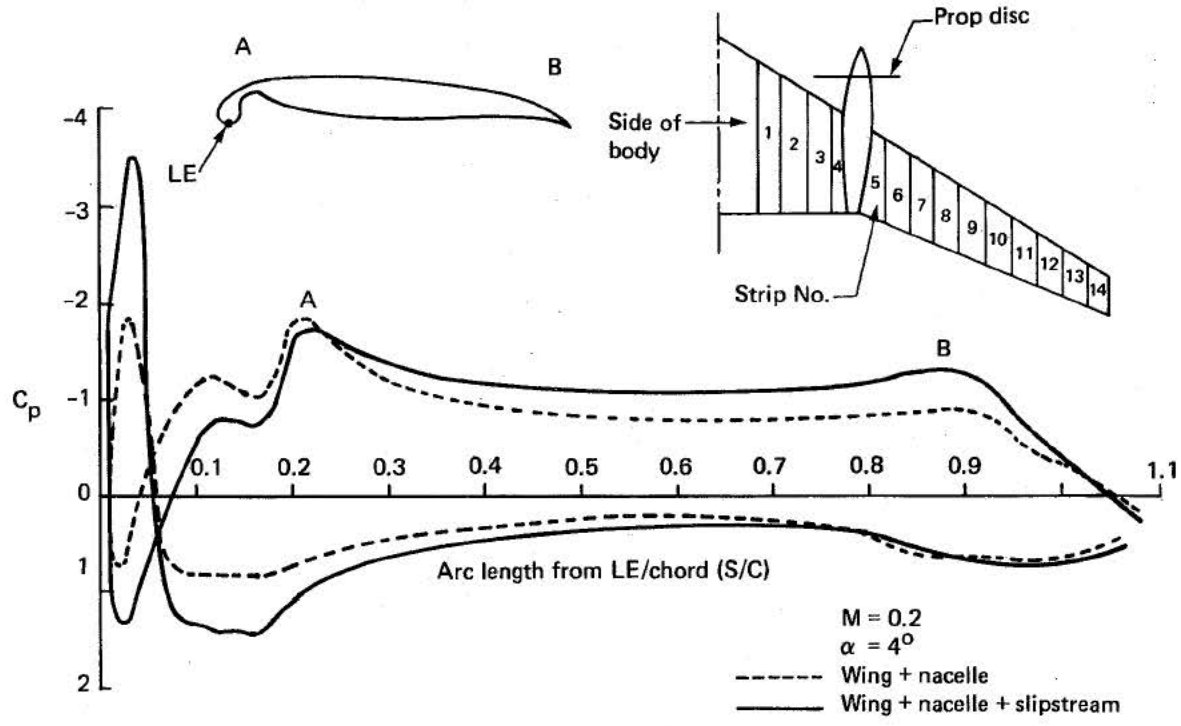


Figure 42. Low-Speed Wing Pressure Profiles with Slipstream: Strip 5

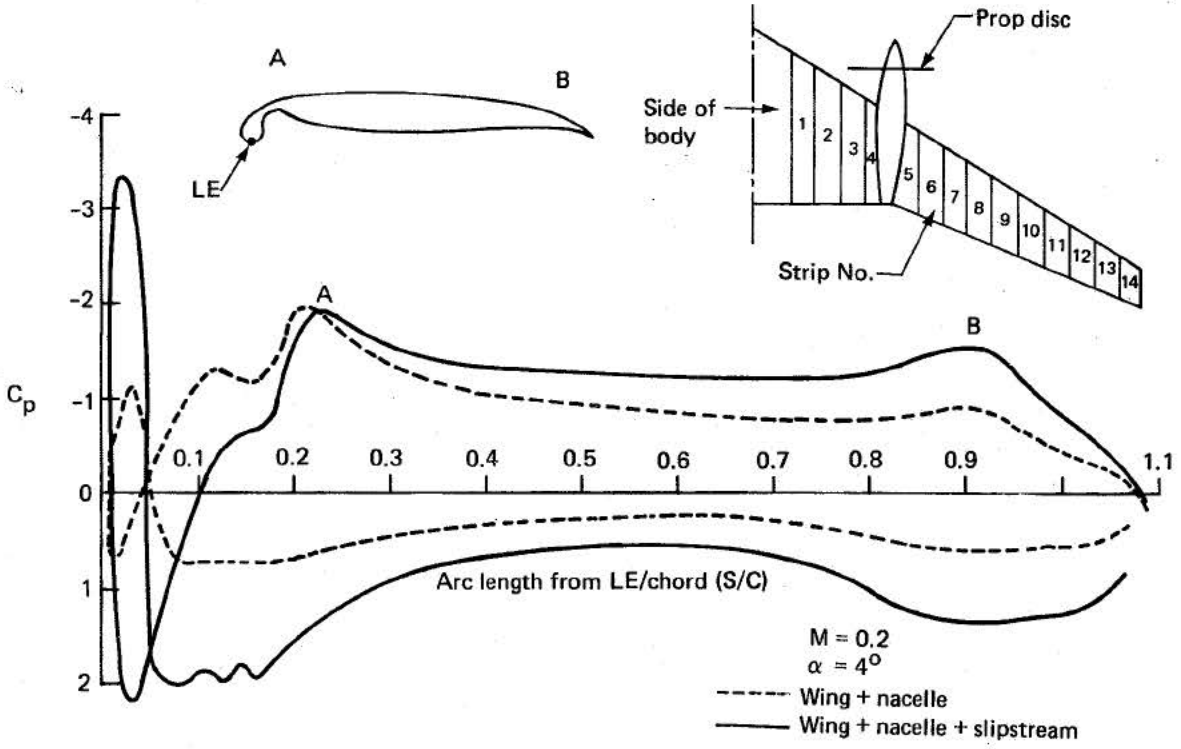


Figure 43. Low-Speed Wing Pressure Profiles with Slipstream: Strip 6

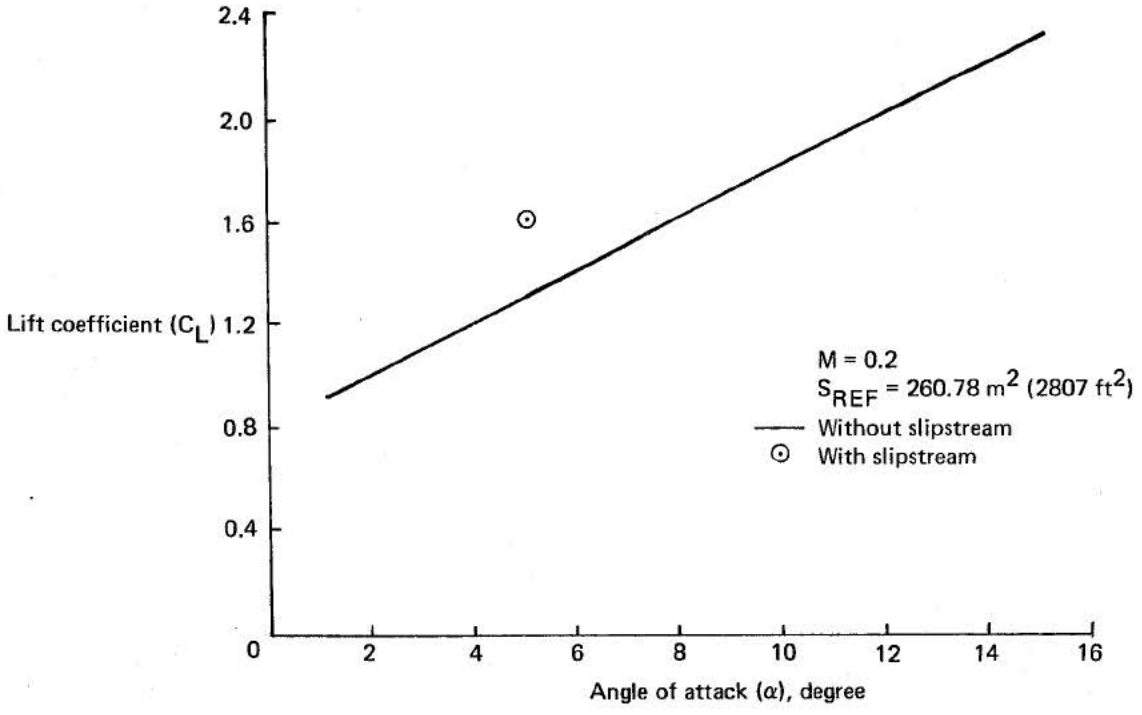


Figure 44. Krueger Wing—Low-Speed Configuration Lift Curve

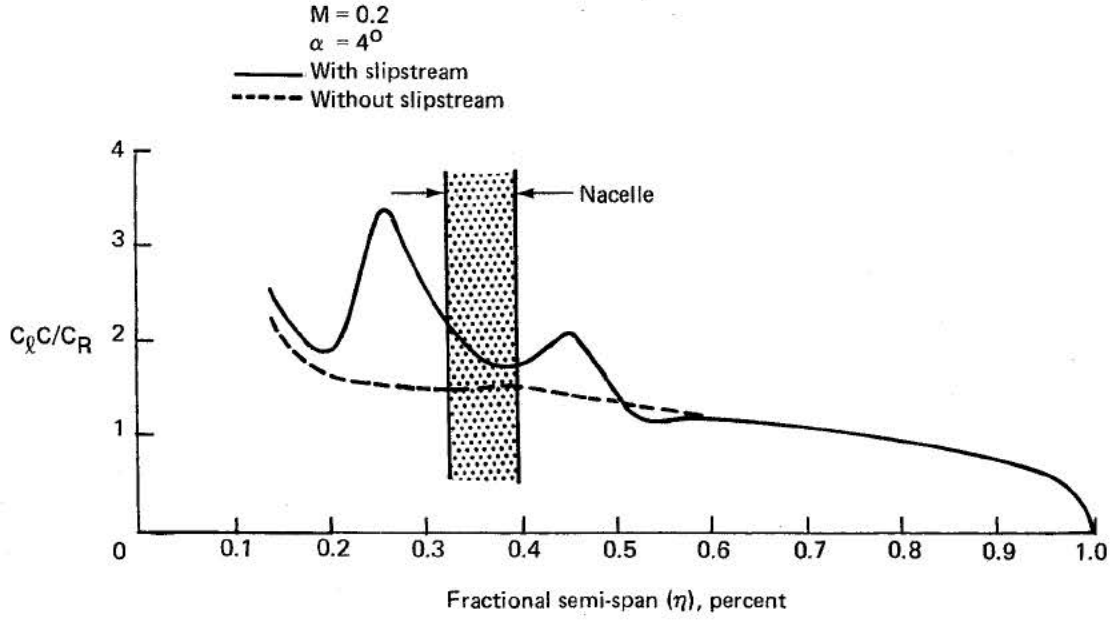


Figure 45. Krueger Wing—Low-Speed Configuration Spanwise Load Distribution

6.6 DRAG AND THRUST RECOVERY

Induced drag of the wing/body/nacelle configuration, calculated from the span load distribution of Figure 45, is shown in Figure 46. The effect of the slipstream (shown in fig. 46) was calculated as an increment in the integrated surface pressures over the configuration. This vector is largely composed of a C_L increment ($\Delta C_L = 0.282$) with 36 counts of drag reduction, which contributes to thrust recovery. If, however, the effect of the slipstream is to be considered at constant C_L, the thrust recovery could be as high as 350 counts, depending on the general shape of the polar.

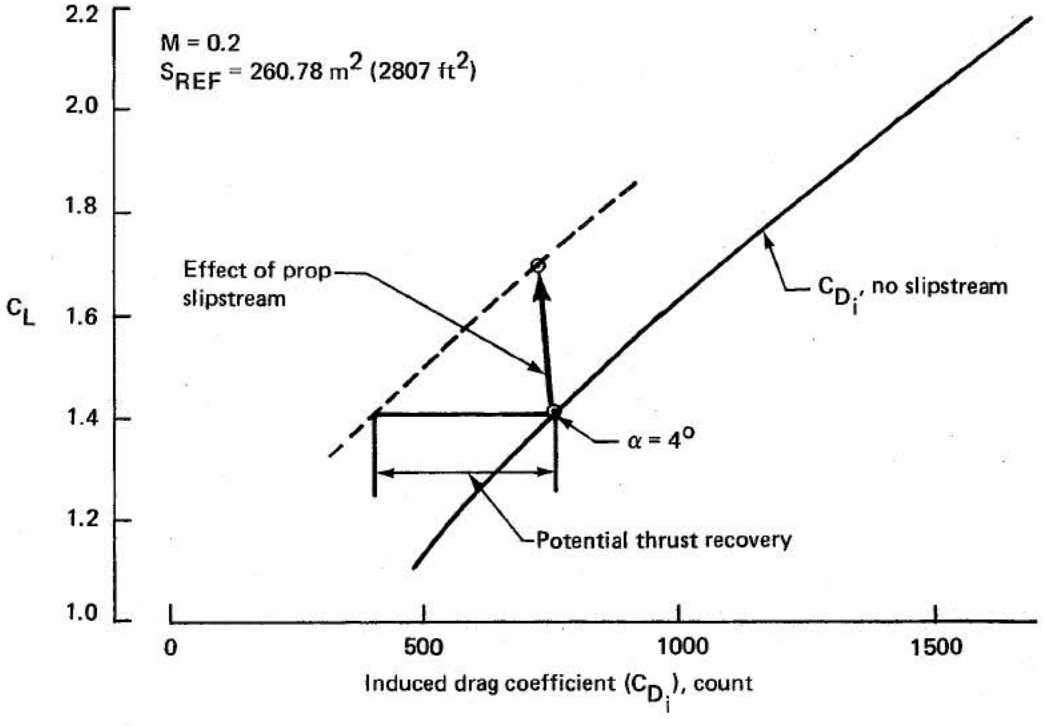


Figure 46. Krueger Wing—Low-Speed Configuration Induced Drag Due to Slipstream

6.7 EFFECT OF ONE-ENGINE FAILURE

In the case of a one-engine failure, the aerodynamic forces and moments attributed to the slipstream will act only on one side of the airplane, creating a general aerodynamic imbalance that must be trimmed.

Figure 47 depicts the rolling moment C_{MX} as a function of C_L for only one-half of the configuration. The effect of the slipstream, calculated by integration of the surface pressures, is shown on the figure as a vector composed of:

$$\Delta C_L = 0.141$$
$$\Delta C_{MX} = 0.018$$

This represents the engine-out increment of the prop-fan over the turbofan. It is substantially smaller than preliminary estimates for the Reference 1 study, as indicated in Figure 48.

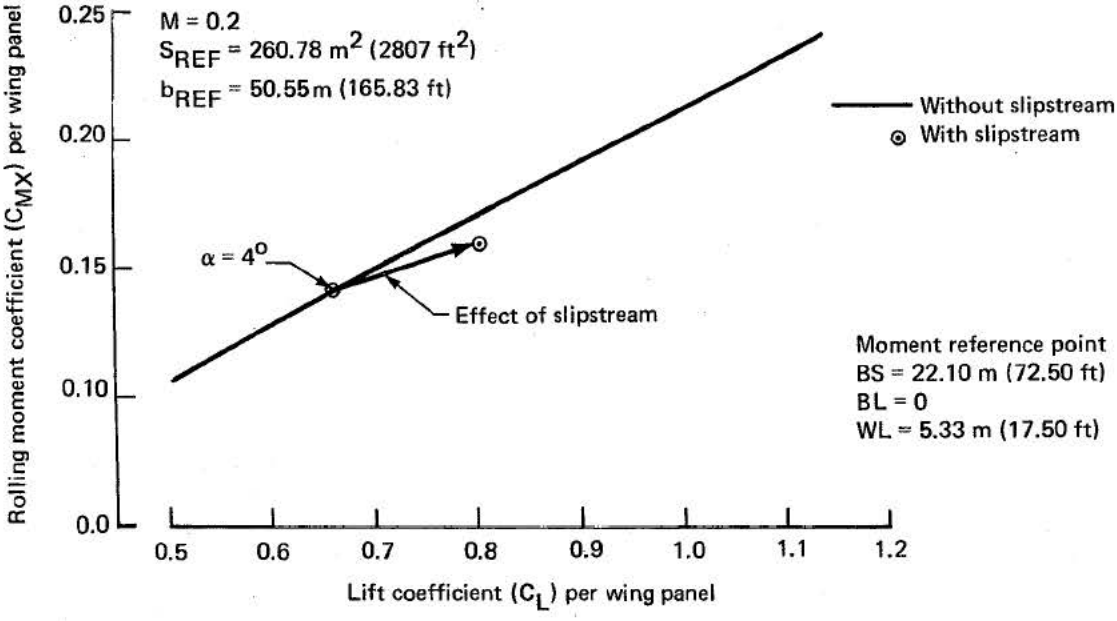


Figure 47. Krueger Wing—Low-Speed Configuration Rolling Moment Coefficient

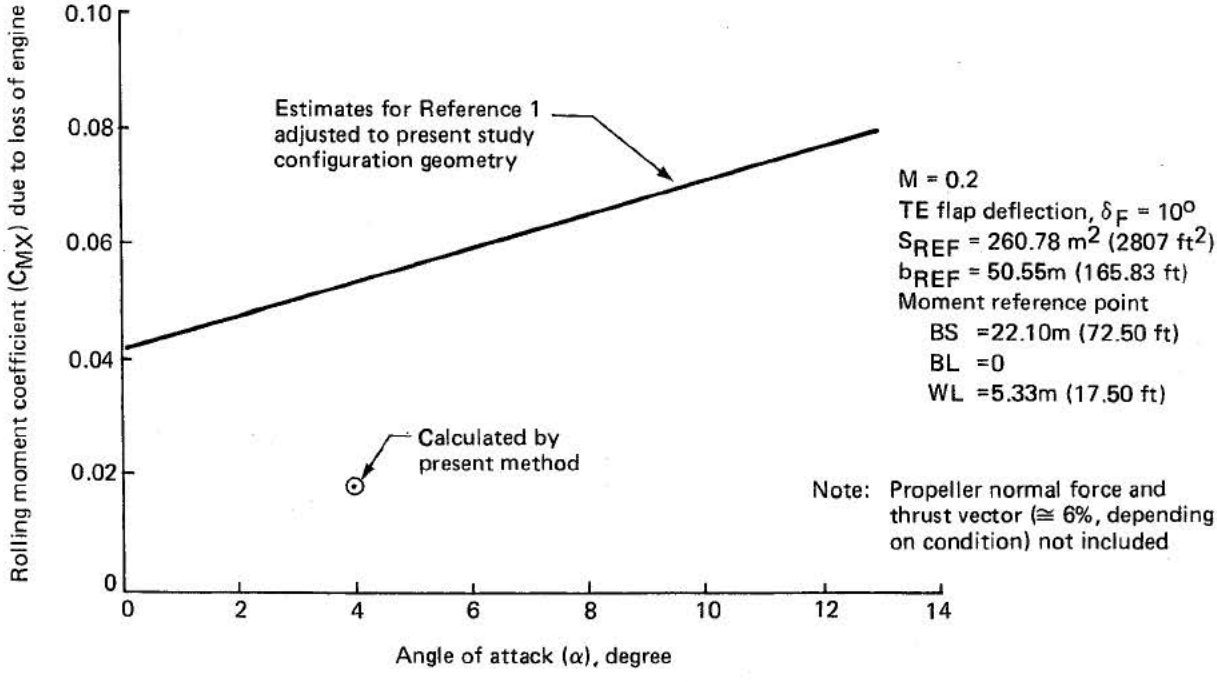


Figure 48. Rolling Moment Due to Engine-Out Comparison with Preliminary Estimates

6.8 ASSESSMENT

Leading- and trailing-edge flaps were defined for the modified cruise wing, and are suitable for both landing and takeoff. The flap definition was intended for potential flow analysis only, and would normally undergo extensive tailoring prior to hardware application. The analysis showed the nature and extent of the problems associated with the wing-slipstream interaction during takeoff; landing approach problems would be similar but less severe. Based upon the calculated data, the following observations were made:

- Leading-edge Krueger flaps had more than enough deflection (δ_K) to eliminate all pressure peaks on the upper surface. The extra margin in δ_K ensures safe operation at $C_{L_{MAX}}$. For maximum L/D during climb, the Krueger flap should be partially retracted.

- Unlike the high-speed condition, the axial velocity increment, rather than the swirl, dominates the slipstream effect at the takeoff condition. As a consequence, the portions of the wing scrubbed by the slipstream experience large, local increases in loading.

- An engine failure at takeoff results in an asymmetric loading that appears to be well within the trim capabilities of the lateral control system for this type of airplane.

7.0 AFT-MOUNTED PROP-FAN

7.1 CONFIGURATION AND FLIGHT CONDITIONS

Paneling of the aft-mounted prop-fan configuration is shown in Figures 49 and 50. The wing was moved aft for longitudinal stability and was represented by a single vortex panel network placed over its mean surface. Accordingly, wing thickness effects were ignored in calculating the flow over the aft-body assembly and the body was partially coke-bottled in the vicinity of the empennage for improved area distribution. The vertical tail and the strut have symmetrical profiles of 12 and 10.5% thick, respectively. The strut plane of symmetry has 2.6^{o} of pitch and 19^{o} of dihedral and the horizontal tail has a cambered, 10.5 percent thick section.

The longitudinal, cross sectional area distribution along the aft body stations has a direct bearing on the local pressure. Figure 51 shows a buildup of the cross sectional area in that region. Maximum area occurs at body station 1640 and generally corresponds to the location of minimum body pressure in Figure 52. Smoothing the cross sectional area distribution could greatly improve the flow field in the body-nacelle channel but is not readily feasible. For example, additional necking of the body is limited by structural considerations. Moving the strut-nacelle assembly forward could require large increases in body noise attenuation provisions. It should be noted that the area profile of Figure 51 is typical of T-tail, aft-mounted engine arrangements and is not necessarily objectionable or undesirable.

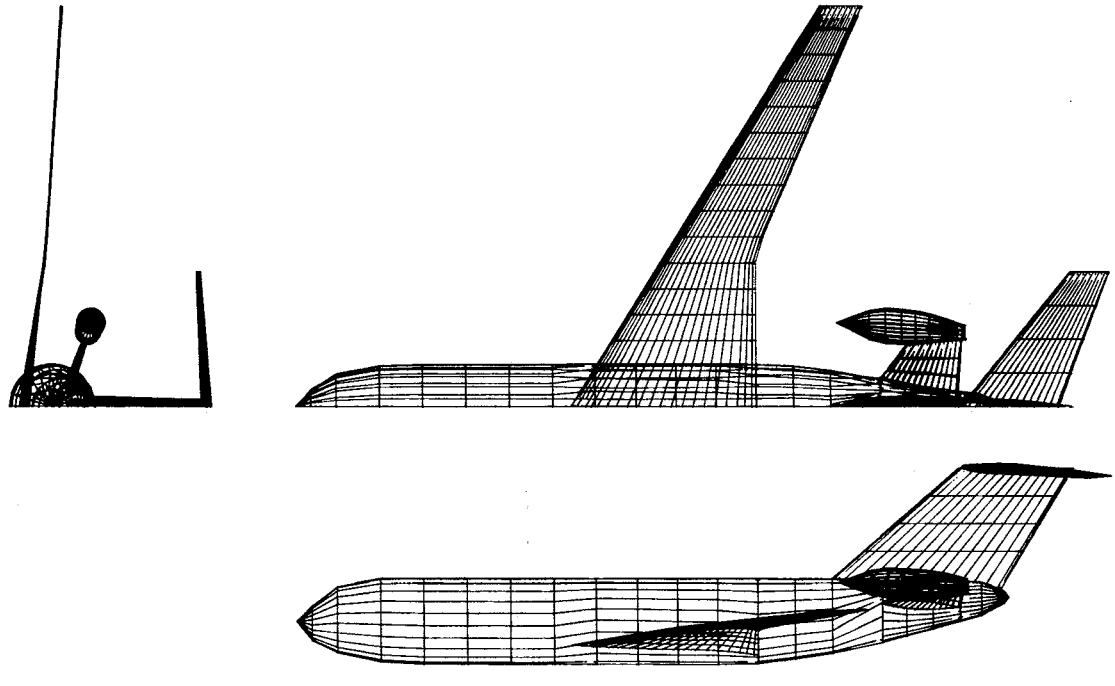


Figure 49. Paneling of Aft-Mounted Prop-Fan

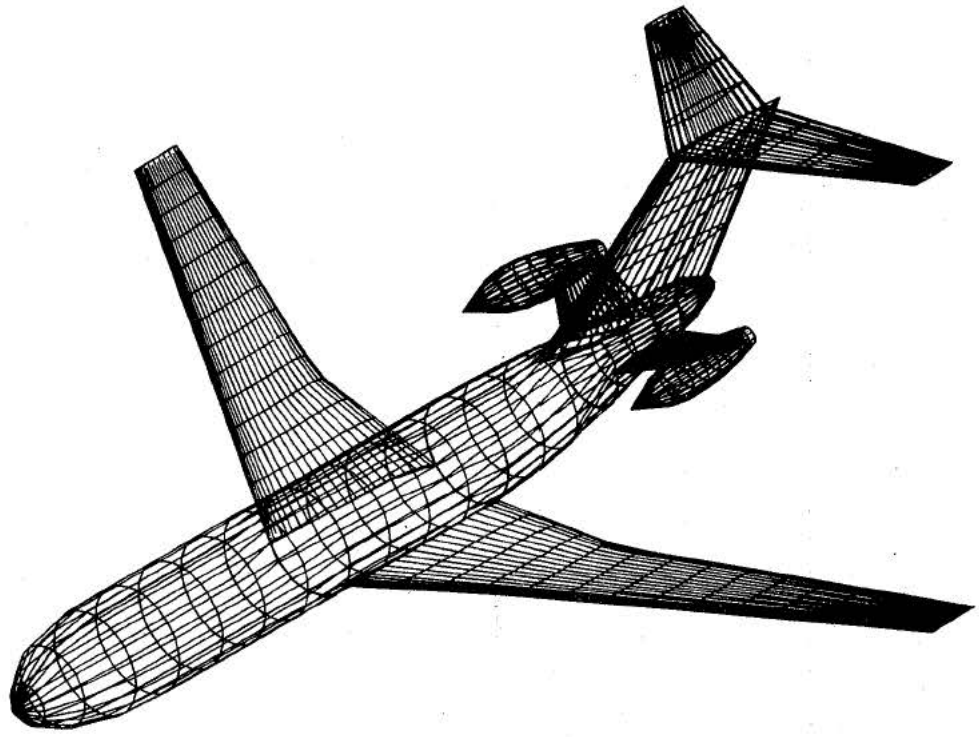


Figure 50. Aft-Mounted Prop-Fan Isometric Projection

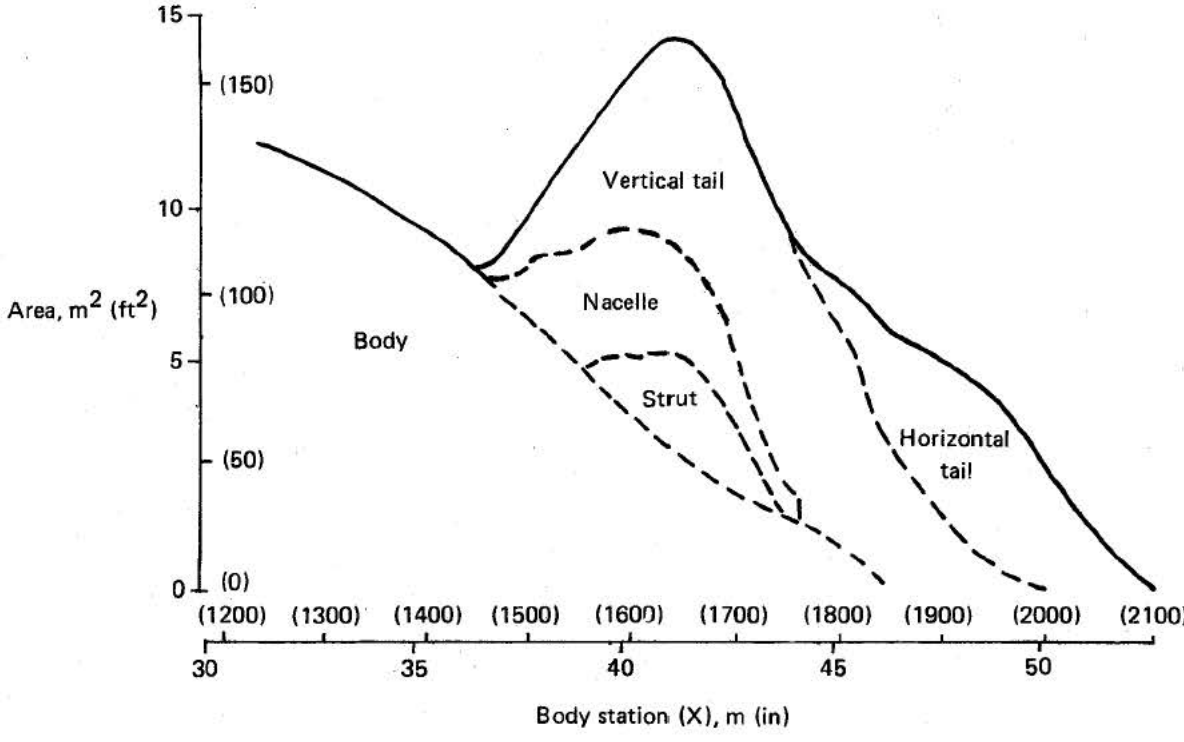


Figure 51. Aft-Mounted Prop-Fan Cross Sectional Area Distribution

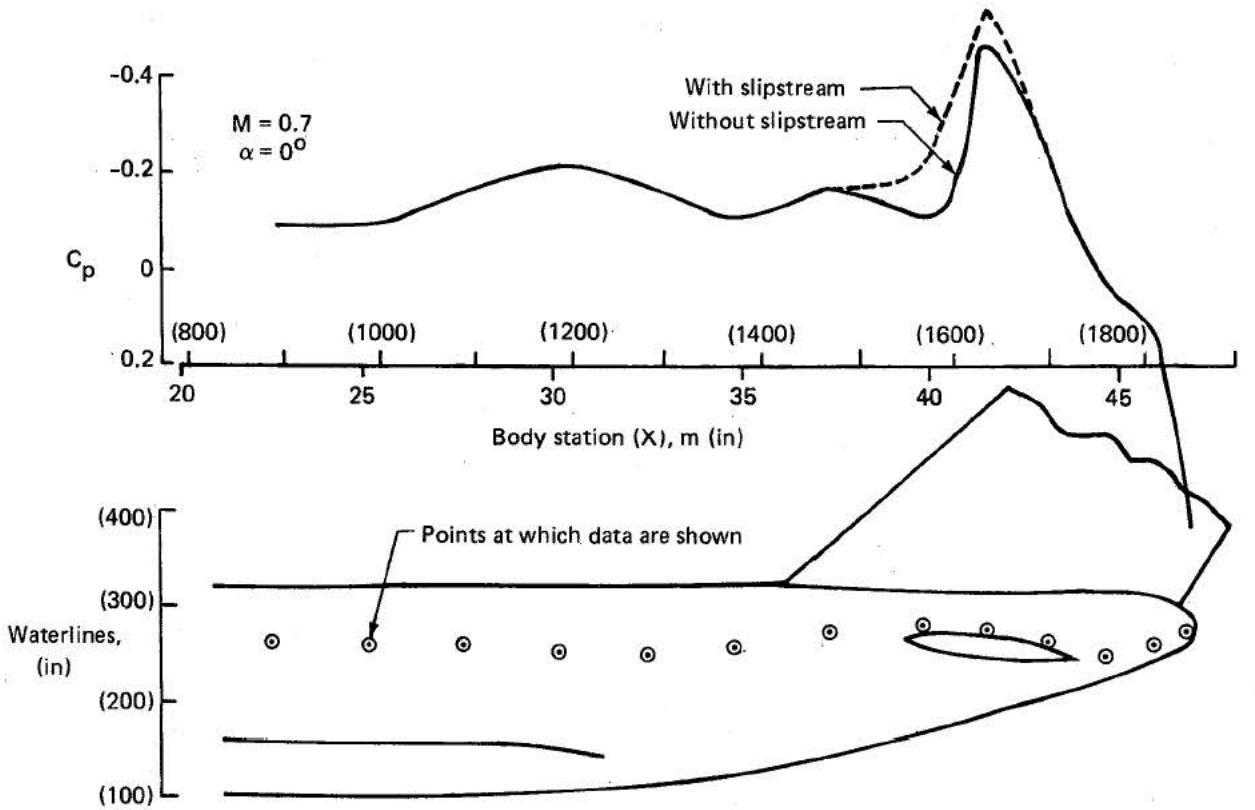


Figure 52. Aft-Mounted Prop-Fan Side-of-Body Pressure Profile

The configuration was analyzed on potential flow program A 230 at Mach 0.7 and angles-of-attack of -2 to 5°.

7.2 SLIPSTREAM CHARACTERISTICS

Radial distribution of swirl angle and total pressure ratio aft of the propeller corresponds to the cruise condition defined in Figure 13 for the wing-mounted prop-fan. Only the strut, in the present case, is washed by the propeller slipstream. However, the effect of the slipstream extends to the body and the vertical tail because of its impact on the channel cross sectional area distribution.

7.3 PRESSURE DISTRIBUTION AND SPAN LOADING

The pressure distribution along the side of the body is shown in Figure 52. The pressure is most critical at about 50% chord of the strut-body intersection on the upper side of the strut. This condition is further aggravated by the propeller slipstream, in spite of the fact

that the latter does not impinge on the body. From the point of minimum pressure, the pressure recovery occurs over a relatively short distance, increasing the danger of separation over the tail end of the body and possibly increasing drag by one or two counts.

Strut pressure profiles showing the effect of the slipstream are presented in Figures 53 through 55. In the absence of the slipstream, the strut is influenced by the downwash from the wing and suction peaks are in evidence on its lower surface. The chordwise load distribution exhibits two loops of opposite signs that integrate to produce a strut C_L close to zero. The propeller slipstream produces a strong upwash counteracting the downwash from the wing and it causes a collapse of the negative pressure loop on the strut leading edge, generally increasing the total load on the strut. This effect is particularly pronounced on strip 2 because, as shown in the figure inserts, strip 3 is close to the axis of the propeller and strip 1 is out of its range. Vertical-tail pressure profiles are presented in Figures 56 through 59 and show that the influence of the propeller slipstream clearly extends to the vertical tail and that this effect is more pronounced on the lower parts of the vertical tail and diminishes toward the tip.

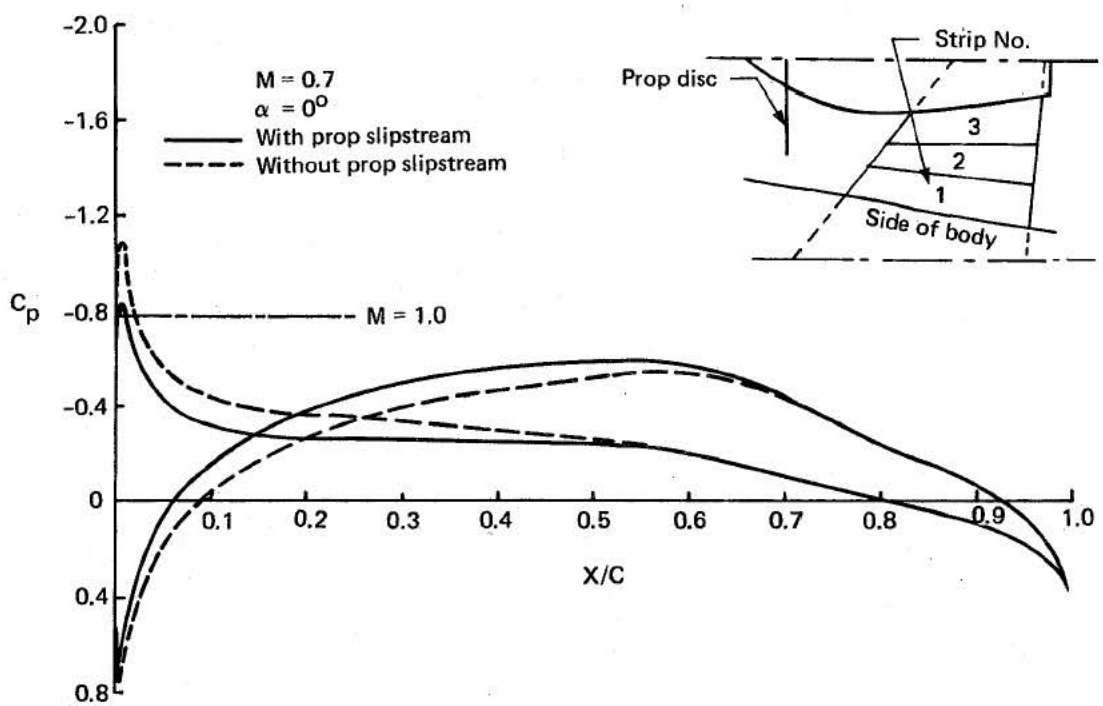


Figure 53. Aft-Mounted Prop-Fan Strut Pressure Profiles: Strip 1

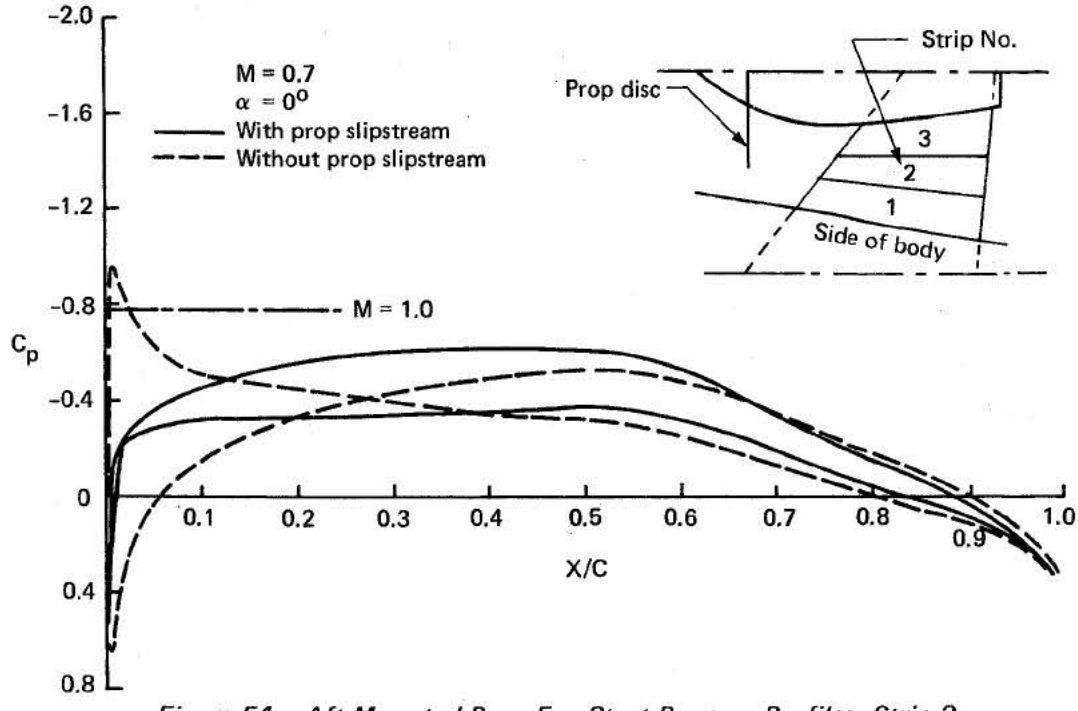


Figure 54. Aft-Mounted Prop-Fan Strut Pressure Profiles: Strip 2

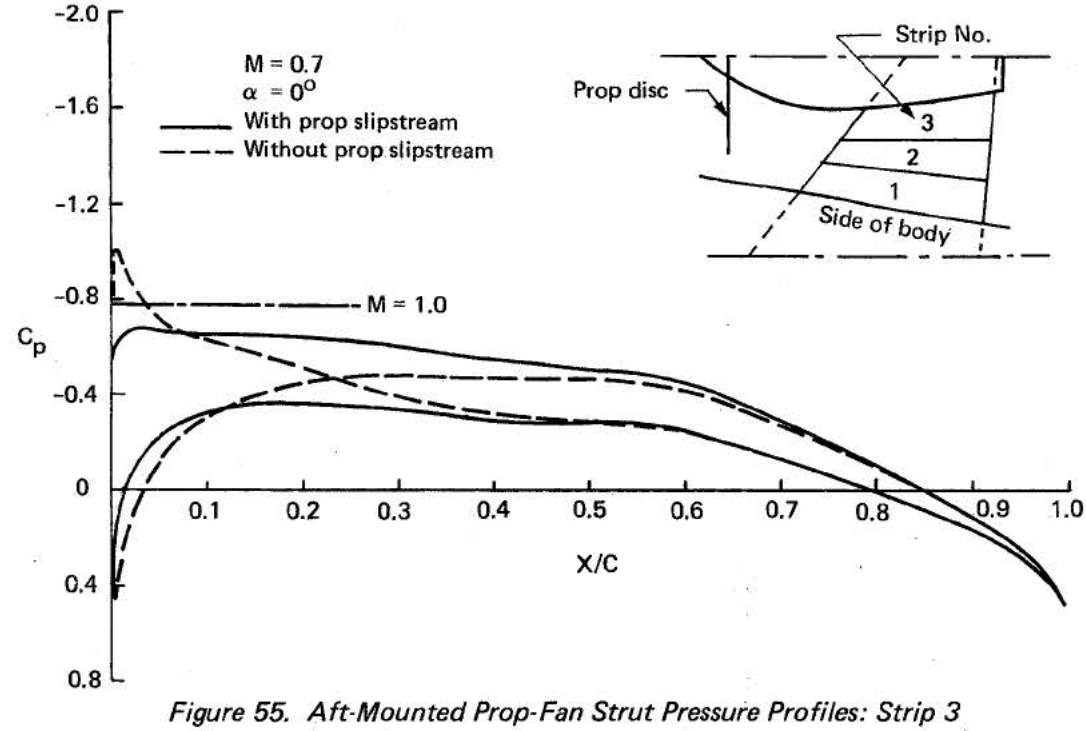


Figure 55. Aft-Mounted Prop-Fan Strut Pressure Profiles: Strip 3

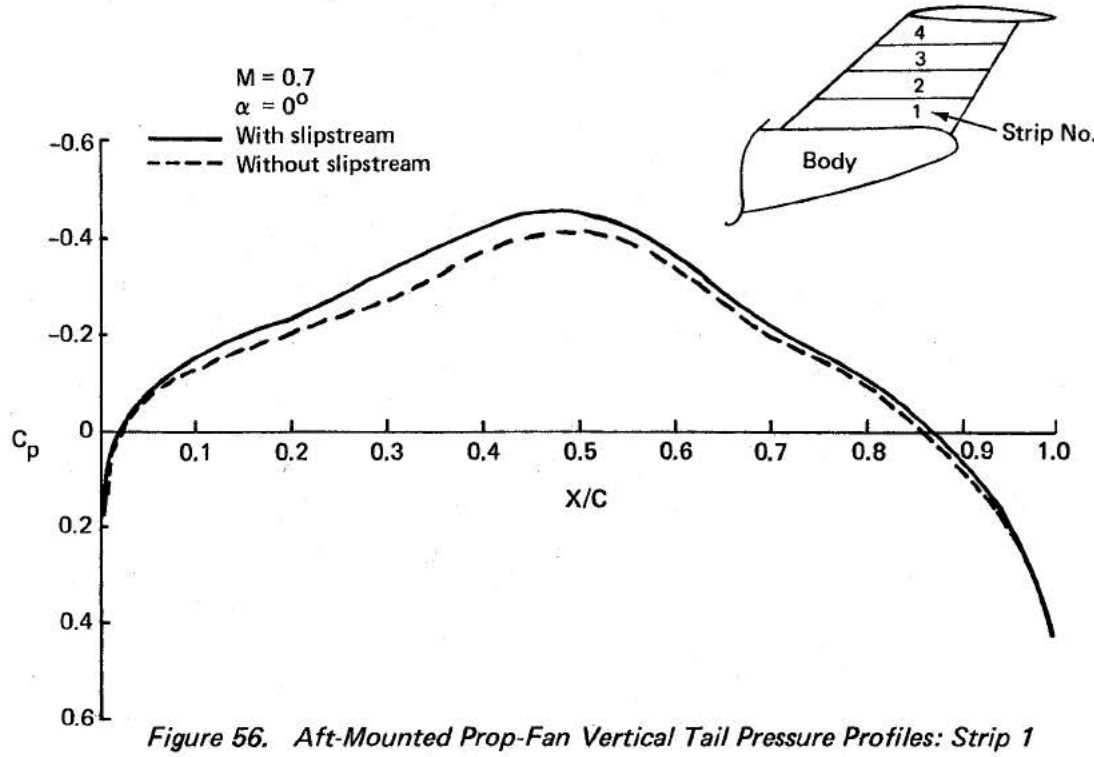


Figure 56. Aft-Mounted Prop-Fan Vertical Tail Pressure Profiles: Strip 1

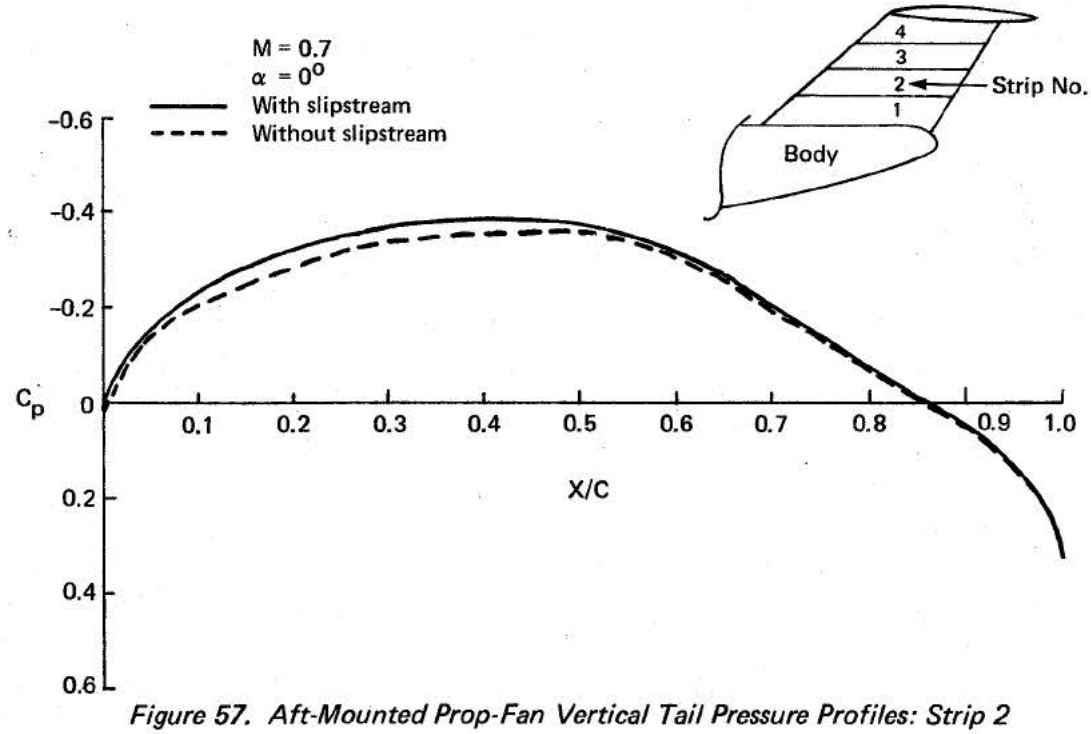


Figure 57. Aft-Mounted Prop-Fan Vertical Tail Pressure Profiles: Strip 2

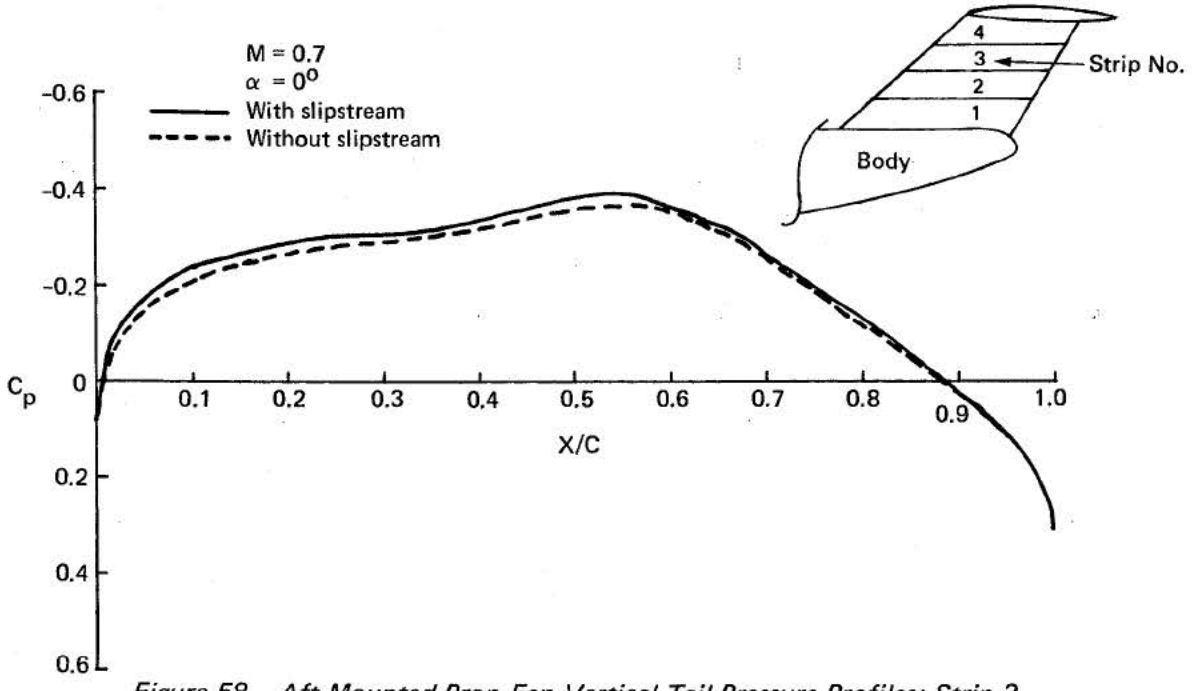


Figure 58. Aft-Mounted Prop-Fan Vertical Tail Pressure Profiles: Strip 3

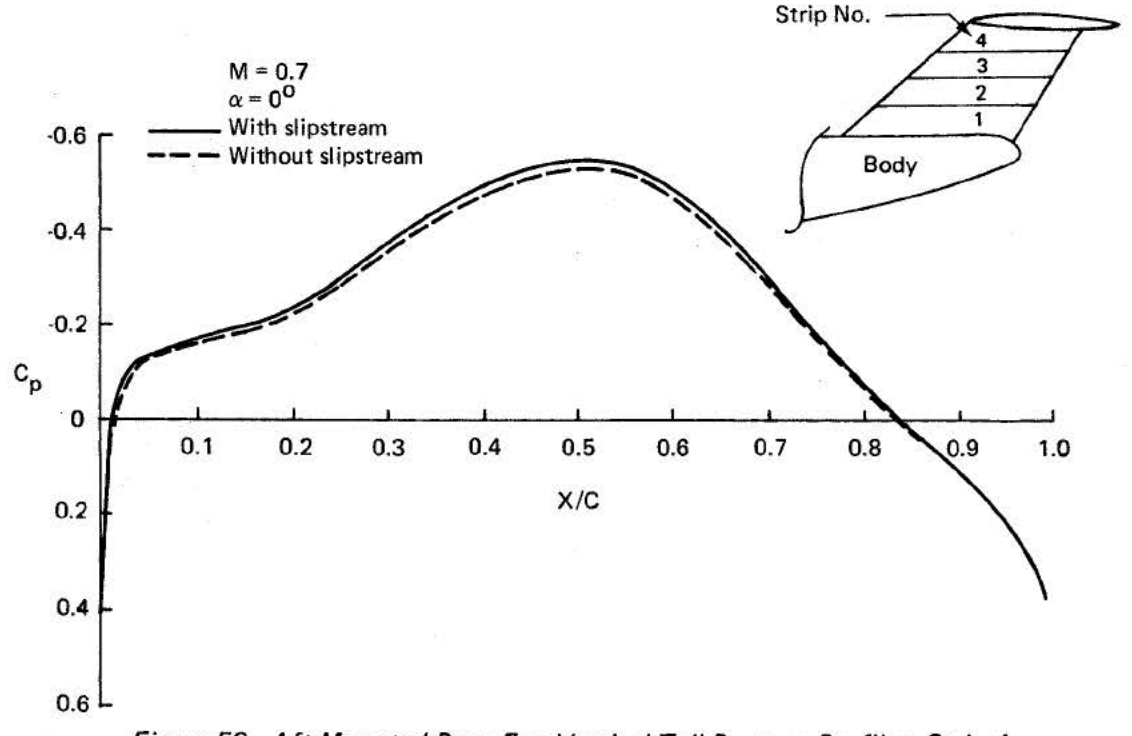


Figure 59. Aft-Mounted Prop-Fan Vertical Tail Pressure Profiles: Strip 4

Figure 60, strut spanwise load distribution, shows that the propeller slipstream clearly increases the upward load on the strut, which, to some extent, contributes to thrust recovery. This force, however, is very small due to the limited strut area. Because loading the strut serves no useful purpose, the strut could be twisted and pitched down to uniformly eliminate the span load in the presence of the slipstream. The load increment of the slipstream would probably remain unaffected as would the thrust recovery and the strut drag would be reduced.

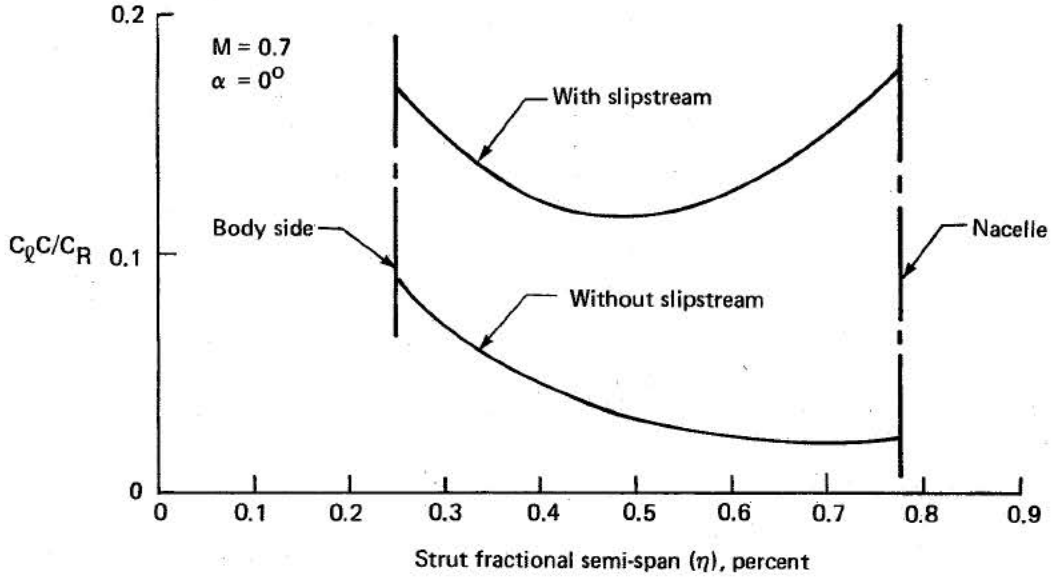


Figure 60. Aft-Mounted Prop-Fan Effect of Slipstream on Strut Loading

7.4 DRAG AND THRUST RECOVERY

Figure 61 shows a plot of induced drag of the clean wing versus C_L. The lift and drag increments due to the slipstream were calculated by integration of the surface pressures and are shown as a thrust recovery vector. Computed at $\alpha = 0^o$, this vector is

$\Delta C_L = 0.017$
$\Delta C_D = 0.8$ drag counts.

Considered at constant C_L, an equivalent three counts of drag reduction could be interpreted as thrust recovery. However, the uncertainties in the above calculations are sufficient to offset any gain attributed to thrust recovery.

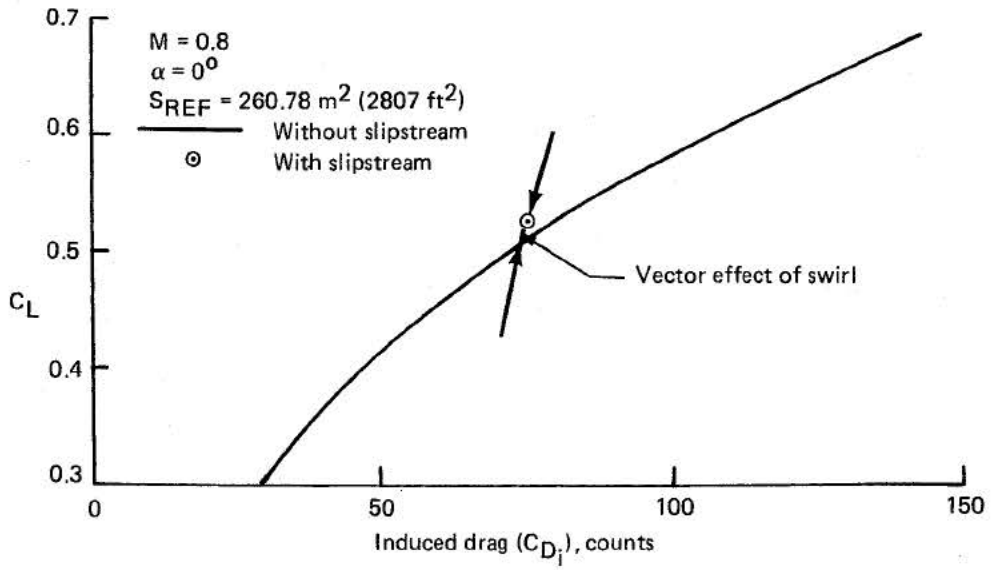


Figure 61. Aft-Mounted Prop-Fan Effect of Slipstream on Induced Drag

7.5 ASSESSMENT

In the absence of the wing-slipstream interference problem, there is little aerodynamic difference between the aft-mounted prop-fan and an equivalent turbofan configuration. Therefore, only airplane size and power plant characteristics for a given mission determine the difference in operating economics between the two airplanes.

The aft-mounted prop-fan requires relatively long struts for the propeller to clear the side of the body, so a higher incentive exists to optimize these struts for minimum drag and maximum thrust recovery. The present analysis shows the type and extent of strut loading caused by the prop slipstream and the interference effects between the various components involved. Proper loading of the strut and careful contouring of its leading edge should enhance thrust recovery without incurring drag penalties.

8.0 REFERENCES

1. *Energy Consumption Characteristics of Transports Using the Prop-Fan Concept.* NASA CR-137937, October 1976.

2. Rubbert, P.E. et al.; *A General Method for Determining the Aerodynamic Characteristics of Fan-in-Wing Configurations.* Technical Report 67-61A, USAAVLABS, 1967.

3. Geller, E.W. and Bailey, D.C.; *TEA 236, Subsonic Wing Design and Analysis Program.* Boeing Document D6-29337, 1968.

4. Rohrback, Carl; *A Report on the Aerodynamic Design and Wind Tunnel Test of a Prop-Fan Model.* AIAA Paper No. 76-667, July 1976.

5. Lundry, J.L.; *The Calculation of Lift and Induced Drag from a Curve-Fitting of Sparse Span Loading Points.* Boeing Document D6-40274 TN, August 1972.

APPENDIX A

BASELINE AND MODIFIED WING GEOMETRY

Definitions of the baseline and modified cruise wing are given in the following pages. Figure A-1 gives the planform definition which is common to both wings. The wing has the following reference quantities:

Area, m^2 (ft^2)	260.8 (2807)
Aspect ratio	10
Taper ratio	0.353
C/4 sweep, deg	30
MAC, m (in)	5.496 (216.37)
Span, m (in)	51.066 (2010.49)

Each of the two wings is defined at 16 wing buttock lines, including one on each side of the nacelle.

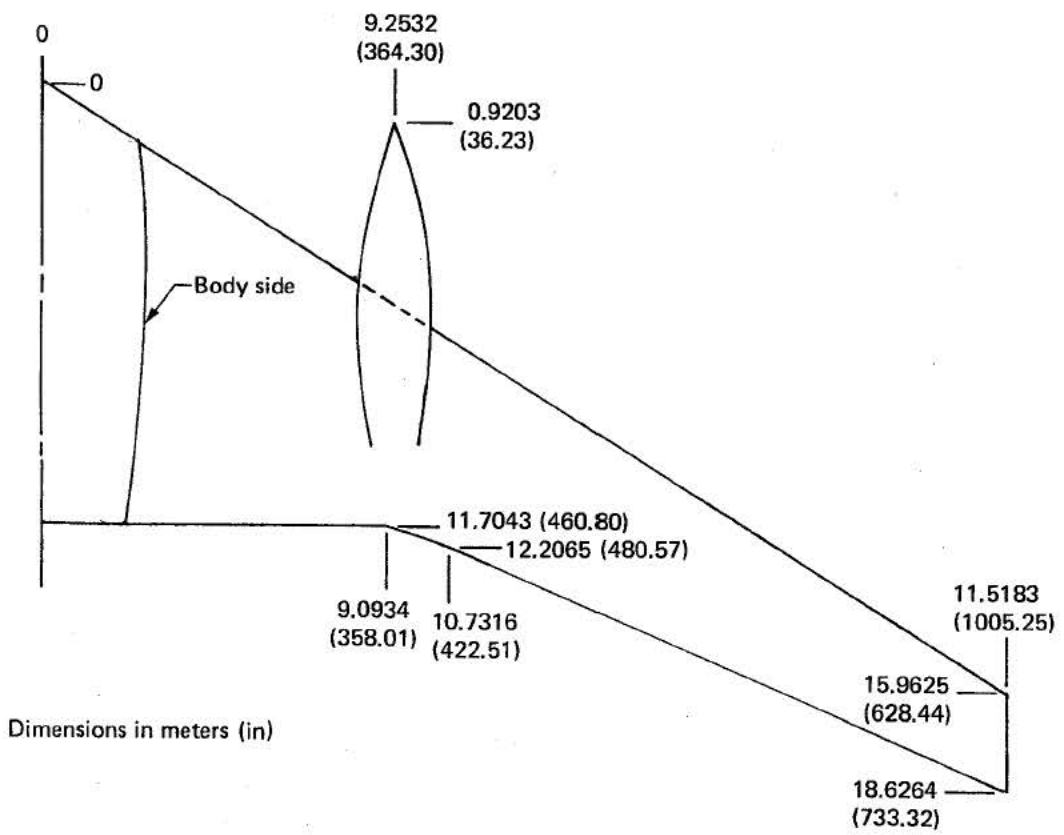


Figure A-1. Wing Planform Dimensions

WBL: 2.7686 m (9.0833 FT) η = .1084

(DIMENSIONS IN METERS)

BASELINE WING		MODIFIED WING	
X	Z	X	Z
25.719227	3.857153	25.719227	3.852128
25.469891	3.906314	25.470089	3.899553
25.095883	3.980513	25.096084	3.970965
24.701932	4.059131	24.702130	4.040687
24.113495	4.177093	24.113693	4.160154
23.525058	4.293674	23.525259	4.271840
22.940612	4.400042	22.940711	4.373753
22.353173	4.496513	22.353273	4.468338
21.769725	4.586399	21.769824	4.552925
21.181289	4.666473	21.181388	4.629998
20.590856	4.734596	20.590957	4.695828
20.004418	4.791428	20.004517	4.751019
19.415981	4.836274	19.416080	4.794796
18.837519	4.866086	18.837618	4.824557
18.239110	4.878393	18.239209	4.836151
17.740434	4.870072	17.740432	4.832264
17.241761	4.839536	17.241756	4.805385
16.910540	4.809508	16.910538	4.778215
16.615623	4.772312	16.615621	4.744049
16.359007	4.728383	16.359005	4.703003
16.139988	4.677306	16.139985	4.654769
15.961662	4.598637	15.961660	4.579422
15.852206	4.498833	15.852206	4.482493
15.759501	4.369234	15.759499	4.357342
15.745737	4.267363	15.728694	4.241966
15.759501	4.170462	15.789946	4.158094
15.852206	4.061828	15.836743	4.063622
15.961662	3.951206	15.961660	3.955456
16.139988	3.837074	16.139985	3.844160
16.359007	3.754727	16.359005	3.763510
16.615623	3.679629	16.615623	3.689642
16.910540	3.609868	16.910540	3.621156
17.241761	3.548555	17.241759	3.561113
17.740434	3.482386	17.740432	3.496236
18.239110	3.445673	18.239207	3.460276
18.837519	3.421878	18.837618	3.436483
19.415981	3.413376	19.416080	3.427506
20.004418	3.424362	20.004517	3.437557
20.590858	3.456429	20.590957	3.468304
21.181289	3.517024	21.181388	3.527263
21.769725	3.600455	21.769824	3.609172
22.353173	3.691981	22.353273	3.699281
22.940612	3.775761	22.940711	3.781529
23.525058	3.840124	23.525259	3.844435
24.113495	3.877739	24.113696	3.880556
24.701932	3.895192	24.702130	3.898060
25.095883	3.906794	25.096084	3.905806
25.469891	3.851847	25.470089	3.826369
25.719227	3.797417	25.719227	3.792083

WBL: 4.1786 m (13.7092 FT) η = .1637

(DIMENSIONS IN METERS)

BASELINE WING		MODIFIED WING	
X	Z	X	Z
25.719227	4.096922	25.719227	4.082755
25.491926	4.144831	25.492108	4.133706
25.150975	4.214737	25.151156	4.208698
24.791839	4.287256	24.792021	4.284871
24.255409	4.393529	24.255591	4.396694
23.719979	4.496016	23.719160	4.503843
23.180186	4.588094	23.180276	4.599264
22.650664	4.672040	22.650755	4.685564
22.118780	4.746030	22.118870	4.760730
21.582350	4.812642	21.582440	4.827375
21.044101	4.868466	21.044191	4.882461
20.509490	4.914326	20.509579	4.926796
19.973059	4.949525	19.973149	4.959727
19.445721	4.971574	19.445810	4.976775
18.900199	4.976285	18.900288	4.981757
18.445597	4.967814	18.445595	4.967892
17.990995	4.938235	17.990993	4.935097
17.089048	4.909843	17.889046	4.904811
17.420197	4.875165	17.420195	4.866952
17.180259	4.834555	17.180256	4.824311
16.980597	4.787506	16.980595	4.782205
16.824032	4.737293	16.824030	4.736853
16.709017	4.686593	16.709015	4.685695
16.639736	4.513546	16.639734	4.519191
16.627189	4.423658	16.627187	4.437090
16.639736	4.336276	16.639734	4.356769
16.709017	4.259888	16.709015	4.285104
16.824032	4.142967	16.824030	4.172775
16.980597	4.045156	16.980595	4.079227
17.180259	3.973747	17.180256	4.008964
17.420197	3.909924	17.420195	3.943974
17.889048	3.848930	17.889046	3.882575
17.990995	3.796214	17.990993	3.827352
18.445597	3.739322	18.445595	3.765597
18.900199	3.707099	18.900288	3.727629
19.445721	3.686320	19.445810	3.699669
19.973059	3.679397	19.973149	3.685460
20.509490	3.689600	20.509579	3.688151
21.044101	3.718625	21.044191	3.709961
21.582350	3.773065	21.582440	3.757978
22.118780	3.848972	22.118870	3.826867
22.650664	3.933625	22.650755	3.910133
23.180186	4.014073	23.180276	3.988998
23.719979	4.078432	23.719160	4.054070
24.255409	4.118812	24.255591	4.096911
24.791839	4.128750	24.792021	4.110167
25.150975	4.111710	25.151156	4.095174
25.491926	4.070840	25.492108	4.062052
25.719227	4.041990	25.719227	4.028150

WBL: 5.8169 m (19.0842 FT) η = .2278

(DIMENSIONS IN METERS)

BASELINE WING		MODIFIED WING	
X	Z	X	Z
25.719227	4.375522	25.719227	4.460109
25.517531	4.421977	25.517693	4.492497
25.214988	4.486893	25.215149	4.536776
24.896308	4.552327	24.896470	4.578997
24.420306	4.645016	24.420467	4.636819
23.944304	4.731125	23.944465	4.688808
23.471529	4.806601	23.471609	4.731471
22.996334	4.873670	22.996414	4.766783
22.524306	4.931514	22.524446	4.793827
22.048364	4.982484	22.048444	4.814739
21.570748	5.024062	21.570828	4.826905
21.096360	5.057129	21.096439	4.831560
20.620358	5.081116	20.620437	4.827817
20.152423	5.094144	20.152502	4.814053
19.668354	5.094354	19.668433	4.787219
19.264962	5.081384	19.264960	4.752681
18.861570	5.052920	18.861569	4.704113
18.593638	5.020429	18.593636	4.665677
18.355072	4.994674	18.355070	4.625064
18.147487	4.957921	18.147485	4.581990
17.970317	4.915556	17.970315	4.536269
17.820064	4.855166	17.820062	4.475494
17.721344	4.779368	17.721341	4.401988
17.662529	4.681250	17.662527	4.327207
17.651396	4.605264	17.651393	4.270245
17.662529	4.553272	17.662527	4.225182
17.721344	4.446765	17.721341	4.154951
17.820064	4.365763	17.820062	4.092522
17.970317	4.286942	17.970315	4.036858
18.147487	4.228237	18.147485	3.998072
18.355072	4.175353	18.355070	3.965083
18.593638	4.126720	18.593636	3.936413
18.861570	4.083981	18.861569	3.914732
19.264962	4.037870	19.264960	3.890684
19.668354	4.010804	19.668433	3.894320
20.152423	3.993004	20.152502	3.902815
20.620358	3.988501	20.620437	3.919516
21.096360	3.997794	21.096439	3.948044
21.570748	4.023264	21.570828	3.990452
22.048364	4.070571	22.048444	4.052280
22.524306	4.137739	22.524446	4.131958
22.996334	4.214834	22.996414	4.220010
23.471529	4.290982	23.471609	4.305917
23.944304	4.355335	23.944465	4.380068
24.420306	4.398926	24.420467	4.434994
24.896308	4.411751	24.896470	4.461424
25.214988	4.396291	25.215149	4.457382
25.517531	4.361624	25.517693	4.435817
25.719227	4.320173	25.719227	4.410121

WBL: 7.4552 m (24.4592 FT) η = .2920

(DIMENSIONS IN METERS)

BASELINE WING		MODIFIED WING	
X	Z	X	Z
25.719227	4.654121	25.719227	4.797032
25.543137	4.699123	25.543277	4.841065
25.279001	4.759050	25.279141	4.896094
25.000778	4.817397	25.000918	4.950349
24.565204	4.896502	24.565344	4.982752
24.169630	4.966235	24.169770	5.013419
23.750873	5.025109	23.750943	5.031164
23.342004	5.075301	23.342073	5.039065
22.929952	5.116998	22.930021	5.038509
22.514378	5.152325	22.514447	5.031043
22.097395	5.179638	22.097465	5.015159
21.683230	5.199931	21.683299	4.992289
21.267656	5.212711	21.267725	4.961557
20.859126	5.216715	20.859195	4.922479
20.436509	5.210424	20.436577	4.871154
20.084327	5.194954	20.084325	4.817800
19.732146	5.167605	19.732144	4.752925
19.498227	5.143014	19.498225	4.706479
19.269947	5.114103	19.269945	4.651511
19.108715	5.081267	19.108713	4.602163
18.954037	5.043605	18.954034	4.544300
18.828097	4.993039	18.828094	4.482316
18.730670	4.930143	18.730668	4.419604
18.685322	4.848913	18.685320	4.365402
18.675602	4.756871	18.675600	4.339556
18.685322	4.725200	18.685320	4.338987
18.730670	4.653061	18.730668	4.347622
18.828097	4.568599	18.828094	4.196710
18.954037	4.528726	18.954034	4.162641
19.108715	4.482727	19.108713	4.140742
19.269947	4.441781	19.269945	4.125253
19.498227	4.404505	19.498225	4.109821
19.732146	4.371749	19.732144	4.100713
20.084327	4.336419	20.084325	4.096079
20.436509	4.314630	20.436577	4.099819
20.859126	4.300861	20.859195	4.111167
21.267656	4.297605	21.267725	4.126120
21.683230	4.305987	21.683299	4.153449
22.097395	4.327944	22.097465	4.189400
22.514378	4.368077	22.514447	4.241649
22.929952	4.426505	22.930021	4.311285
23.342004	4.495844	23.342073	4.392510
23.750873	4.567890	23.750943	4.480055
24.169630	4.632238	24.169770	4.569410
24.565204	4.679041	24.565344	4.648953
25.000778	4.694753	25.000918	4.703856
25.279001	4.680872	25.279141	4.730400
25.543137	4.646203	25.543277	4.747206
25.719227	4.610356	25.719227	4.749910

WBL: 8.3820 m (27.5000 FT) η = .3283

(DIMENSIONS IN METERS)

BASELINE WING		MODIFIED WING	
X	Z	X	Z
25.719227	4.811735	25.719227	4.853132
25.557622	4.855914	25.557752	4.912020
25.315215	4.913016	25.315344	4.986457
25.059879	4.967356	25.060008	5.047257
24.678493	5.038776	24.678622	5.115547
24.297104	5.099246	24.297234	5.167622
23.916304	5.148725	23.916307	5.205433
23.537563	5.189370	23.537626	5.232055
23.159408	5.221935	23.159469	5.246866
22.778019	5.246412	22.778082	5.253896
22.395337	5.267655	22.395404	5.251869
22.015244	5.280718	22.015308	5.242209
21.633856	5.287157	21.633919	5.224061
21.258934	5.286057	21.258995	5.196873
20.871081	5.276088	20.871144	5.159830
20.547871	5.259205	20.547808	5.116500
20.224661	5.232486	20.224659	5.062367
20.009985	5.208971	20.009963	5.020587
19.818840	5.181793	19.818838	4.973094
19.652516	5.151079	19.652513	4.924488
19.510563	5.116045	19.510563	4.871006
19.394983	5.071039	19.394980	4.811349
19.311076	5.015443	19.311109	4.743544
19.263965	4.943191	19.263965	4.684316
19.255034	4.888588	19.255031	4.648152
19.263970	4.837339	19.263970	4.609158
19.311193	4.769140	19.311186	4.548683
19.395194	4.713323	19.395168	4.500555
19.510802	4.664547	19.510802	4.464723
19.652776	4.625955	19.652776	4.437751
19.819046	4.592061	19.819046	4.413603
20.010006	4.561622	20.010013	4.392092
20.224661	4.534550	20.224661	4.372315
20.547871	4.505317	20.547871	4.350583
20.871081	4.486481	20.871144	4.336118
21.258934	4.474716	21.258995	4.326631
21.633856	4.472475	21.633922	4.324955
22.015244	4.480344	22.015308	4.332270
22.395337	4.500301	22.395404	4.351114
22.778019	4.536387	22.778082	4.386811
23.159408	4.589871	23.159471	4.441739
23.537563	4.654822	23.537626	4.511751
23.916304	4.724547	23.916307	4.590959
24.297104	4.786891	24.297234	4.669244
24.678493	4.837514	24.678620	4.739645
25.059879	4.874857	25.060008	4.787547
25.315215	4.891670	25.315344	4.805837
25.557622	4.897255	25.557752	4.814331
25.719227	4.771128	25.719227	4.811291

WBL: 10.1600 m (33.3333 FT) η = .3979

(DIMENSIONS IN METERS)

BASELINE WING		MODIFIED WING	
X	Z	X	Z
26.046189	5.042913	26.046189	4.669998
25.904198	5.084958	25.904312	4.724806
25.691214	5.137396	25.691325	4.796348
25.466868	5.185809	25.466980	4.863170
25.131771	5.246764	25.131883	4.950396
24.796674	5.295392	24.796786	5.028143
24.466847	5.333182	24.466903	5.096324
24.129319	5.362242	24.129375	5.161519
23.797062	5.383906	23.797118	5.217493
23.461965	5.399959	23.462018	5.268443
23.125732	5.409824	23.125788	5.313142
22.791771	5.414599	22.791824	5.351958
22.456673	5.413880	22.456727	5.384848
22.127256	5.407172	22.127309	5.410972
21.786479	5.393355	21.786532	5.430830
21.502497	5.375275	21.502497	5.440053
21.218517	5.349814	21.218515	5.440644
21.029897	5.328001	21.029894	5.435362
20.861950	5.303263	20.861947	5.424560
20.715813	5.275666	20.715813	5.408605
20.591089	5.244399	20.591087	5.386415
20.489537	5.206573	20.489537	5.355021
20.415816	5.160350	20.415814	5.314655
20.374412	5.100970	20.374409	5.236169
20.366576	5.056754	20.366573	5.203274
20.374412	5.015367	20.374409	5.159246
20.415816	4.956605	20.415814	5.098773
20.489537	4.911908	20.489537	5.052197
20.591089	4.875708	20.591089	5.004559
20.715813	4.845764	20.715813	4.962395
20.861950	4.819851	20.861947	4.922091
21.029897	4.796858	21.029894	4.882294
21.218517	4.776645	21.218515	4.842807
21.502497	4.754923	21.502494	4.791479
21.786479	4.739947	21.786532	4.747133
22.127256	4.730856	22.127309	4.705542
22.456673	4.729940	22.456727	4.670621
22.791771	4.737209	22.791826	4.647123
23.125732	4.754646	23.125786	4.636176
23.461965	4.785553	23.462021	4.641591
23.797062	4.832305	23.797115	4.666671
24.129319	4.890945	24.129375	4.706899
24.466847	4.956371	24.466903	4.754405
24.796674	5.019093	24.796786	4.793866
25.131771	5.068509	25.131883	4.809866
25.466868	5.087422	25.466980	4.786193
25.691214	5.075763	25.691325	4.744725
25.904198	5.042215	25.904309	4.684819
26.046189	5.006607	26.046189	4.633227

WBL: 10.7317 m (35.2088 FT) η = .4203

(DIMENSIONS IN METERS)

BASELINE WING		MODIFIED WING	
X	Z	X	Z
26.221434	5.161976	26.221433	4.705816
26.063997	5.143212	26.064106	4.757215
25.877642	5.194314	25.877951	4.824307
25.660691	5.241199	25.660800	4.887676
25.336339	5.299739	25.336448	4.970649
25.011988	5.345800	25.012097	5.044546
24.689836	5.381169	24.689869	5.112292
24.366034	5.407969	24.366088	5.174607
24.044431	5.427547	24.044485	5.229037
23.720080	5.441655	23.720133	5.279619
23.394629	5.449814	23.394682	5.324753
23.071377	5.453118	23.071430	5.364940
22.747025	5.451171	22.747078	5.400080
22.426171	5.443557	22.426224	5.429052
22.098322	5.429193	22.098375	5.452641
21.823448	5.411052	21.823446	5.466105
21.548574	5.386005	21.548572	5.472328
21.366002	5.364664	21.366001	5.471283
21.203442	5.340552	21.203440	5.464608
21.061992	5.313729	21.061990	5.453436
20.941267	5.283389	20.941265	5.434316
20.842972	5.247125	20.842970	5.408084
20.771615	5.202926	20.771613	5.370544
20.731538	5.146193	20.731536	5.271090
20.723951	5.104067	20.723949	5.271147
20.731538	5.064755	20.731536	5.249901
20.771615	5.008106	20.771613	5.199868
20.842972	4.965771	20.842970	5.146717
20.941267	4.932094	20.941265	5.102122
21.061992	4.903944	21.061990	5.061143
21.203442	4.879691	21.203440	5.022650
21.366002	4.858234	21.366001	4.984486
21.548574	4.839423	21.548572	4.946669
21.823448	4.819216	21.823446	4.897241
22.098322	4.805096	22.098375	4.853949
22.426171	4.796589	22.426224	4.810626
22.747025	4.795990	22.747078	4.776967
23.071377	4.803152	23.071430	4.751352
23.394629	4.820060	23.394682	4.736874
23.720080	4.844856	23.720133	4.736588
24.044431	4.895125	24.044485	4.753812
24.366034	4.952097	24.366088	4.784433
24.689836	5.010171	24.689869	4.821255
25.011988	5.078028	25.012097	4.850744
25.336339	5.127119	25.336448	4.855567
25.660691	5.146200	25.660800	4.829457
25.877642	5.134886	25.877951	4.785621
26.063997	5.101868	26.064106	4.723471
26.221434	5.060960	26.221433	4.664706

WBL: 12.3784 m (40.6050 FT) η = .4847

(DIMENSIONS IN METERS)

BASELINE WING		MODIFIED WING	
X	Z	X	Z
26.934809	5.220370	26.934808	4.869270
26.805244	5.264934	26.805347	4.931929
26.610695	5.312606	26.610998	4.986352
26.406182	5.356262	26.406285	5.037229
26.100406	5.410564	26.100510	5.102629
25.794633	5.453082	25.794736	5.157829
25.490932	5.485610	25.490983	5.205742
25.185676	5.510157	25.185726	5.247198
24.882492	5.527954	24.882543	5.282103
24.576718	5.540653	24.576768	5.312365
24.269907	5.547812	24.269958	5.337536
23.965169	5.550446	23.965220	5.358407
23.659395	5.548171	23.659445	5.374861
23.356803	5.540627	23.356853	5.386134
23.047846	5.526737	23.047896	5.392234
22.788715	5.509393	22.788713	5.392047
22.529584	5.485569	22.529582	5.385683
22.357469	5.465354	22.357467	5.377246
22.204219	5.442574	22.204217	5.364937
22.070870	5.417292	22.070868	5.349446
21.957060	5.388762	21.957058	5.326254
21.864395	5.354787	21.864393	5.298309
21.797125	5.313444	21.797123	5.260307
21.759343	5.260449	21.759341	5.211954
21.752191	5.221039	21.752189	5.162254
21.759344	5.184490	21.759341	5.102149
21.797125	5.131650	21.797123	5.110300
21.864395	5.092237	21.864393	5.075497
21.957060	5.060929	21.957058	5.045962
22.070870	5.034794	22.070868	5.012140
22.204219	5.012321	22.204217	4.982781
22.357469	4.992470	22.357467	4.954556
22.529584	4.975133	22.529582	4.927783
22.788715	4.956607	22.788713	4.894749
23.047846	4.943795	23.047896	4.867172
23.356803	4.936283	23.356853	4.841570
23.659395	4.930133	23.659445	4.823655
23.965169	4.945253	23.965220	4.812309
24.269907	4.959461	24.269958	4.809811
24.576718	4.987714	24.576768	4.818564
24.882492	5.030344	24.882543	4.841083
25.185676	5.083999	25.185726	4.874241
25.490932	5.144283	25.490983	4.913277
25.794633	5.202611	25.794736	4.945995
26.100406	5.249050	26.100510	4.970975
26.406182	5.287010	26.406285	4.985212
26.610695	5.257047	26.610998	4.939801
26.805244	5.220245	26.805347	4.896236
26.934809	5.193582	26.934808	4.855516

WBL: 14.0211 m (46.0008 FT) η = .5491

(DIMENSIONS IN METERS)

BASELINE WING		MODIFIED WING	
X	Z	X	Z
27.048140	5.350769	27.048139	5.056865
27.526446	5.386648	27.526542	5.094979
27.343904	5.431011	27.344001	5.139937
27.151627	5.471359	27.151724	5.181456
26.864428	5.521383	26.864525	5.233642
26.577230	5.560357	26.577326	5.274901
26.291978	5.590025	26.292026	5.306961
26.005267	5.612298	26.005314	5.331558
25.720502	5.628354	25.720550	5.349807
25.433303	5.639646	25.433351	5.363164
25.145131	5.645803	25.145179	5.371322
24.856906	5.647769	24.856954	5.375027
24.571708	5.645165	24.571755	5.374039
24.289377	5.637692	24.289424	5.368037
23.997310	5.624276	23.997358	5.355645
23.753922	5.607728	23.753920	5.340460
23.510533	5.585127	23.510532	5.318814
23.348875	5.566037	23.348873	5.300302
23.204935	5.544590	23.204933	5.279180
23.079687	5.520850	23.079685	5.255961
22.972790	5.494168	22.972789	5.228365
22.885755	5.462441	22.885753	5.193907
22.822571	5.423956	22.822569	5.157138
22.787085	5.374698	22.787083	5.120826
22.780367	5.338003	22.780365	5.077289
22.787086	5.304236	22.787083	5.046952
22.822571	5.255128	22.822569	5.003803
22.885755	5.218695	22.885753	4.969365
22.972790	5.189755	22.972789	4.935077
23.079687	5.165636	23.079685	4.907996
23.204935	5.144942	23.204933	4.886078
23.348875	5.126710	23.348873	4.866510
23.510533	5.110835	23.510532	4.849351
23.753922	5.093989	23.753920	4.830752
23.997310	5.082485	23.997358	4.817602
24.289377	5.075970	24.289424	4.809430
24.571708	5.076267	24.571755	4.808213
24.856906	5.083306	24.856954	4.815748
25.145131	5.098854	25.145179	4.827645
25.433303	5.125563	25.433351	4.852418
25.720502	5.165555	25.720550	4.890138
26.005267	5.215893	26.005314	4.937828
26.291978	5.272358	26.292026	4.991402
26.577230	5.327187	26.577326	5.043444
26.864428	5.370975	26.864525	5.084883
27.151627	5.389025	27.151724	5.101073
27.343904	5.379201	27.344001	5.090135
27.526446	5.350594	27.526542	5.060057
27.048140	5.320176	27.048139	5.028461

WBL: 15.6657 m (51.3967 FT) η = .6135

(DIMENSIONS IN METERS)

BASELINE WING		MODIFIED WING	
X	Z	X	Z
28.361471	5.475161	28.361470	5.177551
28.247647	5.508362	28.247738	5.210414
28.070913	5.549355	28.077003	5.251108
27.897072	5.586436	27.897163	5.288251
27.628449	5.632202	27.628540	5.334527
27.359827	5.667633	27.359917	5.370709
27.093025	5.694440	27.093070	5.398295
26.824858	5.714460	26.824902	5.419239
26.558512	5.728755	26.558556	5.434523
26.289889	5.738639	26.289933	5.445436
26.020356	5.743794	26.020400	5.451737
25.752643	5.745091	25.752688	5.454173
25.484021	5.742159	25.484065	5.452479
25.219951	5.734757	25.219995	5.446269
24.946775	5.721815	24.946819	5.434650
24.719129	5.706063	24.719127	5.420081
24.491483	5.684685	24.491481	5.399884
24.340280	5.666720	24.340278	5.382756
24.205650	5.646605	24.205648	5.363267
24.068503	5.624407	24.068501	5.341816
23.980521	5.599555	23.980519	5.316406
23.907114	5.570096	23.907113	5.285009
23.848017	5.534467	23.848016	5.250733
23.814827	5.488947	23.814825	5.212671
23.808543	5.454967	23.806542	5.179267
23.814828	5.423906	23.814825	5.151751
23.848017	5.378602	23.848016	5.110502
23.907114	5.345153	23.907113	5.076760
23.980521	5.318582	23.980519	5.048393
24.068503	5.296478	24.068501	5.024031
24.205650	5.277505	24.205648	5.004412
24.340280	5.260943	24.340278	4.987011
24.491483	5.246538	24.491481	4.971881
24.719129	5.231371	24.719127	4.955568
24.946775	5.221176	24.946819	4.944254
25.219951	5.215656	25.219995	4.937388
25.484021	5.216402	25.484065	4.936810
25.752643	5.223379	25.752688	4.942263
26.020356	5.238247	26.020400	4.955468
26.289889	5.263412	26.289933	4.978802
26.558512	5.300760	26.558556	5.014187
26.824858	5.347786	26.824902	5.059052
27.093025	5.400492	27.093070	5.109703
27.359827	5.451763	27.359917	5.159157
27.628449	5.492899	27.628540	5.196918
27.897072	5.510433	27.897163	5.215466
28.070913	5.501355	28.077003	5.205724
28.247647	5.474943	28.247738	5.178352
28.361471	5.446770	28.361470	5.149377

WBL: 17.3104 m (56.7925 FT) η = .6780

(DIMENSIONS IN METERS)

BASELINE WING		MODIFIED WING	
X	Z	X	Z
29.074801	5.599554	29.074801	5.293654
28.968849	5.630075	28.968934	5.323799
28.809921	5.667700	28.810006	5.361022
28.642517	5.701513	28.642601	5.394753
28.392470	5.743021	28.392554	5.436461
28.142424	5.774908	28.142508	5.466784
27.894072	5.798855	27.894114	5.493246
27.644449	5.816621	27.644491	5.511601
27.396521	5.829155	27.396563	5.524701
27.146474	5.837632	27.146516	5.533830
26.895580	5.841766	26.895621	5.538607
26.646361	5.842413	26.646422	5.540073
26.396334	5.839153	26.396375	5.537606
26.150525	5.831821	26.150566	5.531088
25.896240	5.819354	25.896281	5.519497
25.684336	5.804398	25.684335	5.505333
25.472432	5.784243	25.472431	5.485995
25.331685	5.767403	25.331684	5.469644
25.206365	5.748620	25.206364	5.451251
25.097319	5.727964	25.097318	5.431116
25.004251	5.704941	25.004249	5.407273
24.926474	5.677750	24.926473	5.383593
24.873464	5.644979	24.873462	5.351256
24.842568	5.603196	24.842567	5.309257
24.836720	5.571931	24.836718	5.279697
24.842570	5.543735	24.842567	5.250093
24.873464	5.502079	24.873462	5.212077
24.926474	5.471612	24.926473	5.186761
25.004251	5.447409	25.004249	5.159434
25.097319	5.427319	25.097318	5.159738
25.206365	5.410187	25.206364	5.119782
25.331685	5.395177	25.331684	5.104195
25.472432	5.382240	25.472431	5.090701
25.684336	5.368753	25.684335	5.076333
25.896240	5.359806	25.896281	5.066641
26.150525	5.355342	26.150566	5.061081
26.396334	5.356556	26.396375	5.061220
26.646361	5.363452	26.646422	5.067018
26.895580	5.377640	26.895621	5.080021
27.146474	5.401261	27.146516	5.102326
27.396521	5.435977	27.396563	5.135683
27.644449	5.479660	27.644491	5.178085
27.894072	5.526596	27.894114	5.225798
28.142424	5.576339	28.142508	5.272603
28.392470	5.614824	28.392554	5.310526
28.642517	5.631842	28.642601	5.327351
28.809921	5.623508	28.810006	5.318824
28.968849	5.599292	28.968934	5.294082
29.074801	5.573364	29.074801	5.267596

WBL: 18.9550 m (62.1883 FT) η = .7424

(DIMENSIONS IN METERS)

BASELINE WING		MODIFIED WING	
X	Z	X	Z
29.788132	5.723946	29.788132	5.408466
29.690051	5.751769	29.690129	5.435964
29.542930	5.786044	29.543008	5.469865
29.387962	5.816590	29.388040	5.500352
29.156491	5.853840	29.156569	5.537764
28.925020	5.882184	28.925098	5.566443
28.695119	5.903269	28.695157	5.587954
28.464040	5.918782	28.464078	5.603890
28.234531	5.929555	28.234569	5.615138
28.003060	5.936624	28.003098	5.622718
27.770804	5.939777	27.770842	5.626422
27.540118	5.939736	27.540156	5.626971
27.308647	5.936147	27.308685	5.624005
27.081099	5.928886	27.081137	5.617394
26.845705	5.916892	26.845743	5.606095
26.649543	5.902732	26.649542	5.592560
26.453381	5.883801	26.453380	5.574297
26.323091	5.868086	26.323089	5.558950
26.207081	5.850636	26.207079	5.541758
26.106136	5.831522	26.106134	5.523025
26.019981	5.810327	26.019980	5.500956
25.949834	5.785405	25.949833	5.474251
25.898910	5.755490	25.898909	5.446011
25.870310	5.717445	25.870308	5.414233
25.864896	5.668896	25.864894	5.384099
25.870311	5.663483	25.870308	5.358129
25.898910	5.625555	25.898909	5.324271
25.949834	5.598070	25.949833	5.299168
26.019981	5.576236	26.019980	5.274664
26.106136	5.556161	26.106134	5.254860
26.207081	5.542809	26.207079	5.239037
26.323091	5.529410	26.323089	5.225106
26.453381	5.517942	26.453380	5.213156
26.649543	5.506135	26.649542	5.200609
26.845705	5.498557	26.845743	5.192315
27.081099	5.495026	27.081137	5.187894
27.308647	5.496670	27.308685	5.188624
27.540118	5.503524	27.540156	5.194571
27.770804	5.517032	27.770842	5.207063
28.003060	5.539111	28.003098	5.228135
28.234531	5.571187	28.234569	5.259160
28.464040	5.611574	28.464078	5.298541
28.695119	5.656700	28.695157	5.342831
28.925020	5.700915	28.925098	5.386465
29.156491	5.736746	29.156569	5.422066
29.387962	5.753250	29.388040	5.438624
29.542930	5.745662	29.543008	5.431040
29.690051	5.723641	29.690129	5.408643
29.788132	5.699957	29.788132	5.384550

WBL: 20.5997 m (67.5842 FT) η = .8068

(DIMENSIONS IN METERS)

BASELINE WING		MODIFIED WING	
X	Z	X	Z
30.501463	5.048339	30.501463	5.522942
30.411253	5.873503	30.411325	5.547650
30.275939	5.904389	30.276011	5.578482
30.133407	5.931666	30.133479	5.605689
29.920512	5.964658	29.920584	5.638805
29.707617	5.989459	29.707689	5.663972
29.496165	6.007684	29.496201	5.682544
29.283631	6.020944	29.283667	5.696177
29.072540	6.029956	29.072576	5.705586
28.859645	6.035617	28.859680	5.711693
28.646029	6.037766	28.646064	5.714302
28.433855	6.037056	28.433890	5.714107
28.220960	6.033141	28.220995	5.710730
28.011673	6.025950	28.011708	5.704029
27.795170	6.014431	27.795205	5.693128
27.614750	6.001067	27.614749	5.680296
27.434331	5.983359	27.434329	5.663131
27.314496	5.968769	27.314495	5.648896
27.207796	5.952652	27.207795	5.633046
27.114952	5.935079	27.114951	5.615708
27.035712	5.915714	27.035710	5.596206
26.971194	5.893060	26.971192	5.572954
26.924357	5.866002	26.924355	5.550809
26.898052	5.831694	26.898050	5.520791
26.893072	5.805860	26.893071	5.486947
26.898054	5.783231	26.898050	5.460285
26.924357	5.749051	26.924355	5.430271
26.971194	5.724528	26.971192	5.410425
27.035712	5.705063	27.035710	5.389709
27.114952	5.689002	27.114951	5.372700
27.207796	5.675430	27.207795	5.358818
27.314496	5.663643	27.314495	5.346585
27.434331	5.653644	27.434329	5.336197
27.614750	5.643517	27.614749	5.325447
27.795170	5.637247	27.795205	5.318560
28.011673	5.634714	28.011708	5.315311
28.220960	5.636805	28.220995	5.316693
28.433855	5.643597	28.433890	5.322719
28.646029	5.656425	28.646064	5.334753
28.859645	5.676960	28.859680	5.354480
29.072540	5.706398	29.072576	5.383084
29.283631	5.743468	29.283667	5.419377
29.496165	5.784805	29.496201	5.460159
29.707617	5.825491	29.707689	5.500458
29.920512	5.858673	29.920584	5.533560
30.133407	5.874659	30.133479	5.549795
30.275939	5.867815	30.276011	5.543008
30.411253	5.847990	30.411325	5.522960
30.501463	5.826551	30.501463	5.501248

WBL: 22.2443 m (72.9800 FT) η = .8712

(DIMENSIONS IN METERS)

BASELINE WING		MODIFIED WING	
X	Z	X	Z
31.214794	5.972731	31.214794	5.637265
31.132455	5.995217	31.132521	5.659592
31.008947	6.022733	31.009013	5.686921
30.878852	6.046743	30.878918	5.710948
30.684533	6.075477	30.684599	5.739891
30.490214	6.096735	30.490279	5.761438
30.297212	6.112099	30.297244	5.777161
30.103222	6.123105	30.103255	5.786498
29.910550	6.130356	29.910582	5.796129
29.716231	6.134610	29.716263	5.800779
29.521253	6.135760	29.521285	5.802324
29.327592	6.134380	29.327624	5.801369
29.133273	6.130135	29.133305	5.797611
28.942247	6.123015	28.942279	5.790955
28.744635	6.111970	28.744667	5.780448
28.579958	6.099402	28.579956	5.768328
28.415280	6.082917	28.415279	5.752344
28.305901	6.069452	28.305900	5.739190
28.208512	6.054667	28.208510	5.724718
28.123768	6.038657	28.123767	5.708952
28.051442	6.021100	28.051441	5.691911
27.992554	6.000714	27.992552	5.671929
27.949803	5.976513	27.949802	5.647843
27.925794	5.945943	27.925792	5.617681
27.921248	5.922825	27.921247	5.594508
27.925796	5.902979	27.925792	5.574559
27.949803	5.872507	27.949802	5.544350
27.992554	5.850987	27.992552	5.522722
28.051442	5.833890	28.051441	5.505506
28.123768	5.819844	28.123767	5.491334
28.208512	5.808052	28.208510	5.479230
28.305901	5.797877	28.305900	5.468757
28.415280	5.789346	28.415279	5.459897
28.579958	5.780899	28.579956	5.450945
28.744635	5.775938	28.744667	5.445478
28.942247	5.774400	28.942279	5.443318
29.133273	5.776959	29.133305	5.445284
29.327592	5.783670	29.327624	5.451367
29.521253	5.795818	29.521285	5.462858
29.716231	5.814809	29.716263	5.481154
29.910550	5.841609	29.910582	5.507298
30.103222	5.875361	30.103255	5.540461
30.297212	5.912909	30.297244	5.577572
30.490214	5.950067	30.490279	5.614513
30.684533	5.980597	30.684599	5.645087
30.878852	5.996067	30.878918	5.660866
31.008947	5.989969	31.009013	5.654925
31.132455	5.972339	31.132521	5.637149
31.214794	5.953145	31.214794	5.617760

WBL: 23.8890 m (78.3758 FT) η = .9356

(DIMENSIONS IN METERS)

BASELINE WING		MODIFIED WING	
X	Z	X	Z
31.928125	6.097124	31.928125	5.751647
31.853657	6.116931	31.853717	5.771345
31.741956	6.141078	31.742015	5.795395
31.624297	6.161820	31.624357	5.816204
31.448554	6.186290	31.448613	5.840925
31.272811	6.204010	31.272870	5.858919
31.098259	6.216514	31.098288	5.871727
30.922813	6.225207	30.922843	5.880797
30.748560	6.230757	30.748589	5.886630
30.572816	6.233602	30.572845	5.889811
30.396477	6.233751	30.396506	5.890311
30.221329	6.231703	30.221358	5.888617
30.045586	6.227129	30.045615	5.884452
29.872822	6.220079	29.872850	5.877783
29.694100	6.209509	29.694128	5.867644
29.545165	6.197737	29.545163	5.856277
29.396229	6.182475	29.396228	5.841449
29.297307	6.170155	29.297306	5.829365
29.209227	6.156662	29.209226	5.816219
29.132585	6.142194	29.132584	5.801906
29.067172	6.126467	29.067171	5.786718
29.013914	6.108369	29.013912	5.768983
28.975250	6.087025	28.975249	5.747664
28.953535	6.060192	28.953534	5.721091
28.949425	6.039769	28.949423	5.700571
28.953537	6.022727	28.953534	5.683312
28.975250	5.995984	28.975249	5.656510
29.013914	5.977445	29.013912	5.637709
29.067172	5.962717	29.067171	5.622821
29.132565	5.950666	29.132584	5.610692
29.209227	5.940674	29.209226	5.600394
29.297307	5.932111	29.297306	5.591506
29.396229	5.925048	29.396228	5.584202
29.545165	5.918261	29.545163	5.576949
29.694100	5.914628	29.694128	5.572818
29.872822	5.914086	29.872850	5.571718
30.045586	5.917074	30.045615	5.574173
30.221329	5.923742	30.221358	5.580291
30.396477	5.935211	30.396506	5.591205
30.572816	5.952658	30.572845	5.608083
30.748560	5.976620	30.748589	5.631665
30.922813	6.007255	30.922843	5.661595
31.098259	6.041013	31.098288	5.695046
31.272811	6.074643	31.272870	5.728553
31.448554	6.102521	31.448613	5.756583
31.624297	6.117476	31.624357	5.771893
31.741956	6.112122	31.742015	5.766773
31.853657	6.096668	31.853717	5.751376
31.928125	6.079738	31.928125	5.734323

WBL: 25.5332 m (83.7705 FT) η = 1.0000

(DIMENSIONS IN METERS)

BASELINE WING		MODIFIED WING	
X	Z	X	Z
32.641301	6.221469	32.641301	5.866040
32.574703	6.238618	32.574757	5.883152
32.474806	6.259397	32.474859	5.903886
32.369581	6.276872	32.369634	5.921476
32.212410	6.297091	32.212463	5.941972
32.055238	6.311263	32.055291	5.956395
31.899132	6.320906	31.899159	5.966321
31.742227	6.327406	31.742254	5.973098
31.586388	6.331135	31.586414	5.977102
31.429216	6.332574	31.429242	5.978833
31.271512	6.331721	31.271538	5.978279
31.114874	6.329004	31.114899	5.975866
30.957702	6.324102	30.957728	5.971294
30.803194	6.317122	30.803220	5.964640
30.643359	6.307026	30.643385	5.954882
30.510163	6.296051	30.510162	5.944245
30.376967	6.282012	30.376966	5.930571
30.288498	6.270797	30.288497	5.919574
30.209726	6.258676	30.209725	5.907738
30.141183	6.245729	30.141182	5.895037
30.082683	6.231850	30.082682	5.881568
30.035052	6.216000	30.035051	5.866083
30.000475	6.197512	30.000473	5.847598
29.981055	6.174416	29.981053	5.824656
29.977378	6.156728	29.977377	5.806821
29.981057	6.142449	29.981053	5.792265
30.000475	6.119433	30.000473	5.768937
30.035052	6.103876	30.035051	5.752972
30.082683	6.091515	30.082682	5.740425
30.141183	6.081499	30.141182	5.730292
30.209726	6.073268	30.209725	5.721733
30.288498	6.066315	30.288497	5.714479
30.376967	6.060721	30.376966	5.708613
30.510163	6.055653	30.510162	5.703040
30.643359	6.053289	30.643385	5.700221
30.803194	6.053742	30.803220	5.700163
30.957702	6.057178	30.957728	5.703128
31.114874	6.063785	31.114899	5.709236
31.271512	6.074574	31.271538	5.719572
31.429216	6.090477	31.429242	5.735001
31.586388	6.112002	31.586414	5.756007
31.742227	6.139121	31.742254	5.782734
31.899132	6.169090	31.899159	5.812492
32.055238	6.199192	32.055291	5.842552
32.212410	6.224419	32.212463	5.868009
32.369581	6.238856	32.369634	5.882876
32.474806	6.254249	32.474859	5.878611
32.574703	6.221010	32.574757	5.865592
32.641301	6.206305	32.641301	5.850946

END OF DOCUMENT